Reactions of dithianitronium hexafluoroarsenate(v) and some plasma studies

Hibbert, Thomas G.

REACTIONS OF DITHIANITRONIUM HEXAFLUOROARSENATE(V) AND SOME PLASMA STUDIES

Thomas G. Hibbert BSc
Graduate Society

A thesis submitted in fulfillment of the degree of Master of Science at the University of Durham.

November 1993

" Come up to the lab, and see what's on the slab ".

The Rocky Horror Picture Show

Acknowledgements

To Dr Arthur Banister, for his knowledge, guidance and inexhaustable enthusiasm for life in general and chemistry in particular.

To Drs Jeremy Rawson and Ian Lavender, who provided me with experienced advice and a lot of understanding. It has been a priviledge to work with them both. Also, thanks to Jeremy for conducting esr experiments for me at Edinburgh.

To Zdenek ('Stan') Hauptman, whose gentle genius became apparent to all who worked with him.

To all the members of lab. 100, namely Christine Aherne, Simon Lawrence, Iain May and Colin Campbell. It's been a lot of fun.

To Dr Keith Dillon for sage ^{31}P nmr advice, without which I would drown under a sea of spectra.

To Professor William Clegg and his research group for working hard to solve the solid state structures featured in this thesis.

To the glassblowers, Ray and Gordon, for making the impossible for the disorganised.

To Julia Say, for performing the nmr spectra featured in this thesis, and for not laughing at my early attempts to flame-seal nmr tubes.

To the microanalytical staff at Durham (Jaraka Dostal, Judith Magee and Bob Coult) for their stalwart services.

To Leela Sequeira, for supplying me with samples of hard-won diphosphene.

And to Lisa, for love, encouragement and clean socks.

Memorandum

The work described in this thesis was carried out by me, in the Department of Chemistry at the University of Durham between October 1992 and October 1993. I declare that this work has not been submitted previously for a degree at this or any other University. This thesis is a report of my own original work, except where acknowledged by reference. The copyright of this thesis rests with the author. No quotation should be published without written consent, and information derived from it should be acknowledged.

Abstract

This work is chiefly concerned with the varied reactions of the compound dithianitronium hexafluoroarsenate(V), [SNS][AsF_6].

Chapter one provides a brief review of the properties and uses of [SNS][AsF_6], and chapter two outlines the experimental techniques required in this area of chemistry.

Chapter three describes the synthesis and characterisation of *ortho*-substituted 1,3,2,4-dithiadiazolium salts, along with two crystal structures and reduction studies.

The fourth and fifth chapters outline reactions of [SNS][AsF_6] with double and single bonds respectively, to form novel cations.

Chapter six demonstrates the surface area expansion of silver when subjected to several plasma oxidation/reduction cycles.

Appendix I outlines the synthesis and characterisation of the radical cation [$NSSNCC_6H_4CNSNS]^{+\cdot}$[$AsF_6$]. Appendix II illustrates the ability of [PhNSNSNPh][AsF_6] to polymerise thf. Appendix III lists colloquia, lectures and seminars attended by the author, and appendix IV contains supplementary crystallographic data.

Abbreviations

Ar	aryl
Bu	butyl
C_6H_4	phenylene
C. I.	chemical ionisation
-CNSNS	the 1,3,2,4-dithiadiazolyl/ium ring system
-CNSSN	the 1,2,3,5-dithiadiazolyl/ium ring system
C.V.	cyclic voltammagram
dmso	dimethylsulphoxide
dsc	differential scanning calorimetry
E. I.	electron impact
esr	electron spin resonance
Et	ethyl
FMO	frontier molecular orbital
HOMO	highest occupied molecular orbital
IR	Infrared
LUMO	lowest unoccupied molecular orbital
Me	methyl
MNDO	modified neglect of diatomic overlap
nmr	nuclear magnetic resonance
Ph	phenyl
R	organic substituent
t-Bu	tertiary butyl
thf	tetrahydrofuran

Contents

Chapter 1 A Brief review of the Chemistry of Dithianitronium Hexafluoroarsenate(V)

Chapter 2 Experimental Techniques

Chapter 3 Preparation and characterisation of some ortho- substituted dithiadiazolium salts

Chapter 4 Novel reactions of [SNS][AsF_6] with double bonds

Chapter 5 Reactions of [SNS][AsF_6] with single bonds

Chapter 1 A Brief Review of the Chemistry of Dithianitronium Hexafluoroarsenate(V)

The dithianitronium cation, $[SNS]^+$, is a versatile cycloaddition reagent, especially for the high-yield synthesis of carbon-sulphur-nitrogen heterocycles (see figure **1.2.**), and delocalised compounds containing other main group elements. It thus provides a convenient route to 1,3,2,4-dithiadiazolylium salts and their related free radicals. M.J.Schriver[1] and I.Lavender[2] have both extensively catalogued the chemistry of the dithianitronium cation in recent times, and this chapter is intended merely as a brief review of the chemistry of the most commonly used dithianitronium compound, $[SNS][AsF_6]$.

1.1. Preparation of dithianitronium salts

1.1.1. Introduction: the first dithianitronium salts

The first dithianitronium compound to be prepared was the hexachloroantimonate(V) salt, $[SNS][SbCl_6]$, synthesised by Gillespie and co-workers[3] in 1978 from the reaction of $SbCl_5$ with a number of SN reagents. The imido compounds S_7NH, 1,4-$S_6N_2H_2$ and S_7NBCl_3 all reacted with $SbCl_5$ in liquid SO_2 to give $[SNS][SbCl_6]$ in unspecified yields. The stoichiometries of the three reactions were not established with certainty, but they are believed to be as shown in equations **1.1.** to **1.3.**

$$S_7NH + 2SbCl_5 \xrightarrow{l.SO_2} [SNS][SbCl_6] + HCl + {}^5/_8\,S_8 + SbCl_3 \qquad \textbf{[Eq. 1.1.]}$$

$$1,4\text{-}S_6N_2H_2 + 4SbCl_5 \xrightarrow{l.SO_2} 2[SNS][SbCl_6] + 2HCl + {}^1/_4S_8 + 2SbCl_3 \qquad \textbf{[Eq.1.2.]}$$

$$S_7NBCl_3 + 2SbCl_5 \xrightarrow{l.SO_2} [SNS][SbCl_6] + {}^5/_8\,S_8 + BCl_3 \qquad \textbf{[Eq. 1.3.]}$$

The corresponding hexafluoroarsenate(V) salt, $[SNS][AsF_6]$, was first prepared via the reaction of $S_8[AsF_6]_2$ with sodium azide in liquid SO_2[4] (equation **1.5.**), with a yield of approximately 20%. The synthesis of the precursor, $S_8[AsF_6]_2$[5], is illustrated in figure **1.4.**, below.

$$S_8 + 3AsF_5 \longrightarrow S_8[AsF_6]_2 + AsF_3 \qquad \textbf{[Eq. 1.4.]}$$

$$S_8[AsF_6]_2 + NaN_3 \xrightarrow{l.SO_2} [SNS][AsF_6] + NaAsF_6 + {}^3/_4\,S_8 + N_2 \qquad \textbf{[Eq. 1.5.]}$$

The non-interacting nature of the $[AsF_6]^-$ anion facilitates the clean reaction of $[SNS][AsF_6]$ with organic nitriles, alkenes and alkynes (see section **1.3.1.**).

1.1.2. Synthetic routes to $[SNS][AsF_6]$

The low yield for the above reaction led researchers to develop a better, higher-yielding route to $[SNS][AsF_6]$ [6,7,8]. This route involved reacting S_4N_4 with AsF_5, sulphur and a trace of bromine, using liquid SO_2 as a solvent (equation **1.6.**). This reaction remains a standard preparative route to $[SNS][AsF_6]$ for those with facilities to handle AsF_5, and is routinely used to synthesise 10g - 20g of product.

$$S_8 + 2S_4N_4 + 12AsF_5 \xrightarrow{1.SO_2} 8[SNS][AsF_6] + 4AsF_3 \qquad \textbf{[Eq. 1.6.]}$$

Yields in excess of 75% were obtained using this method, and this was increased to 95% by washing with CH_2Cl_2[8]. Yields were also increased by washing with SO_2 / CCl_3F at -78°C [6], and by vacuum thermolysis at 250°C [9].

Although the syntheses shown above give excellent yields of high purity $[SNS][AsF_6]$, they do involve the use of hazardous reagents (S_4N_4 is explosive; AsF_5 is an extremely toxic gas). Thus a synthesis of $[SNS][AsF_6]$ that did not require such reagents was sought, and this was acheived by reacting $[SN][AsF_6]$ with sulphur[7] (equation **1.7.**).

$$1/8\ S_8 + [SN][AsF_6] \xrightarrow{1.SO_2} [SNS][AsF_6] \qquad \textbf{[Eq. 1.7.]}$$

This preparative method provoked initial interest, not least because $[SNS][SbCl_6]$ could be made by an analogous reaction[10]. Unfortunately, the yield was only 50% and $[SN][AsF_6]$ proved to be very moisture-sensitive.

In an attempt to devise a simpler preparative method, researchers[11] developed a synthetic route involving the *in situ* generation of [SN][X] salts from the appropriate silver salt and $(NSCl)_3$, followed by addition of a slight excess of SCl_2 to give the salt $[N(SCl)_2][X]$ (equation **1.8.**). These salts were then dechlorinated using $SnCl_2$ to yield the corresponding dithianitronium salt (equation **1.9.**).

$$AgX + 1/3\ (NSCl)_3 \xrightarrow{1.SO_2} [SN][X] \xrightarrow{1.SO_2} [N(SCl)_2][X] \qquad \textbf{[Eq. 1.8.]}$$

$$[N(SCl)_2][X] + SnCl_2 \xrightarrow{1.SO_2} [SNS][X] + SnCl_4 \qquad \textbf{[Eq. 1.9.]}$$

Many dithianitronium salts were made in this manner (see table **1.1.**), but the hexafluoroarsenate(V) salt is again produced in the highest yield. This route has the advantage of avoiding hazardous reagents, although the silver salts used tend to be expensive ($AgAsF_6$ is *ca.* £11/g.). To date, attempts to use cheaper alkali metal $[AsF_6]^-$ salts in place of $AgAsF_6$ have proved unsuccessful[12].

1.1.3. Other dithianitronium salts

Whilst $[SNS][AsF_6]$ is by far the most common dithianitronium compound used in synthesis; other dithianitronium salts, [SNS][X], have been prepared, as shown in table **1.1.**.

Table 1.1. Preparations of [SNS][X]

Anion $[X]^-$	Yield (%)	Reference(s)
AsF_6	95	**4,6,7,8,11**
$SbCl_6$	90	**3,11,13,14**
SbF_6	75	**11**
$AlCl_4$	86	**11,13**
$FeCl_4$	72	**11,15**
CF_3SO_3	70	**11,16**

1.2. Molecular orbital studies

M.J. Schriver[1] and I. Lavender[2] are amongst those who have previously performed molecular orbital calculations in order to determine the nature of the frontier orbitals of the $[SNS]^+$ cation. The symmetries of HOMOs and LUMO are illustrated in figure **1.1.** It should be noted that both HOMO and LUMO are doubly degenerate in the $[SNS]^+$ cation.

Molecular orbital studies were also carried out by the author .These calculations were performed using the MOPAC software[17] applied at the PM3 level. The S-N-S angle was set at 180°, as the $[SNS]^+$ cation is known to be linear, and both S-N distances were set at 1.510Å, the corrected distance obtained from the X-ray crystal structure of $[SNS][AsF_6]$[18]. The results obtained are compared with those of both Schriver and Lavender in table **1.2.**

Figure 1.1. The HOMO and LUMO of $[SNS]^+$

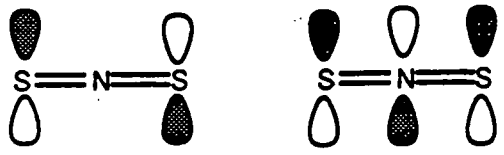

HOMO LUMO

Table 1.2. Molecular orbital data for the $[SNS]^+$ cation

Reference	HOMO orbital coefficients (p_z)	LUMO orbital coefficients (p_z)	Eigenvalues
1	(S1) +0.67 (S2) -0.67	(S1) +0.51 (S2) +0.51 (N) -0.38	HOMO -0.71 aU LUMO -0.39 aU
2	(S1) +0.71 (S2) -0.71	(S1) +0.55 (S2) +0.55 (N) -0.64	HOMO -15.69 eV LUMO -8.56 eV
This work	(S1) +0.71 (S2) -0.71	(S1) +0.55 (S2) +0.55 (N) -0.64	HOMO -15.71 eV LUMO -8.41 eV

References	Heat of Formation	S-N bond length Å	Software package
1	N/A	1.51	CNDO/2
2	258 kcal/mol	1.53	MNDO/PM3
This work	259 kcal/mol	1.51	MNDO/PM3

The results obtained from these calculations are in broad agreement with those of Haiduc and co-workers[19], but the PM3 data set assigns more electron density to the nitrogen atom in the LUMO. The LUMO orbital coefficient is greater for the nitrogen than for the sulphurs, which is as expected from a consideration of the relative electronegativities of the atoms,(though Schriver's calculations[1], show less electron density on the nitrogen than the sulphurs).

$[S=N=S]^+$ can be thought of as the most significant valence bond structure, as calculations using Nyburg's equation[1,20] correspond to a bond order of 2.10. However, it has also been claimed[3] that there is a considerable degree of triple bond character, because the bonds are shorter than for the isoelectronic species CS_2[21] (1.55 Å). Reaction takes place

chiefly at the sulphurs, due to their ability to form new bonds by expanding their valency. Assignments of the vibrational spectra of $[SNS][AsF_6]$ are given in table **1.3.**

Table 1.3. Vibrational spectra (cm^{-1}) of $[SNS][AsF_6]$ (From ref. 4)

IR	Raman	Assignment
1494 (m)		ν_3 $[SNS]^+$
1088 (w)		$\nu_1+\nu_2$ $[SNS]^+$
818 (w)		$[AsF_6]^-$
	798 (18, br)	$2\nu_2$ $[SNS]^+$
	779 (3)	$2\nu_2$ $[^{32}SN^{34}S]^+$
697 (vs)		ν_3 $(T_1u)[AsF_6]^-$
	696 (100)	ν_1 $[SNS]^+$
	682 (30)	ν_1 $(A_1g)[AsF_6]^-$
	573 (8)	ν_2 $(Eg)[AsF_6]^-$
391 (s)		ν_4 $(T_1u)[AsF_6]^-$
	368 (10)	ν_5 $(T_2g)[AsF_6]^-$

Note : IR spectra recorded as nujol mulls, raman spectra as solids.

1.3. The reactions of $[SNS][AsF_6]$

1.3.1. Reactions with inorganic materials

As $[SNS]^+$ is an unsaturated, electrophilic cation with a low-lying LUMO and terminal sulphur atoms that can readily expand their valency, it should react with nucleophilic, electron-rich inorganics. Passmore and co-workers[22,23] have studied the reactions of $[SNS][AsF_6]$ with halogens, halogenating agents, halides, azides and S_4N_4. The reactions of $[SNS][AsF_6]$ with NSF[24] and $[SNS][AsF_6]$ with $(NSCl)_3$[25], have also been observed. In all cases it is the sulphur atoms of $[SNS]^+$ that are directly involved in reaction, and the SNS fragment is preserved.

1.3.2. Reactions of $[SNS][AsF_6]$ with organic materials

The first reactions of $[SNS][AsF_6]$ studied were those with alkynes and nitriles, observed in 1983. Acetonitrile gave 5-methyl-1,3,2,4-dithiadiazolylium hexafluoroarsenate(V) on reaction with $[SNS][AsF_6]$[26], and ethyne and propyne yielded the corresponding 1,3,2-dithiazolium hexafluoroarsenate(V) salts[26]. Three years later the reactions of $[SNS][AsF_6]$ with the alkenes trans-but-2-ene and norbornene were studied by Passmore and co-workers[27]. All the above reactions gave novel

products in high yields, illustrating the utility of $[SNS][AsF_6]$ as a synthetic reagent. The generalised reaction schemes for $[SNS][AsF_6]$ with nitriles, alkynes and alkenes are shown in figure **1.2.**, below.

Figure 1.2. The reaction of $[SNS]^+$ with nitriles, alkynes and alkenes

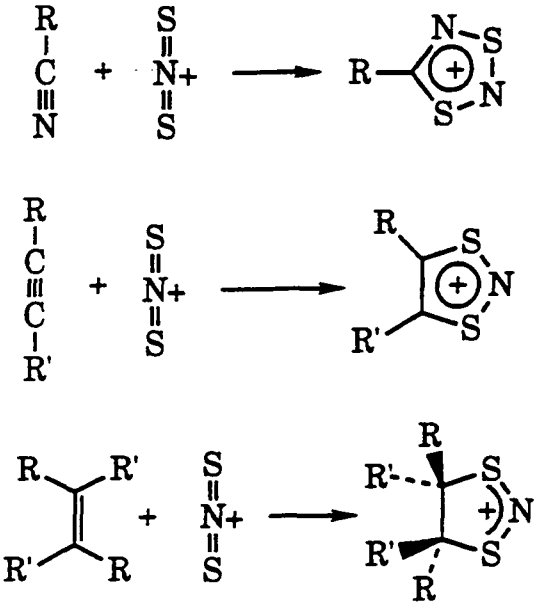

1.3.2.1. General reactivity towards organic compounds

The frontier molecular orbitals for $[SNS]^+$ and the various unsaturated systems ($RC{\equiv}N$, $R_2C{=}CR_2$ and $RC{\equiv}CR$) are shown in figure **1.3.** In general these cycloadditions are believed[28] to proceed predominantly by electron density transfer from the HOMO of the unsaturated species to the LUMO of $[SNS]^+$ (which is at a very low energy compared with the dienes encountered in organic synthesis).This occurs readily for $[SNS]^+$ (unlike to neutral SN heterocycles[29]) as it is cationic and can accept electron density into its low-lying LUMO from the HOMO of the unsaturated organic compounds. Kinetic studies[30] have shown that the reactions of $[SNS][AsF_6]$ with alkynes and nitriles are second order overall, being first order with respect to both reactants. It was also noted that reaction rates increased with an increase in the HOMO-LUMO energy gap, which is expected if the matching of frontier orbitals is considered.

Figure 1.3. The FMOs of $[SNS]^+$, $R_2C{=}CR_2$, RC≡CR and RC≡N

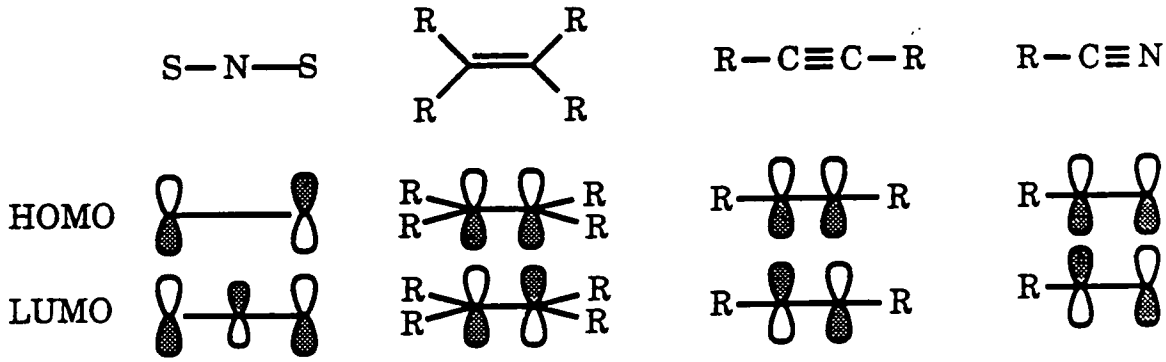

Furthermore, the quantitative reaction of $[SNS][AsF_6]$ with N≡C-C≡C-H occurs in 1:1 stoichiometry only[30], reacting solely with the C≡C moiety. This is as expected, because the lowering of energy of the HOMO in the 1:1 mono-adduct, increases the HOMO-LUMO energy gap thus deactivating the intermediate with respect to further $[SNS]^+$ addition (Ionisation energies: 11.60 eV for C≡C and 14.03 eV for C≡N). Figure **1.4.** illustrates this reaction.

Figure 1.4. The Reaction of $[SNS][AsF_6]$ with N≡C-C≡CH

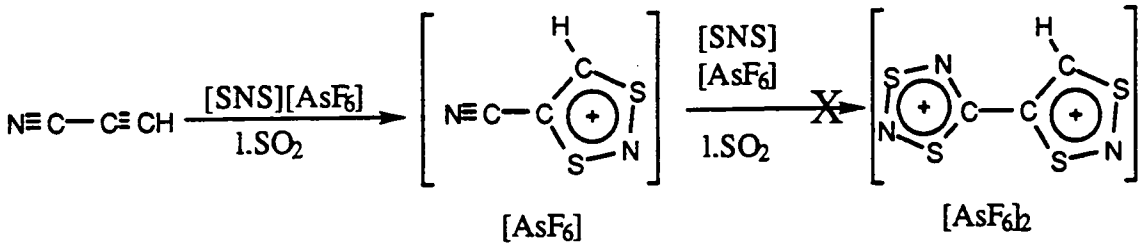

Such specificity of $[SNS]^+$ towards a particular functional group is of great synthetic importance and side reactions are minimised. For example, the addition of further $[SNS][AsF_6]$ to the 1:1 adduct of $[SNS][AsF_6]$ with potassium tricyanomethanide[8] occurs at the C≡N groups only, and not at the C=C functionality.

It can thus be seen that $[SNS][AsF_6]$ is a highly versatile reagent for heterocyclic synthesis, chiefly due to the properties listed below:

1. *Novelty.* $[SNS][AsF_6]$ often provides the only synthetic pathway to new compounds and, indeed, new families of compounds.

2. *High yields.* For most reactions yields are >80%, and for many they are quantitative

3. *Specific.* There are very few side reactions, and the reactivity of a particular functionality can generally be predicted.

One of the few disadvantages of these reactions is that they require a polar aprotic solvent (*eg.* SO_2), so tetrahydrofuran and alcohols cannot be used[31].

1.3.2.2. Reactions with alkenes

[SNS][AsF_6] undergoes a wide range of quantitative reactions with alkenes in liquid SO_2[27], as mentioned previously. The intermediate 1:1 cycloaddition compound, [RR'CSNSCRR']$^+$, can behave in a similar way to [SNS]$^+$, reacting with alkenes and alkynes[1] (see figure **1.5.**), but not with the less reactive nitrile moiety[1]. This reactivity is due to the fact that the LUMO of [RR'CSNSCRR']$^+$ is of similar energy and geometry to that of [SNS]$^+$ itself. Alkenes also undergo analogous reactions with the chlorinated derivative of the dithianitronium cation, [ClSNSCl]$^+$, but with the exception of ethene, yields are lower[32] than for reaction with [SNS]$^+$.

Figure 1.5. Reactions of [RR'CSNSCRR']$^+$ with unsaturated organic compounds

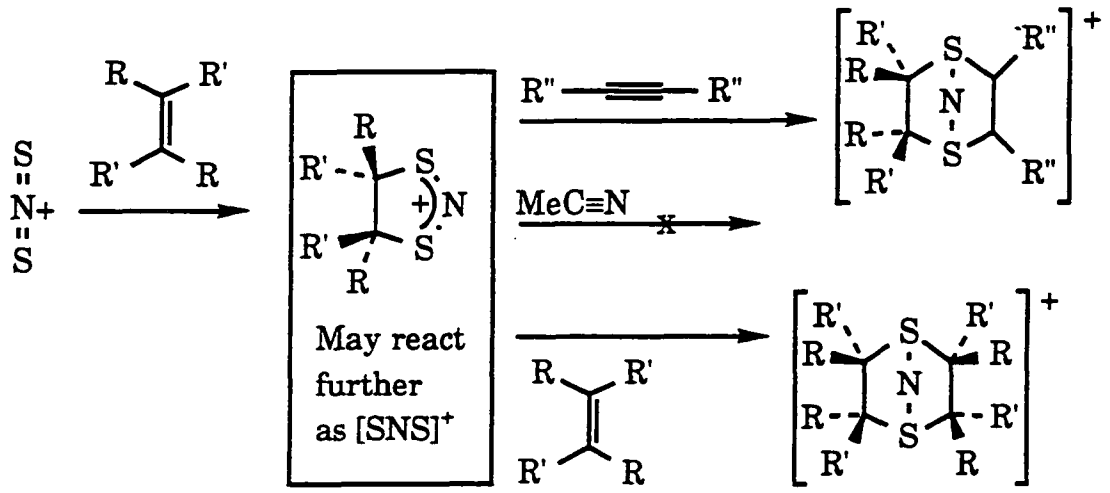

1.3.2.3. Reactions with nitriles

[SNS][AsF_6] reacts with a large range of nitrile-containing organic compounds, including multi-nitriles[8]. Researchers at Durham[33] used a wide variety of *para*-substituted benzonitrile derivatives (see table **1.4.**) in order to prepare the corresponding 1,3,2,4-dithiadiazolylium salts. The cations are readily reduced to give the corresponding dithiadiazolyl free-radicals[34], which although photolytically stable in the solid state are thermally unstable solids[35] and photolytically rearrange in solution to give the corresponding 1,2,3,5-isomer[34]. The syntheses and characterisations of the analogous *ortho*- systems are discussed in Chapter **3** of this work.

Table 1.4. Preparation of some *para*-[X-C_6H_4-CN_2S_2][AsF_6] salts.

X	Yield (%)
CF_3	83%
Br	80%
MeS	86%
MeO	70%
CH_3	87%

These materials and their selenium analogues are the subject of recent interest as potential molecular magnets[36] and conductors[37,38].

1.3.2.4. Reactions with alkynes

The majority of reactions between [SNS][AsF_6] and alkynes are quantitative, as are the reactions between alkynes and $[ClSNSCl]^+$. These further illustrate the synthetic utility of [SNS][AsF_6] and are summarised in table **1.5.**, below.

Table 1.5. The reactions of [SNS][AsF_6] with alkynes

R	R'	Yield (%)	Reference
H	H	100	39
H	Me	94	39
Me	Me	N/A	1
CF_3	CF_3	95	40
$SiMe_3$	$SiMe_3$	100	25
CO_2Me	CO_2Me	95	1
H	CF_3	100	1
H	CN	96	29

1.3.2.5 Reactions with other multiple bonds

In principle, $[SNS]^+$ can react with a wide range of multiple bonds, provided the LUMO - HOMO energy gap is not too high.The reaction of [SNS][AsF_6] with R-C≡P[41] has recently been established, and there are suggestions that [SNS]+ may also react with Ar-N=S=O[16] and R-N≡C[12]. In Chapter 4 of this work the reactions of [SNS][AsF_6] with N=N, P=P, P=N and C=N are described.

1.5. References

1. M.J. Schriver, PhD Thesis, University of New Brunswick, 1988.

2. I. Lavender,.PhD Thesis, University of Durham, 1992.

3. R. Faggiani, R.J. Gillespie, C.J.L. Lock and J.D. Tyler, *Inorg. Chem.*, 1978, **17**, 2975.

4. A.J. Banister, R.G. Hey, G.K. MacLean and J. Passmore, *Inorg. Chem.*, 1982, **21**, 1679.

5. C.G. Davies, R.J. Gillespie, J.J. Park and J. Passmore, *Inorg. Chem.*, **10**, 1971, 2781.

6. E.G. Awere and J. Passmore, *J. Chem. Soc., Dalton Trans.*, **1992**, 1343.

7. A. Apblett, A.J. Banister, D. Biron, A.G. Kendrick, J.Passmore, M.J. Schriver and M. Stojanac, *Inorg. Chem.*, 1986, **25**, 4451.

8. A.J. Banister, I. Lavender, J.M. Rawson and W. Clegg, *J. Chem. Soc., Dalton Trans.*, **1992**, 859.

9. Z.V. Hauptman, unpublished results.

10. R. Hey, PhD Thesis, University of Durham, 1980.

11. B. Ayres, A.J. Banister, P.D. Coates, M.I. Hansford, J.M. Rawson, C.E.F. Rickard, M.B. Hursthouse, K.M.A. Malik and M Motevalli,*J. Chem. Soc., Dalton Trans.*, **1992**, 3097.

12. J.M. Rawson, unpublished results.

13. A.J. Banister and J.M. Rawson, *J. Chem. Soc., Dalton Trans.*, **1990**, 1517.

14. A.J. Banister and A.G. Kendrick, *J. Chem. Soc., Dalton Trans.*, **1987**, 1565.

15. U. Thewalt, K. Berhalter and P. Müller, *Acta. Cryst.*, 1982, **B38**, 1280.

16. M.I. Hansford, PhD Thesis, University of Durham, 1989.

17. (a) J.J.P. Stewart, No. 445 (MOPAC) Quantum Chemistry Program Exchange, 1984. (b) M.J.S. Dewar and W.J. Thiel, *J. Am. Chem. Soc.*, 1977, **99**, 4899. (c) PM3 parameters for C,H,N and S, J.J.P. Stewart, *J. Comp. Chem.*, 1989, **10**, 209.

18. A.J. Banister, A.G. Kendrick, J.P. Johnson, J. Passmore and P.S. White, *Acta. Cryst.*, 1987, **C43**, 1651.

19. I. Silaghi-Dumitrescy and I. Haiduc, *J. Mol. Struc, Theochem.*, 1984, **106**, 217.

20. S.C. Nyburg and C.H. Faerman, *Acta Cryst.*, 1985, **B41**, 274.

21. A.H. Guenther, T.A. Wiggins and D.H. Rank, *J. Chem. Phys.*, 1958, **28**, 682.

22. W.V.F. Brooks, G.K. MacLean, J. Passmore, P.S. White and C.M. Wong, *J. Chem. Soc., Dalton Trans.*, **1983**, 1961.

23. G.K. MacLean J. Passmore and P.S. White, *J. Chem. Soc., Dalton Trans.*, **1984**, 211.

24. A.G. Kendrick, PhD Thesis, University of Durham, 1986.

25. S. Parsons, J. Passmore, M.J. Schriver and X. Sun, *Inorg. Chem.*,1991, **30**, 3342.

26. G.K. MacLean, J. Passmore, M.J. Schriver, P.S.White, D. Bethell, R.S. Pilkington and L.H. Sutcliffe, *J. Chem. Soc., Chem. Commun.*, **1983**, 807.

27. N. Burford, J.P. Johnson, J. Passmore, M.J. Schriver and P.S. White, *J. Chem. Soc., Chem. Commun.*, **1986**, 966.

28. A.W. Cordes, S.W. Liblong, M.C. Noble and R.T. Oakley, *Can. J. Chem.*, 1983, **61**, 2062.

29. R. Jones, J.L. Morris, C.W. Rees and D.J. Williams, *J. Chem. Soc., Chem. Commun.*, **1985**, 1654.

30. S. Parsons, J. Passmore, M.J. Schriver and P.S. White, *J. Chem. Soc., Chem. Commun.*, **1991**, 369.

31. A.W. Luke, PhD Thesis, University of Durham, 1992.

32. S. Parsons, J. Passmore, M.J. Schriver and P.S. White, *Can. J. Chem.* , 1990, **68**, 852.

33. C.M. Aherne, A.J. Banister, A.W. Luke, M.I. Hansford, Z.V. Hauptman and J.M. Rawson, *J. Chem. Soc., Dalton Trans.*, 1993, 697.

34. N. Burford, J. Passmore and M.J. Schriver; *J. Chem. Soc., Chem. Commun.*, **1986**, 140.

35. (a) C.M. Aherne, A.J. Banister, A.W.Luke, J.M. Rawson and R.J. Whitehead; *J. Chem. Soc., Dalton Trans.*, **1992**, 1277.
(b) W.V. Brooks, N. Burford, J. Passmore, M.J. Schriver and L.H. Sutcliffe, . *Chem. Soc., Chem. Commun.*, **1987**, 69.

36. A.J. Banister, I. Lavender, J.M. Rawson, W. Clegg, B.K. Tanner and R.J. Whitehead, *J. Chem. Soc., Dalton Trans.*, **1993**, 1421.

37. M.P. Andrew, A.W. Cordes, D.C. Douglas, R.M. Fleming, S.H. Glarum, R.C. Haddon, P. Marsh, R.T. Oakley, T.T.M. Palstra, L.F. Schneemeyer, G.W. Trucks, R. Tycho, J.V. Waszczak, K.M. Young and N.M. Zimmerman, *J. Am. Chem. Soc.*, 1991, **113**, 3559.

38. A.W. Cordes, R.C. Haddon, R.G. Hicks, R.T. Oakley, T.T.M. Palstra, L.F. Schneemeyer and J.V. Waszczak, *J. Am. Chem. Soc.*, 1992, **114**, 1729.

39. G.K. McLean, J. Passmore, M.N.S. Rao, M.J. Schriver, P.S. White, D. Bethell, R.S. Pilkington and L.H. Sutcliffe, *J. Chem. Soc., Dalton Trans.*, **1985**, 1405.

40. E.G. Awere, N. Burford, C. Mailer, J. Passmore, M.J. Schriver, P.S. White, A.J. Banister, H. Oberhammer and L.H. Sutcliffe, *J. Chem. Soc., Chem. Commun.*, **1987**, 66.

41. Y-L. Chung, S.A. Fairhurst, D.G. Gillies, K.F. Preston and L.H. Sutcliffe, *Mag Res. Chem.*, 1992, **30**, 666.

Chapter 2 Experimental Techniques

2.1. General techniques

All of the compounds synthesised in the course of this work are moisture-sensitive, although some are reasonably stable in dry air. Hence, inert atmosphere techniques are required and these have been rigorously employed during this work.

All air- and moisture-sensitive materials were handled under dry nitrogen in a Vacuum Atmospheres HE43-2 glove box fitted with an HE493 Dri-Train. All glassware was oven dried overnight at *c.* 130°C before use. Most reactions required standard vacuum-line methods and oxygen free nitrogen (BOC white spot, further dried by passage through a P_4O_{10} column) as the inert gas. Liquid sulphur dioxide was handled on a Monel vacuum line (fitted with stainless steel and Monel 'Whitey' taps (IKS4), themselves fitted with teflon compression ferrules).This apparatus was designed and built by Dr Z.V.Hauptman of the Department of Chemistry.

2.2. Specialised apparatus

2.2.1 The "Dog"

This is a twin-bulbed reaction vessel incorporating a glass sinter in the horizontal tube connecting the two legs, (shown in figure **2.1.**). Teflon vacuum taps (J. Young Co.) enable this apparatus to be used for all reactions incorporating liquified gases (*eg* SO_2). The $^1/_4$ - inch tubing allows connection to the Monel vacuum line via Swagelok Teflon compression fittings or alternatively to the double-manifold line via a suitable glass adapter and Swagelok fitting. Solid material was recovered from either bulb after scoring with a glass knife, followed by breaking the bulb off in the glove box. The fragments were then cleaned, reassembled and annealed.

2.2.2 The closed extractor

This apparatus (shown in figure **2.2.**) was designed by Dr Hauptman and is based on the more common Soxhlet extractor. The Teflon vacuum tap and closed design allow the apparatus to be used for extractions involving liquid sulphur dioxide as well as with less volatile solvents (*eg.* n-pentane; acetonitrile). A partial vacuum may be applied, enabling low temperature operation. The bulb was usually warmed in a water bath, and the solvent condensed onto the solid in the cooling jacket. Solid material obtained after extraction was recovered from the bulb in a manner similar to that described above.

Figure 2.1. The twin-bulbed reaction vessel or 'dog'

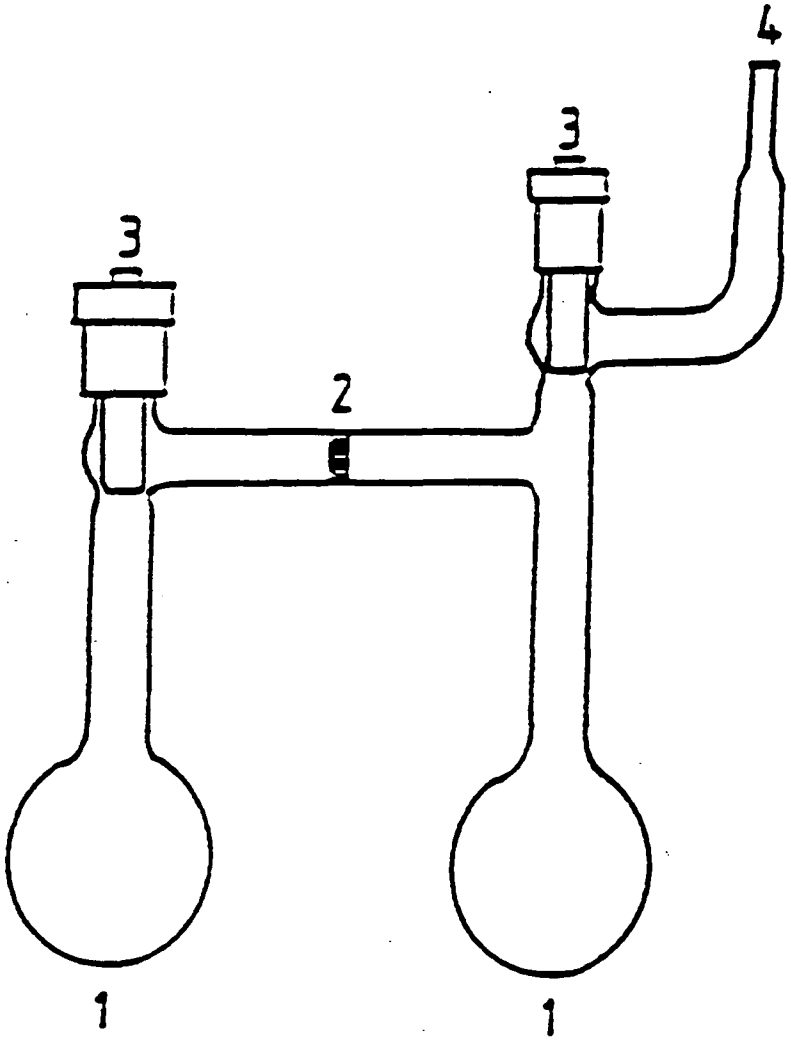

1. Reaction bulb.
2. Glass sinter (usually porosity grade 3).
3. J. Young teflon tap.
4. ¼" ground glass.

Figure 2.2. The closed extractor

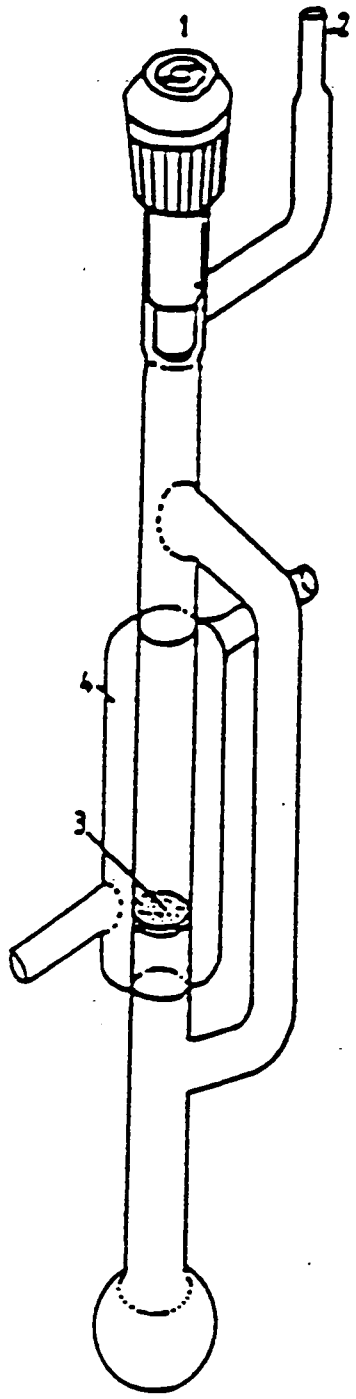

1. J. Young teflon tap.
2. ¼" Ground glass.
3. Glass sinter (usually porosity grade 3).
4. Cooling jacket.

2.3 Temperature control

Reactions were carried out at room temperature unless otherwise stated. Where necessary water baths were used to maintain reactions at a constant temperature.

For slow heating and cooling of a solution, as in the 'ripple' technique of crystal growth[1], a Haake F2 circulator with methylated spirit coolant, and a Haake PG10 programmer were used. This afforded controlled cycling between *ca.* -40°C and +40°C.

2.4. Physical methods [Operator(s) in brackets]

2.4.1. Infrared spectroscopy

Infrared spectra were recorded as Nujol mulls between KBr plates unless otherwise indicated. Spectra were recorded using either Perkin-Elmer 577 or 457 grating infrared spectrophotometers, or Perkin-Elmer FT 1720X or 1600 FTIR spectrophotometers. For all moisture-sensitive samples, mulls were made up in the glove box and the plates sealed in a brass holder. The Nujol was stored over sodium in the glove box.

2.4.2 Nuclear magnetic resonance spectrometry (NMR) [Mrs J.M. Say]

NMR spectra were recorded on Varian VXR400S (^{31}P ^{19}F and ^{13}C), Bruker AC250 MHz (^{1}H) and AMX 500 MHz (^{13}C) spectrometers.

2.4.3. Differential scanning calorimetry (DSC)

DSC measurements were carried out using a Mettler FP80 control unit coupled to a Mettler FP85 thermal analysis cell and a Fisons y-t chart recorder. An Opus PC III computer (with a dsc analysis program written by Dr J.M.Rawson) coordinated the apparatus. Samples were cold-sealed in aluminium sample pans in the glove box.

2.4.4. Mass spectrometry [Dr M. Jones, Miss L.M. Turner]

Spectra were recorded on a VG Analytical 7070E spectrometer using electron-impact (E.I.), chemical-ionisation (C.I.) or fast atom bombardment (FAB) techniques. All FAB samples were dissolved in a matrix of tetraglyme and dibenzo-18-crown-6 (*c.* 1:1 molar ratio).

2.4.5. Elemental analyses.

Carbon, hydrogen and nitrogen analyses were performed by Mrs J. Dostal and Miss J. Magee on a Carlo Erba 1106 Elemental Analyser. All other analyses were performed by Mr R. Coult or Miss Magee.

2.5. Electrochemical techniques

2.5.1. General procedures

A steady potential difference was maintained by a Ministat precision potentiostat, supplied by H.G. Thompson Associates, Newcastle upon Tyne. The cyclic voltammograms were recorded using a Bioanalytical Systems type CV-113 potential wave generator and a Linseis type LY1710Q x-y chart recorder.

Before use, the reference electrode was checked against the saturated standard calomel electrode. Connection was via a salt bridge (0.1M $[Bu_4N][BF_4]$ solution in acetonitrile) and the potential difference was measured with a Thandar TM351 digital multimeter.Acetonitrile was the only solvent used for electrochemical work, and a separate supply of purified acetonitrile (see section **2.7.1.**) was retained for this purpose.

2.5.2 Cyclic voltammetry

This was carried out in a 3-limbed undivided cell[2] with a bulb volume of *ca.* 15 ml. Each limb allowed the use of an electrode via modified Swagelok connectors which also provided an air-tight seal. The apparatus used a reference electrode, a working electrode and an auxiliary electrode, all of which were designed by Dr Z.V.Hauptman. The cell is shown in figure **2.3.**.

The reference electrode

This is of the Ag / Ag^+ type previously reported[3] (see figure **2.4.**). This electrode maintains a steady potential for a period of several months and is dependent on room temperature, and not the temperature of the surrounding solution.

The working electrode

This consists of a polished platinum disc mounted in FEP tubing and connected to a $^1/_4$-inch steel bar.

The auxiliary electrode

This consists of a platinum coil connected to a monel bar via two holes which allow the bar to be slotted through a connecting sheet.

Figure 2.3 The cyclic voltammetry cell showing the modified Swagelok glass to metal connector (insert).

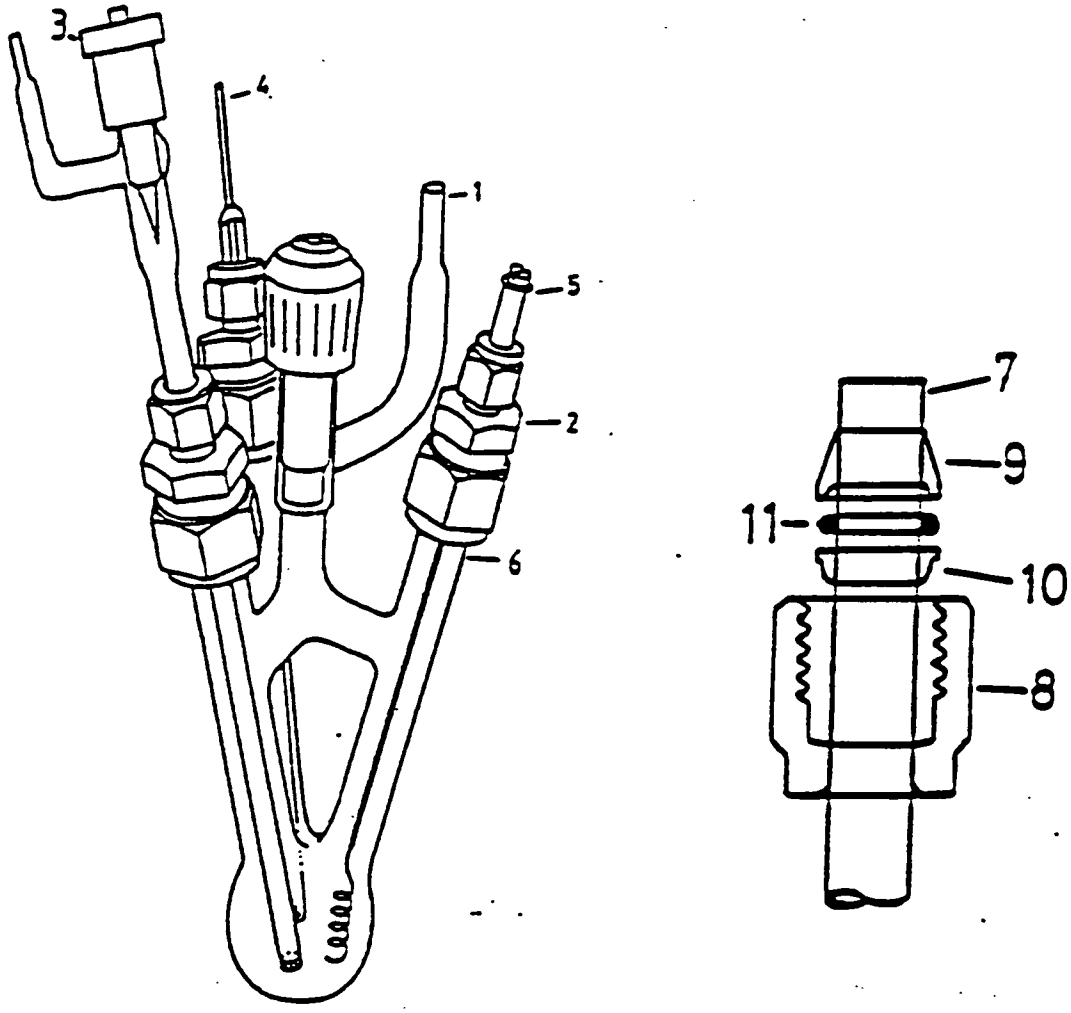

1. 1/4" Ground Glass connection.
2. Swagelock 1/2" to 1/4" reducing union.
3. Reference electrode.
4. Platinum microelectrode.
5. platinum Auxiliary electrode.
6. 1/2" precision O.D. smooth glass.
7. Same as 6.
8. Compression nut.
9. Front ferrule.
10. Back ferrule (reversed).
11. PTFE "O" ring.

Figure 2.4 The Ag / Ag^+ reference electrode

1. Pyrex sinter porosity no.4.
2. 1/4" O.D. smooth glass for air tight Swagelok connection.
3. 0.1M $AgBF_4$ solution in MeCN.
4. Ag metal attched to central through rod.
5. Knife edge to 4. for a tight seal against teflon tap.
6. PTFE stem of Youngs' greaseless tap.
7. Side arm of Youngs' tap down to 1/4" ground glass.
8. Brass ring around PTFE stem to prevent yielding through axial compression.
9. Washer.
10. Stainless steel (or Monel rod). 1/8" diameter, with 5BA thread both ends centrally bored through PTFE stem.

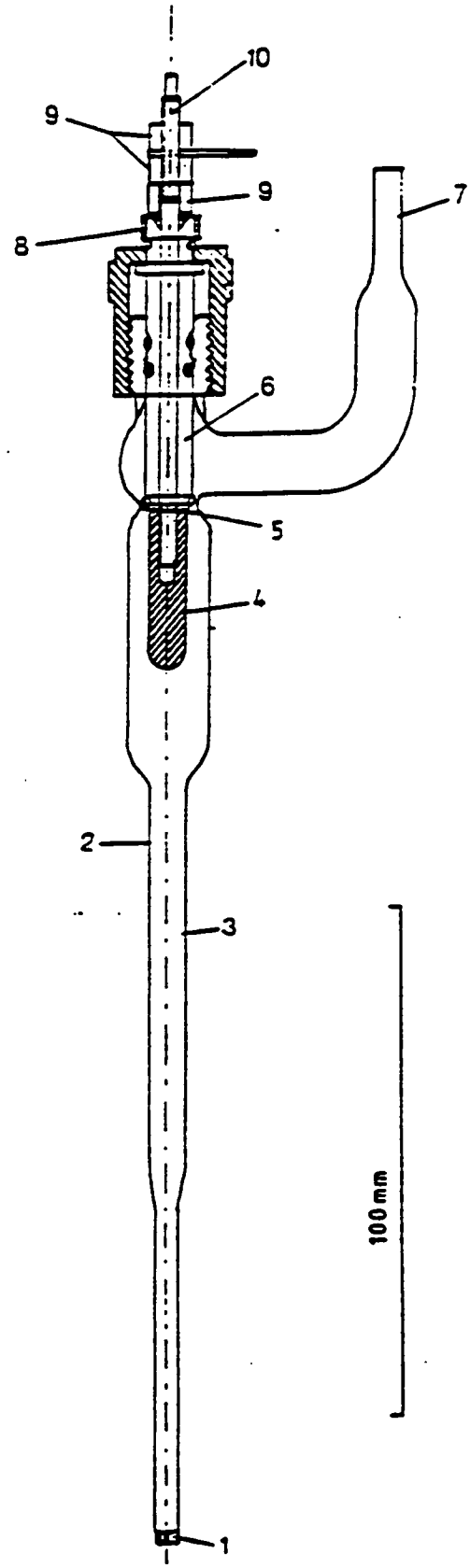

2.6. Single crystal X-ray structure determination.

X-ray structure determination was carried out at the University of Newcastle-upon-Tyne by Dr W. Clegg on a Siemens AED2 diffractometer with a graphite monochromator using MoK_α radiation (λ = 0.71073Å). A ω–θ scan mode was used for data collection with appropriately chosen scan width and time. Programs (SHELTXL, SHELXS[4] and local software[5]) were run on a Data General model 30 computer.

2.7. Chemicals and solvents

2.7.1. Purification of solvents

Acetonitrile (Aldrich HPLC Grade) was dried by refluxing over CaH_2 under an atmosphere of dry nitrogen, followed by distillation (with filtration through a glass column packed with pre-dried Al_2O_3) into clean dry flasks, where it was degassed via freeze-thaw cycles, and then stored under dry nitrogen.

Dichloromethane was dried by distillation from CaH_2 into dry flasks under an atmosphere of dry nitrogen.

Benzene was dried by standing over CaH_2 for seven days, and stored over a molecular sieve.

Toluene was dried by refluxing over lump sodium, followed by distillation under an atmosphere of dry nitrogen onto fresh sodium wire in clean dry flasks.

n- Hexane was dried by refluxing over P_4O_{10}, followed by distillation under an atmosphere of dry nitrogen and degassing by freeze-thaw cycles.

n- Pentane was dried by refluxing over P_4O_{10}, followed by distillation under an atmosphere of dry nitrogen and degassing by freeze-thaw cycles.

Tetrahydrofuran (thf) was purified by fractional distillation from sodium under an atmosphere of dry nitrogen, and stored over sodium wire. It was supplied by Mr B. Hall of the Department of Chemistry.

Sulphur dioxide (BDH GPR Grade) was dried by standing over P_4O_{10} for one week, followed by distillation onto CaH_2 at least 24 hrs before use. It was vacuum transfered onto the solutes at -78°C and used as a liquified gas in either a 'dog' or closed extractor (see sections **2.2.1.** and **2.2.2.**).

Deuterated solvents (Aldrich): CD_3CN was stored over pre-dried magnesium sulphate (ca 130°C, 48 hrs.) and used under an atmosphere of dry nitrogen. CD_2Cl_2, and DMSO-*d*8 were used without further purification under an atmosphere of dry nitrogen

2.7.3. Preparation of starting materials

Dithianitronium Hexaflurorarsenate(V) was prepared according to the literature route[6], with slight modifications[7]. The crude product was washed with dry dichloromethane to remove any residual AsF_3 and coloured impurities. The pure product was pale yellow in colour.

$[Pr_4N]N_3$ was prepared by Dr I.Lavender using the method devised by Dr C.J.Ludman [8].

$[Pr_4N][S_3N_3]$ was prepared via a slightly modified literature method[8,9].

2.8. References

1. A.V. Shubnikov, *Z. Krystallog.* 1914, **54**, 261.

2. A.J. Banister, Z.V. Hauptman and A.G. Kendrick, *J. Chem. Soc., Dalton Trans.*, **1987**, 915.

3. B. Ayres, A.J. Banister, P.D. Coates, M.I. Hansford, J.M. Rawson, C.E.F. Rickard, M.B. Hursthouse, K.M.A. Malik and Majid Motevalli, *J. Chem. Soc., Dalton Trans.*, **1992**, 3097.

4. SHELXS-86 - Program for Crystal Structure Determination. G.M. Sheldrick, University of Göttingen, 1986. SHELX-76 - Program for Crystal Structure Determination. G.M. Sheldrick. University of Göttingen, 1976.

5. W. Clegg, *Acta. Cryst. Sect. A,* 1981, **37**, 22.

6. A.J. Banister, R.G. Hey, G.K. MacLean and J. Passmore, *Inorg. Chem.* 1982, **21**, 1679.

7. A.J. Banister, I. Lavender, J.M. Rawson and W. Clegg, *J. Chem. Soc., Dalton Trans.*, **1992**, 859.

8. S.T. Wait, Ph.D. Thesis, University of Durham, 1989.

9. J. Bojes and T. Chivers, *Inorg. Chem.*, 1978, **17**, 188.

Chapter 3: Preparation and characterisation of some *ortho*-substituted dithiadiazolium salts

3.1. Introduction

Dithiadiazolium salts, $[RCNSSN]^+[X]^-$ (1,2-disulphur) and $[RCNSNS]^+[X]^-$ (1,3-disulphur), have attracted much recent interest as the precursors to a vast array of stable, 7π heterocyclic radicals, designated dithiadiazolyls[1,2]. The nomenclature of dithiadiazolium cations is illustrated in figure **3.1.1.**

Figure 3.1.1. Dithidiazolium cation nomenclature

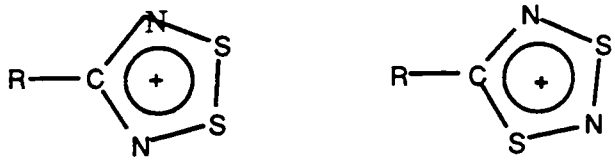

1,2,3,5-Dithiazolium cation 1,3,2,5-Dithiazolium cation

The 1,3-dithiadiazolium cations are usually prepared as the $[AsF_6]^-$ salt using $[SNS][AsF_6]$ as discussed in Chapter 1, whilst the 1,2-dithiadiazoles can be prepared as the chloride by a standard literature method[3]. $[RCNSNS][AsF_6]$ can be easily metathesised to the chloride[4]. As the chloride, both the 1,2- and 1,3-dithiadiazolium cations can be reduced to their corresponding radicals using silver[5], Ph_3Sb[6] or Zn/Cu couple[7]. The 1,2-dithiadiazolyl radicals are stable in the absence of moisture, but the 1,3-dithiadiazolyls rearrange[8] at room temperature to their 1,2-analogues via the mechanism shown in scheme **3.1.1.**. Diselenium analogues of the 1,2-cation and the 1,2 radical are also known[9,10].

Nearly all of these dithiadiazolyl (and diselenadiazolyl) radicals are stabilised in the solid state by dimeric interactions as shown in figure **3.1.2.**, the known exception being *para*-$[(NC)C_6F_4CNSSN]\cdot$ [11].

Scheme 3.1.1. The rearrangement of 1,3-dithiadiazolyls

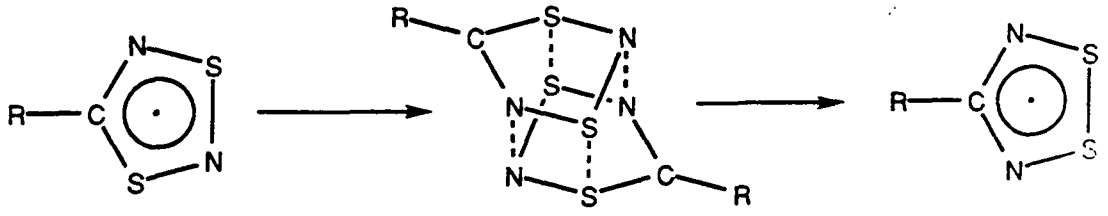

The stability of these radicals has excited interest in their potential use as organic magnets[12]. Di-[13,14] and tri-[15] substituted phenyl rings have been reported, including mixed sulphur/selenium systems[16,17]. Disubstituted dithiadiazolyls are currently under examination as materials for non-linear optics[18].

Figure 3.1.2. Sulphur-sulphur interactions in $(RCNSSN)_2$

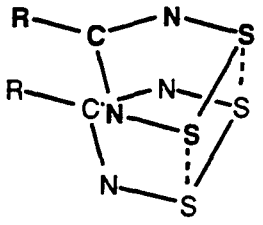

Comparatively little work has been carried out on *ortho*-substituted dithiadiazole systems. The only previously reported syntheses of *ortho*-substituted dithiadiazoles are those of the *ortho*-fluoro and *ortho*-methyl 1,3-cations prepared by Dr Anthony Luke[19]. The intention of the work described in this chapter was to study a series of *ortho*-halogenated dithiadiazoles in order to investigate the interaction of the halogen with the closest sulphur atom, (see figure **3.1.3.**) and to examine what effects this interaction, combined with steric effects, has on the degree of coplanarity of the phenyl and dithiadiazolium rings.

Figure 3.1.3. Sulphur-halogen interaction in *ortho*-halogenated 1,3-dithiadiazoles

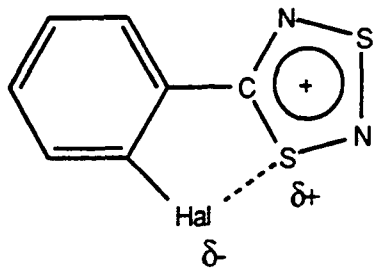

This opened up the possibility of unusual stacking patterns in the solid state, with potentially important consequences for magnetic and optical properties. Another reason for studying these systems was to examine the inductive effects of various *ortho-* substituents on the dithiadiazolium ring.

3.2. Results and discussion

3.2.1. The reaction of [SNS][AsF_6] with *ortho*-bromobenzonitrile

Reaction of [SNS][AsF_6] with ortho-bromobenzonitrile in liquid SO_2 over 18 hours gave 5-(2-bromophenyl)-1,3,2,4-dithiadiazolium hexafluoroarsenate(V), **1**, in 76.2 % yield, as shown in scheme **3.2.2.**. The product, a yellow-green solid, was soluble in SO_2. Comparison of an IR spectrum of **1** with an IR spectrum of *ortho*-bromobenzonitrile showed that the CN peak at 2225 cm^{-1} had disappeared, whilst a strong, broad AsF_6^- peak (701 cm^{-1}) was present in the product. Additional peaks in the region 1400 cm^{-1} to 700 cm^{-1} (namely at 1213, 915, 794 and 780 cm^{-1}) in the spectrum of **1** may be attributed to the dithiadiazolium ring.

Whilst it would be very difficult to assign all these new peaks with absolute certainty, it seems reasonable to assume that the peak at 1213 cm^{-1} is attributable to the C-N bond in the dithiadiazolium ring. It should also be noted that the *ortho*-chloro- and *ortho*-fluoro-substituted dithiadiazolium salts show new peaks at 916 cm^{-1} and 917 cm^{-1} respectively, compared to the new peak at 915 cm^{-1} in **1**, suggesting that the peaks correspond to virtually identical bonds in the three compounds, probably one of the ring S-N bonds. Furthermore, it is important to note that the four new peaks given for **1** may not total number of new peaks; others may be masked by separate peaks, or be too weak to positively identify. Other peaks present in the spectrum of the starting material are also present in the product spectrum, but shifted between 1 and 8 wavenumbers in position.

The mass spectrum (E.I.) of **1** showed a good breakdown pattern for a 1,3-dithiadiazolium cation (see scheme **3.2.1.**) considering that AsF_6^- salts are usually highly involatile. Excellent chemical analysis figures (C,H,N). were obtained. Single crystals of **1** were grown from SO_2 solution over a period of 7 days using the ripple technique discussed in Chapter 2.

Scheme 3.2.1. Mass spectral breakdown pattern (E.I.) of *ortho*-$[BrC_6H_4CNSNS][AsF_6]$

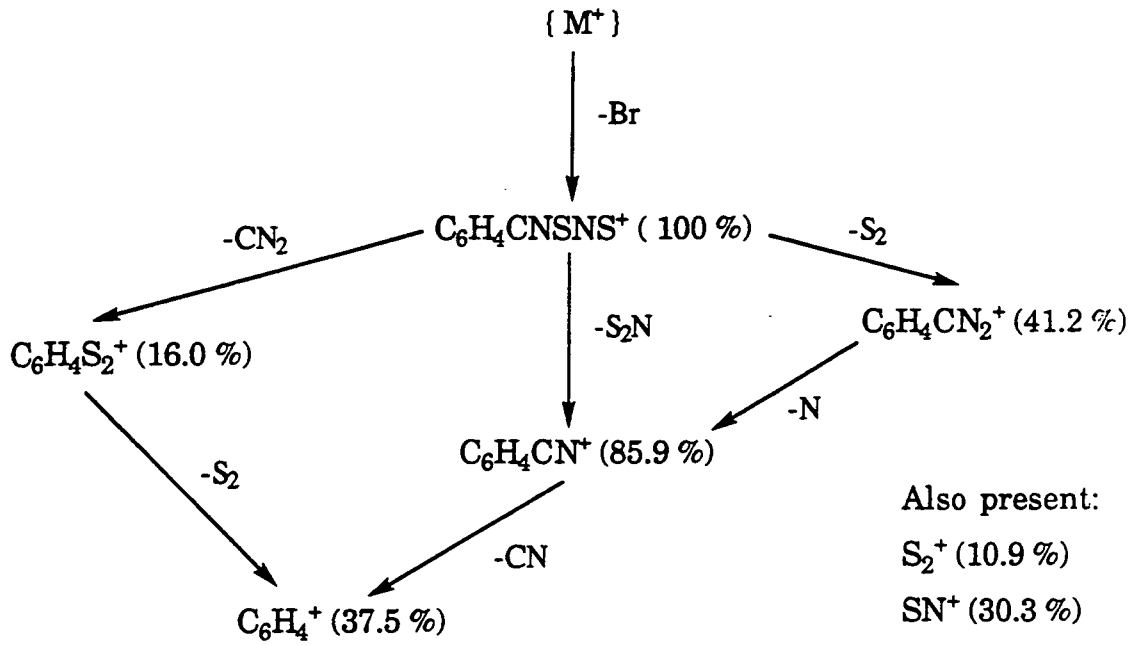

Scheme 3.2.2. Syntheses of *ortho*-substituted 1,3-dithiadiazolium cations

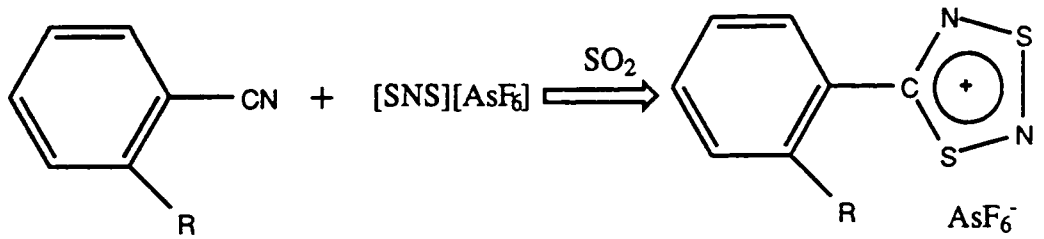

1: R = Br
2: R = Cl
3: R = F
4: R = CH_3
5: R = CF_3
6: R = CN

3.2.2. The reaction of [SNS][AsF6] with *ortho*-chlorobenzonitrile

Reaction of $[SNS][AsF_6]$ with ortho-chlorobenzonitrile in liquid SO_2 over 18 hours gave 5-(2-chlorophenyl)-1,3,2,4-dithiadiazolium hexaflouroarsenate(V), **2**, in 74.7 % yield, as shown in scheme **3.2.2.**. The product, a yellow solid, was soluble in SO_2. An IR spectrum of **2** showed a small residual CN peak (2233 cm^{-1}) but this was greatly reduced in comparison with the same peak in a spectrum of the starting material.

hexafluoroarsenate(V) **4**, in 70.2 % yield, as shown in scheme **3.2.2.**. The product, a bright yellow solid, was soluble in SO_2. An IR spectrum of **4** showed no CN peak (2250 cm^{-1} in a spectrum of the starting material), however a strong, broad AsF_6^- peak (692 cm^{-1}) was present. Additional peaks in the product spectrum (at 1294, 1116, 980 and 806 cm^{-1}) may be attributed to the dithiadiazolium ring.

As with the *ortho*-halogenated dithiadiazolium salts, it is impossible to assign every new peak with total certainty. The new peak at 980 cm^{-1} in **4** is comparable with that at 985 cm^{-1} in the *ortho*-trifluoromethyl-substituted system, suggesting they both correspond to similar bonds, probably one of the dithiadiazolium ring S-N bonds. It seems unlikely that the four new peaks given for **4** are the only new peaks present; other peaks may be masked by separate peaks, or be too weak to be positively identified. Other peaks present in the starting material spectrum are also present in the spectrum of **4**, but shifted between 1 and 9 wavenumbers in position.

The mass spectrum (E.I.) of **4** showed a good breakdown pattern (see scheme **3.2.5.**) considering that AsF_6^- salts are usually involatile. Excellent chemical analysis figures (C,H,N) were obtained. A small quantity of single crystals was grown from SO_2 solution over a period of 7 days using the ripple technique discussed in chapter 2, but proved to be of a different compound to **4**, see section **3.3.**.

Scheme 3.2.5. Mass spectral breakdown pattern (E.I.) of *ortho*-$[CH_3C_6H_4CNSNS][AsF_6]$

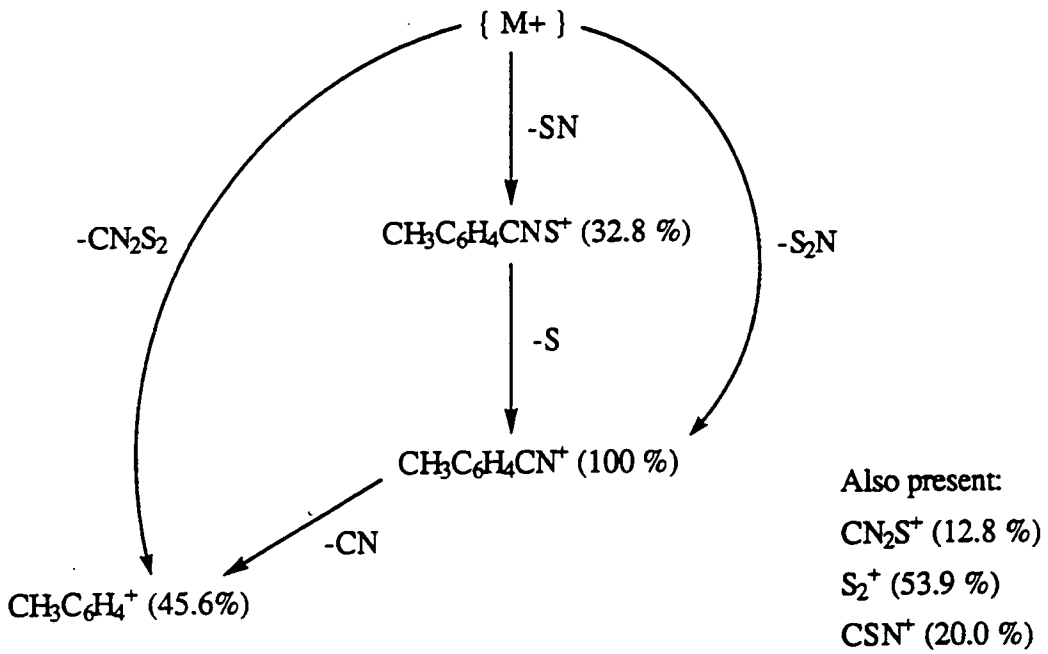

3.2.5. The reaction of [SNS][AsF_6] with *ortho*-(trifluoromethyl)benzonitrile

The reaction of [SNS][AsF_6] with *ortho*-(trifluoromethyl)benzonitrile in liquid SO_2 over 24 hours gave 5-*ortho*-(trifluoromethyl)phenyl)-1,3,2,4-dithiadiazolium hexafluoroarsenate(V), **5**, in 77.4 %.yield, as shown in in scheme **3.2.2.**. The product, a pale beige solid, was soluble in SO_2. An IR spectrum of **5** showed no CN peak (2234 cm^{-1} in an IR spectrum of the starting material), but a strong, broad AsF_6- peak (704 cm^{-1}) was present in **5**. Additional peaks in the product spectrum (at 1419, 1318, 985 and 908 cm^{-1}) may be attributable to the dithiadiazolium ring.

Scheme 3.2.6. Mass spectral breakdown pattern (E.I.) of *ortho*-[$CF_3C_6H_4CNSNS$][AsF_6]

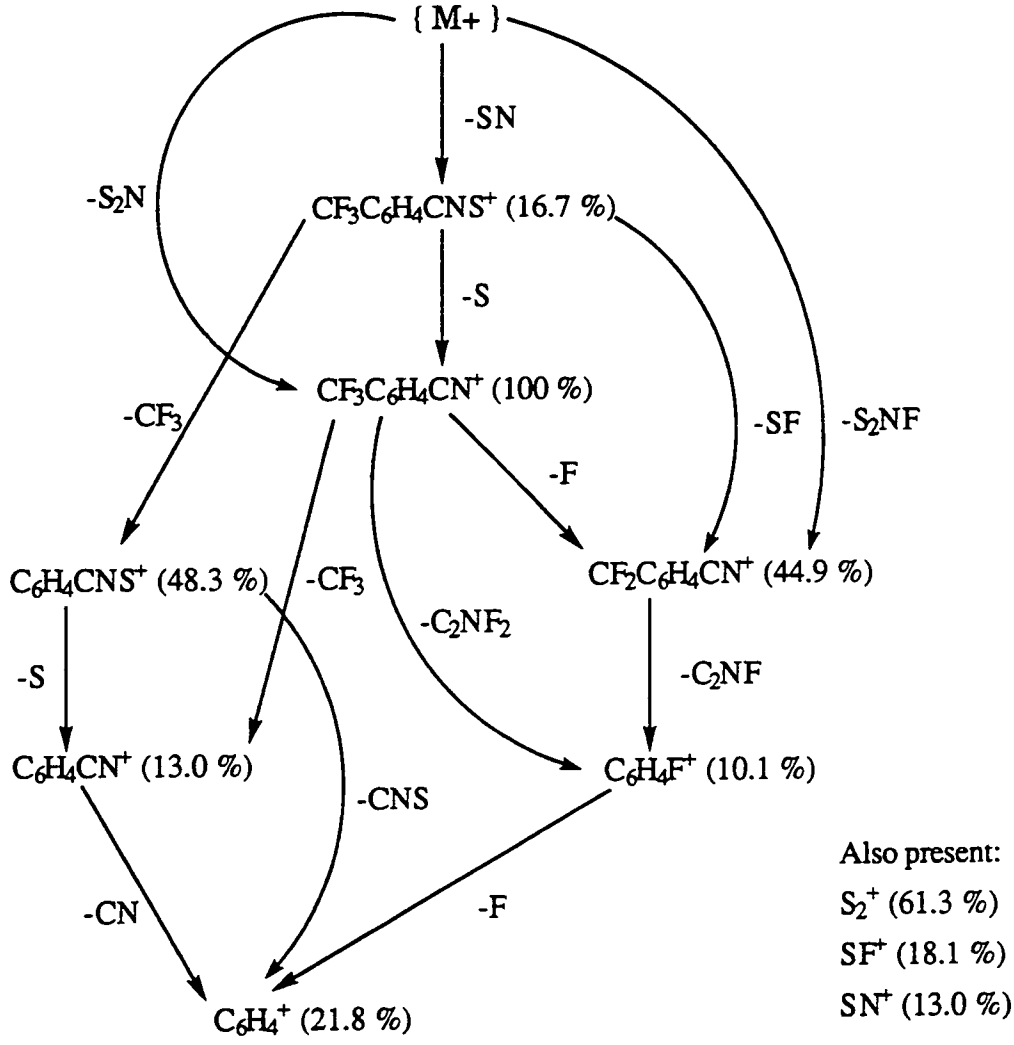

As with the other *ortho*-substituted dithiadiazolium salts, definitive assignment of all the new peaks is very difficult. The new peak at 985 cm^{-1}

in **5** is comparable with that at 980 cm^{-1} in the *ortho*-methyl-substituted system, indicating that they both correspond to similar bonds, probably one of the dithiadiazolium ring S-N bonds. It appears unlikely that the four new peaks given for **5** are the only new peaks present; other peaks may be masked by different peaks, or be too weak to positively identify. Other peaks present in the starting material spectrum are also present in the spectrum of **5**, but are shifted 1 to 8 wavenumbers in position.

The mass spectrum (E.I.) of **5** showed an excellent breakdown pattern for a 1,3-dithiadiazolium ring (see scheme **3.2.6.**). Very good elemental analysis figures (C,H,N) were obtained.

3.2.6. The reaction of [SNS][AsF_6] with *ortho*-dicyanobenzene in 1:1 ratio

The reaction of [SNS][AsF_6] with *ortho*-dicyanobenzene in 1:1 ratio, carried out in liquid SO_2 over 18 hours, yielded a small amount of off-white solid, **6**, that was soluble in SO_2. An IR spectrum of **6** showed sizeable peaks attributable to CN (2263 cm^{-1}) and AsF_6^- (698 cm^{-1}), but comparison with IR spectra of *ortho*-dicyanobenzene and *ortho*-$[C_6H_4(CNSNS)_2]^{2+}[AsF_6^-]_2$ showed that **6** was <u>not</u> a mixture of these compounds. Single crystals of **6** were grown from SO_2 solution over a 5 day period using the ripple technique discussed in Chapter 2. Unfortunately, these crystals decomposed in the glove box before any data could be collected from them. Subsequent attempts to repeat this reaction yielded only dark brown, unworkable oils.

3.2.7 The reaction of [Bu_4N][Cl] with *ortho*-[BrC_6H_4CNSNS][AsF_6]

The reaction of [Bu_4N][Cl] with *ortho*-[BrC_6H_4CNSNS][AsF_6] in CH_2Cl_2 over 24 hours gave 5-(2-bromophenyl)-1,3,2,4-dithiadiazolium chloride,**7**, in 66 % yield. The product, a bright yellow solid, was soluble in CH_2Cl_2. An IR spectrum of **7** showed that the AsF_6^- peak had disappeared (701 cm^{-1} in the starting material spectrum), and other peaks had shifted slightly in position. The peaks attributable to the dithiadiazolium ring had shifted more than the others, which is as expected because the dithiadiazolium ring is more greatly affected than the phenyl ring by any change in the anion.

The mass spectrum (E.I.) of **7** showed the parent cation and a clear breakdown pattern (see scheme **3.2.7.**) Interestingly, it also shows a peak at m/e = 397, corresponding to the association of one parent cation

with one molecule of **7**, (ie. $C_6H_4(CNSNS)_2Cl^+$). Good elemental analysis figures (C,H,N) were also obtained.

Scheme 3.2.7. Mass spectral breakdown pattern (E.I.) of *ortho*-[BrC_6H_4CNSNS][Cl]

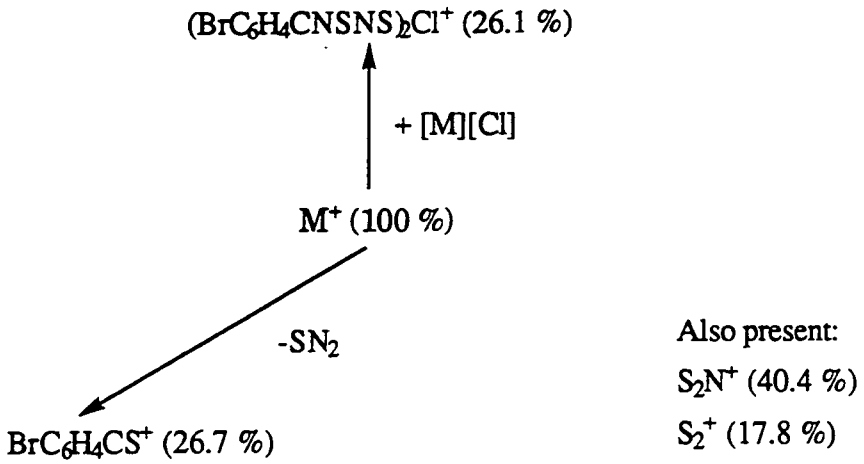

3.2.8. The reduction of *ortho*-[BrC_6H_4CNSNS][Cl] with excess Ph_3Sb

When *ortho*-[BrC_6H_4CNSNS][Cl] and excess Ph_3Sb were reacted in CH_2Cl_2 a green solution was immediately formed, changing to bright blue within 10 minutes (this colour is often indicative of radicals in dithiadiazolyl chemistry). However, upon removal of the solvent after 18 hours stirring, an intractable brown tar was formed.

3.3 Solid state structures

The solid state structures of *ortho*-bromo-dithiadiazolium hexafluoroarsenate(V), **1**, and *ortho*-chloro-dithiadiazolium hexafluoroarsenate(V), **2**, were determined by single crystal x-ray diffraction, by Prof. W. Clegg at the Department of Chemistry, University of Newcastle-upon-Tyne. Crystal parameters, refined atomic coordinates, bond lengths and angles for **1** are given in tables **3.3.1.**, **3.3.2.** and **3.3.3.**, respectively. Crystal parameters, refined atomic coordinates, bond lengths and angles for **2** are given in tables **3.3.4.**, **3.3.5.** and **3.3.6.** respectively (anisotropic displacement parameters, and hydrogen atom coordinates for **1** and **2** are given in appendix IV). Figure **3.3.2.** shows the structure of **1**, illustrating the atomic numbering scheme, whilst figure **3.3.3.** shows the unit cell of **1**, containing two molecules. Figure **3.3.4.** illustrates the packing of **1**, via projection down the y-axis. Figure **3.3.5.**

shows the structure of **2**, illustrating the atomic numbering scheme, whilst figure **3.3.6.** shows the unit cell of **2**, containing four molecules. Figure **3.3.7.** illustrates the packing of **2**, in the crystal.

Two further crystal structures (the *ortho*-fluoro- and *ortho*-methyl-systems) are being studied by single crystal x-ray diffraction. At time of writing data has been collected for both compounds, but neither has been fully refined[20]. The *ortho*-fluoro-dithiadiazolium hexafluoroarsenate(V) sample is isostructural with its *ortho*-chloro analogue, whilst the *ortho*-methyl-dithiadiazolium hexafluoroarsenate(V) sample gave a more surprising structure, **3**, (see figure **3.3.1.**)[20]. This structure is at odds with the expected 1:1 addition product, which is indicated by elemental analysis, and mass and infrared spectra (see section **3.5.4.**). A complete rationalisation of the formation of 3 has not yet been found, but it appears likely to proceed from a rearrangement of the 1:1 addition product in SO_2 solution, from which the crystals were grown.

Figure 3.3.1. The structure of 3,5-(*ortho*-tolyl)-1,2-dithia-4-azolium hexafluoroarsenate(V)

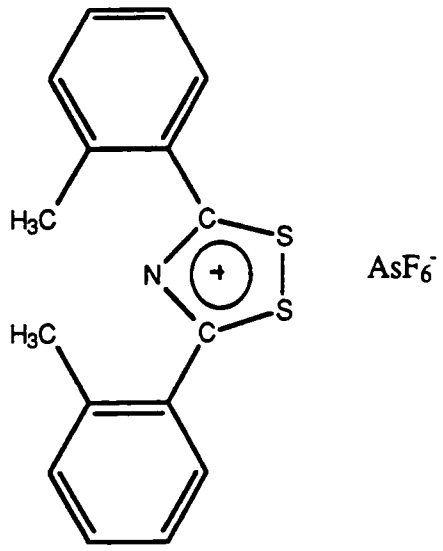

Table 3.3.1. Crystal data, structure solution and refinement for 1

Identification code	ajb39
Chemical formula	$C_7H_4AsBrF_6N_2S_2$
Formula weight	449.07
Temperature	160(2) K
Radiation and wavelength	MoKα, 0.71073 Å
Crystal system, space group	monoclinic, $P2_1/n$
Unit cell dimensions	a = 12.838(5) Å α = 90° b = 8.163(2) Å β = 92.73(4)° c = 24.618(7) Å γ = 90°
Volume	2577(2) $Å^3$
Z	8
Density (calculated)	2.315 g/cm^3
Absorption coefficient μ	6.120 mm^{-1}
F(000)	1712
Reflections for cell refinement	33 (θ range 7.55 to 11.31°)
Crystal colour	pale yellow
Crystal size	0.20 × 0.14 × 0.08 mm
Data collection method	Stoe–Siemens diffractometer, ω/θ scans with on-line profile fitting
θ range for data collection	2.63 to 22.51°
Index ranges	$-13 \le h \le 13$, $0 \le k \le 8$, $0 \le \ell \le 26$
Standard reflections	4 every 60 minutes
Intensity decay of standards	–43%
Reflections collected	3576
Independent reflections	3361 (R_{int} = 0.2087)
Reflections with I>2σ(I)	1727
Absorption correction	semi–empirical from ψ–scans
Max. and min. transmission	0.664 and 0.578
Structure solution	direct methods
Refinement method	full–matrix least–squares on F^2
Weighting parameters a, b	0.2592, 0.0000
Data / restraints / parameters	3355 / 24 / 364
Goodness–of–fit on F^2	1.114
Final R indices [I>2σ(I)]	R1 = 0.1275, wR2 = 0.3323
R indices (all data)	R1 = 0.2082, wR2 = 0.4104
Largest and mean shift/esd	0.000 and 0.000
Largest diff. peak and hole	1.821 and –2.207 $eÅ^{-3}$

Table 3.3.2. Atomic coordinates (x 10^4) and equivalent isotropic displacement parameters ($Å^2$ x 10^3) for **1** U(eq) is defined as one third of the trace of the orthogonalized U_{ij} tensor.

	x	y	z	U(eq)
Br(1)	650(3)	1609(5)	1736.6(13)	51.0(12)
C(1)	52(24)	395(38)	2951(11)	32(7)
C(2)	-817(24)	759(37)	2542(10)	31(7)
C(3)	-1826(21)	555(42)	2721(12)	34(8)
C(4)	-2720(32)	744(53)	2355(15)	62(11)
C(5)	-2539(25)	1470(40)	1860(14)	42(9)
C(6)	-1558(26)	1783(45)	1670(13)	43(9)
C(7)	-668(28)	1354(40)	2021(12)	42(8)
S(1)	845(7)	-248(11)	3843(3)	41(2)
S(2)	1383(6)	421(10)	2836(3)	35(2)
N(1)	-173(19)	121(32)	3441(10)	35(6)
N(2)	1773(20)	-67(33)	3457(12)	45(7)
Br(2)	448(3)	2168(5)	268.5(14)	53.2(12)
C(8)	2342(24)	1754(37)	-570(12)	32(7)
C(9)	1271(21)	2196(38)	-800(11)	30(7)
C(10)	1178(24)	2456(48)	-1348(12)	44(9)
C(11)	233(30)	2874(51)	-1611(14)	57(11)
C(12)	-607(26)	3075(50)	-1319(14)	51(10)
C(13)	-552(29)	2922(47)	-796(19)	65(12)
C(14)	372(23)	2416(39)	-489(12)	32(7)
S(3)	2697(6)	1367(10)	117(3)	34(2)
S(4)	4192(6)	1040(10)	-588(3)	34(2)
N(3)	3910(21)	977(26)	14(9)	33(6)
N(4)	3118(20)	1539(28)	-901(9)	29(6)
As(1)	1131(2)	5156(4)	3184.5(12)	32.6(10)
F(1)	1957(23)	6006(35)	3666(11)	84(10)
F(2)	2063(19)	3972(27)	2935(13)	75(10)
F(3)	842(27)	3611(30)	3622(10)	87(11)
F(4)	174(23)	6331(40)	3387(18)	121(16)
F(5)	1451(22)	6586(30)	2745(10)	71(8)
F(6)	298(23)	4326(32)	2694(12)	81(9)
F(1A)	1046(67)	5789(93)	3812(26)	27(25)
F(2A)	1974(57)	3766(87)	3390(33)	27(25)
F(3A)	180(54)	3872(88)	3262(34)	27(25)
F(4A)	286(58)	6570(88)	2984(34)	27(25)
F(5A)	2080(54)	6475(87)	3108(34)	27(25)
F(6A)	1229(67)	4561(94)	2558(26)	27(25)
As(2)	3173(2)	6287(4)	-324.6(12)	27.3(9)
F(7)	4002(16)	7322(22)	-716(7)	49(5)
F(8)	3820(15)	7151(22)	249(7)	47(5)
F(9)	4016(12)	4620(21)	-292(7)	36(4)
F(10)	2367(15)	5259(23)	81(8)	54(5)
F(11)	2565(15)	5448(22)	-901(8)	50(5)
F(12)	2325(13)	7912(21)	-360(8)	46(5)

Table 3.3.3. Bond lengths (Å) and angles (°) for 1

Br(1)-C(7)	1.87(3)	C(1)-N(1)	1.27(4)
C(1)-C(2)	1.50(4)	C(1)-S(2)	1.74(3)
C(2)-C(7)	1.39(4)	C(2)-C(3)	1.40(4)
C(3)-C(4)	1.43(5)	C(4)-C(5)	1.38(5)
C(5)-C(6)	1.39(5)	C(6)-C(7)	1.44(5)
S(1)-N(2)	1.57(3)	S(1)-N(1)	1.63(3)
S(2)-N(2)	1.63(3)	Br(2)-C(14)	1.87(3)
C(8)-N(4)	1.33(4)	C(8)-C(9)	1.51(4)
C(8)-S(3)	1.76(3)	C(9)-C(10)	1.36(4)
C(9)-C(14)	1.43(4)	C(10)-C(11)	1.39(5)
C(11)-C(12)	1.33(5)	C(12)-C(13)	1.29(5)
C(13)-C(14)	1.44(5)	S(3)-N(3)	1.62(3)
S(4)-N(3)	1.54(2)	S(4)-N(4)	1.60(3)
As(1)-F(6A)	1.63(6)	As(1)-F(3A)	1.63(6)
As(1)-F(2A)	1.63(6)	As(1)-F(1A)	1.64(6)
As(1)-F(4A)	1.64(6)	As(1)-F(5A)	1.64(6)
As(1)-F(4)	1.65(3)	As(1)-F(5)	1.66(2)
As(1)-F(2)	1.68(2)	As(1)-F(1)	1.70(2)
As(1)-F(3)	1.71(2)	As(1)-F(6)	1.71(3)
As(2)-F(10)	1.69(2)	As(2)-F(7)	1.70(2)
As(2)-F(12)	1.72(2)	As(2)-F(11)	1.73(2)
As(2)-F(9)	1.74(2)	As(2)-F(8)	1.75(2)

N(1)-C(1)-C(2)	118(3)	N(1)-C(1)-S(2)	115(2)
C(2)-C(1)-S(2)	126(2)	C(7)-C(2)-C(3)	120(3)
C(7)-C(2)-C(1)	124(3)	C(3)-C(2)-C(1)	116(2)
C(2)-C(3)-C(4)	121(3)	C(5)-C(4)-C(3)	116(3)
C(4)-C(5)-C(6)	125(3)	C(5)-C(6)-C(7)	117(3)
C(2)-C(7)-C(6)	120(3)	C(2)-C(7)-Br(1)	123(3)
C(6)-C(7)-Br(1)	117(2)	N(2)-S(1)-N(1)	103.1(14)
N(2)-S(2)-C(1)	96.0(13)	C(1)-N(1)-S(1)	113(2)
S(1)-N(2)-S(2)	112(2)	N(4)-C(8)-C(9)	120(3)
N(4)-C(8)-S(3)	113(2)	C(9)-C(8)-S(3)	126(2)
C(10)-C(9)-C(14)	118(3)	C(10)-C(9)-C(8)	116(3)
C(14)-C(9)-C(8)	125(3)	C(9)-C(10)-C(11)	122(3)
C(12)-C(11)-C(10)	119(3)	C(13)-C(12)-C(11)	121(3)
C(12)-C(13)-C(14)	124(4)	C(9)-C(14)-C(13)	115(3)
C(9)-C(14)-Br(2)	121(2)	C(13)-C(14)-Br(2)	124(3)
N(3)-S(3)-C(8)	95.2(13)	N(3)-S(4)-N(4)	103.6(14)
S(4)-N(3)-S(3)	115(2)	C(8)-N(4)-S(4)	113(2)
F(6A)-As(1)-F(3A)	91(2)	F(6A)-As(1)-F(2A)	90(2)
F(3A)-As(1)-F(2A)	90(2)	F(6A)-As(1)-F(1A)	179(2)
F(3A)-As(1)-F(1A)	90(2)	F(2A)-As(1)-F(1A)	90(2)
F(6A)-As(1)-F(4A)	90(2)	F(3A)-As(1)-F(4A)	90(2)
F(2A)-As(1)-F(4A)	179(2)	F(1A)-As(1)-F(4A)	89(2)
F(6A)-As(1)-F(5A)	90(2)	F(3A)-As(1)-F(5A)	179(2)
F(2A)-As(1)-F(5A)	90(2)	F(1A)-As(1)-F(5A)	89(2)
F(4A)-As(1)-F(5A)	89(2)	F(4)-As(1)-F(5)	90(2)
F(4)-As(1)-F(2)	176(2)	F(5)-As(1)-F(2)	87.9(13)
F(4)-As(1)-F(1)	90(2)	F(5)-As(1)-F(1)	90.1(14)
F(2)-As(1)-F(1)	93.3(14)	F(4)-As(1)-F(3)	93(2)
F(5)-As(1)-F(3)	177.0(13)	F(2)-As(1)-F(3)	89.1(13)
F(1)-As(1)-F(3)	90(2)	F(4)-As(1)-F(6)	90(2)
F(5)-As(1)-F(6)	89.1(14)	F(2)-As(1)-F(6)	86.9(14)
F(1)-As(1)-F(6)	179.2(14)	F(3)-As(1)-F(6)	90(2)
F(10)-As(2)-F(7)	178.5(11)	F(10)-As(2)-F(12)	90.5(9)
F(7)-As(2)-F(12)	90.0(9)	F(10)-As(2)-F(11)	91.3(10)
F(7)-As(2)-F(11)	90.1(9)	F(12)-As(2)-F(11)	90.3(9)

F(10)-As(2)-F(9)	88.9(8)	F(7)-As(2)-F(9)	90.6(8)
F(12)-As(2)-F(9)	179.1(8)	F(11)-As(2)-F(9)	89.1(8)
F(10)-As(2)-F(8)	90.2(10)	F(7)-As(2)-F(8)	88.4(9)
F(12)-As(2)-F(8)	90.3(9)	F(11)-As(2)-F(8)	178.4(9)
F(9)-As(2)-F(8)	90.4(8)		

Figure 3.3.2. The structure of **1**, illustrating the atomic numbering scheme

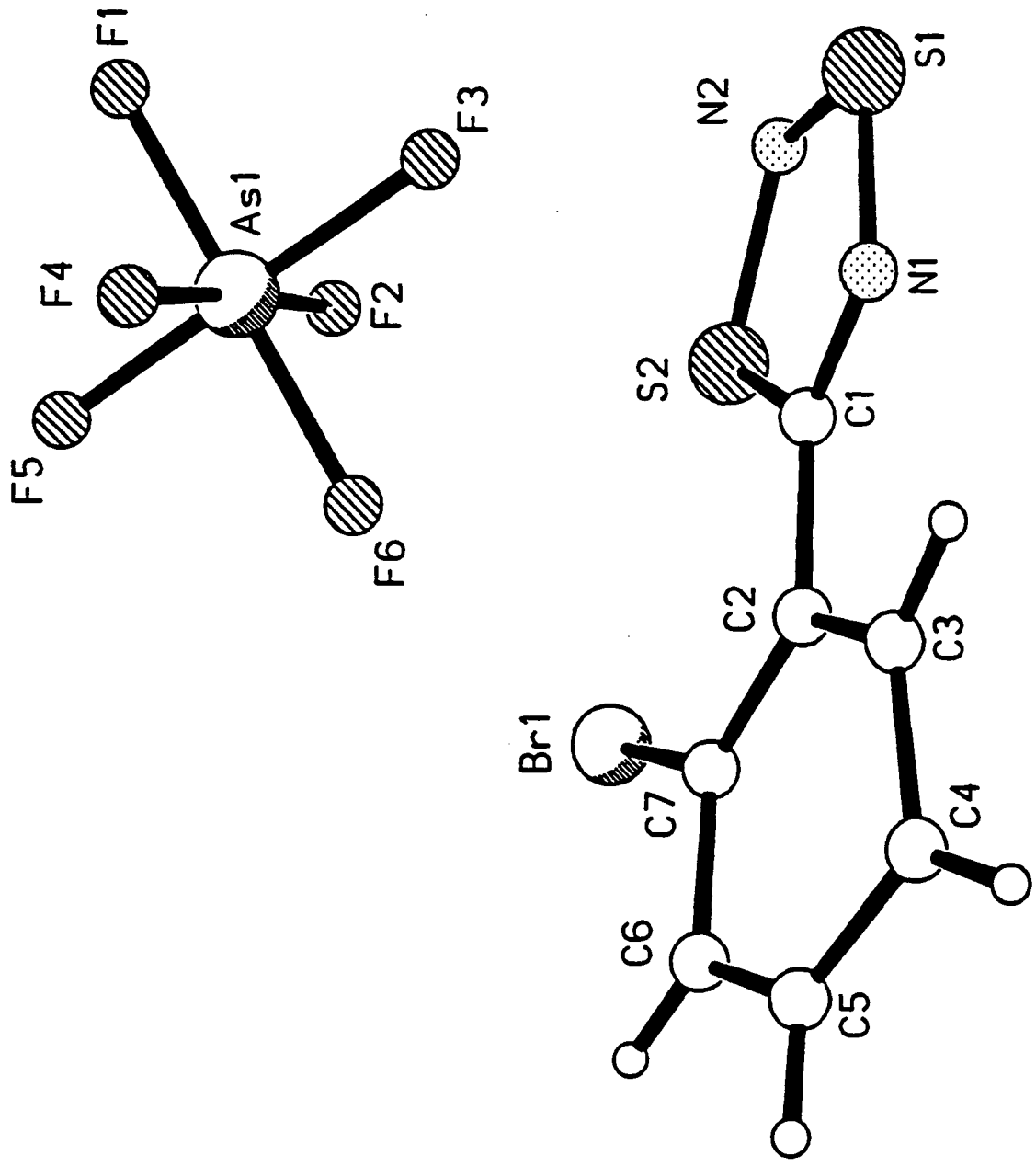

Figure 3.3.3. The unit cell of 1 containing two molecules

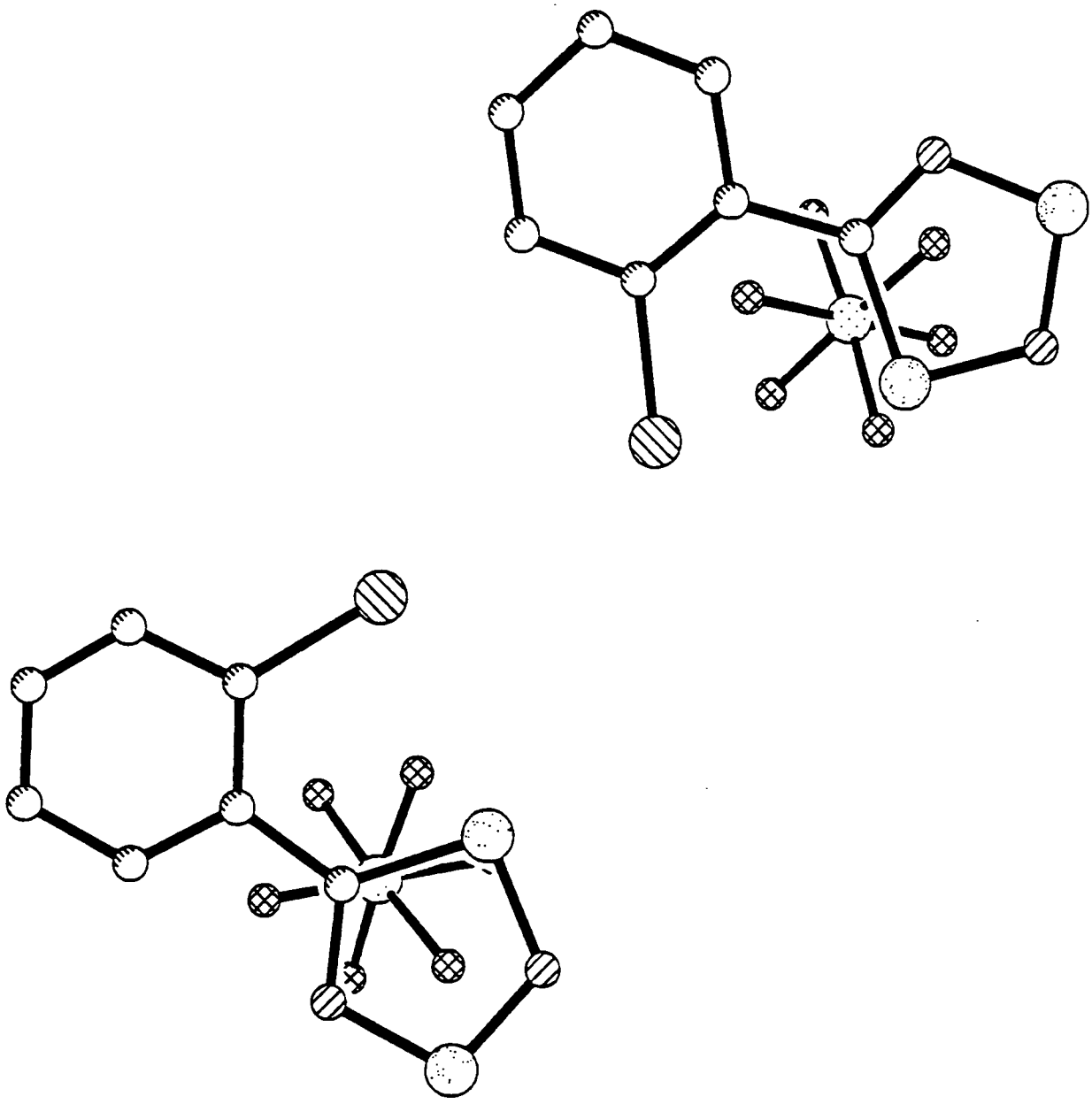

Figure 3.3.4. Projection along the y-axis of **1**

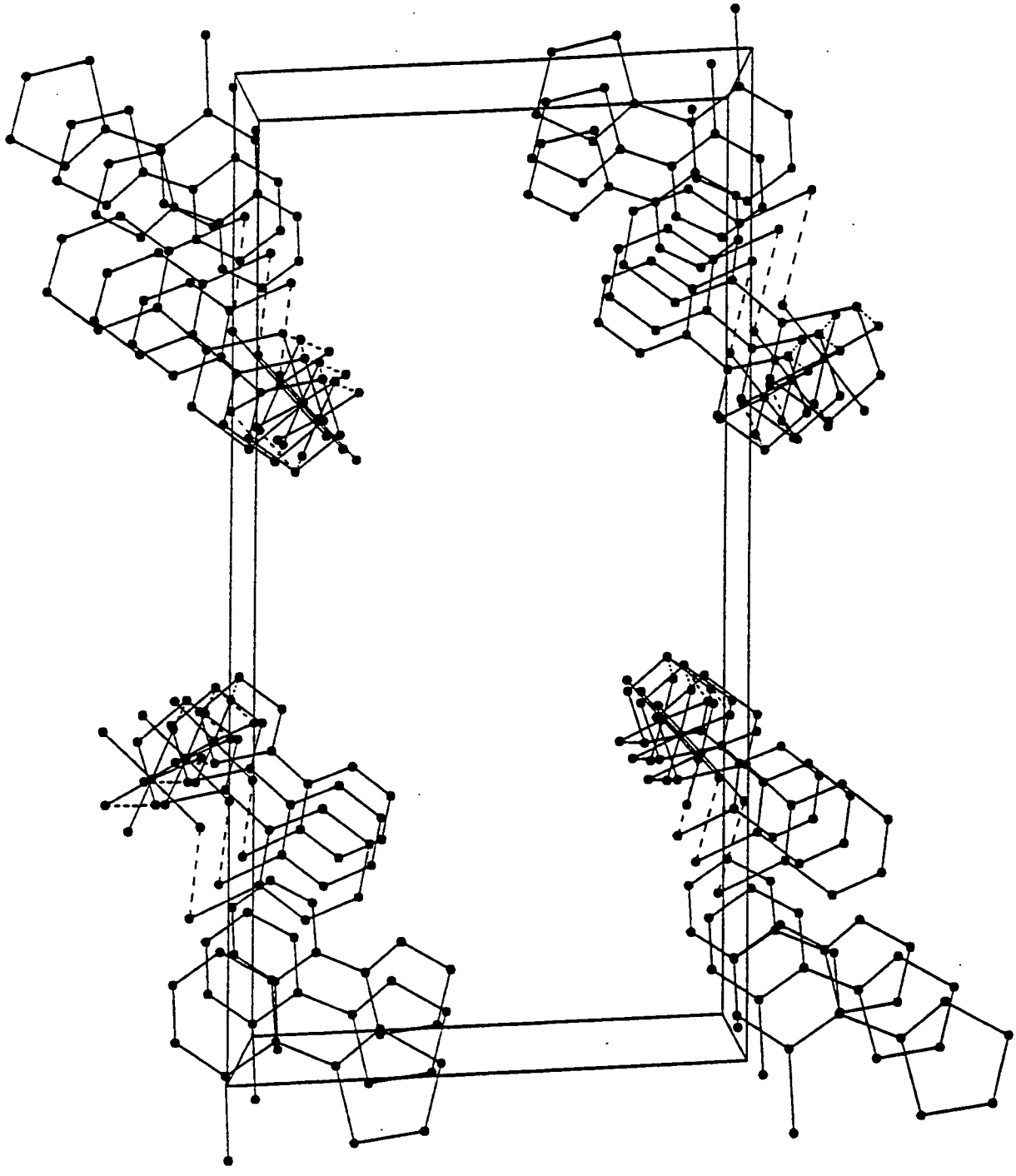

Table 3.3.4. Crystal data, structure solution and refinement for **2**

Identification code	ajb41
Chemical formula	$C_7H_4AsClF_6N_2S_2$
Formula weight	404.61
Temperature	160(2) K
Radiation and wavelength	MoKα, 0.71073 Å
Crystal system, space group	monoclinic, $P2_1/n$
Unit cell dimensions	a = 25.760(4) Å α = 90° b = 8.159(2) Å β = 116.257(12)° c = 27.156(4) Å γ = 90°
Volume	5119(2) $Å^3$
Z	16
Density (calculated)	2.100 g/cm^3
Absorption coefficient μ	3.249 mm^{-1}
F(000)	3136
Reflections for cell refinement	28 (θ range 11.03 to 12.47°)
Crystal colour	pale yellow
Crystal size	0.44 × 0.26 × 0.20 mm
Data collection method	Stoe–Siemens diffractometer, ω/θ scans with on-line profile fitting
θ range for data collection	2.63 to 22.51°
Index ranges	$-27 \le h \le 27$, $-5 \le k \le 8$, $-26 \le \ell \le 29$
Standard reflections	4 every 60 minutes
Intensity decay of standards	0%
Reflections collected	7376
Independent reflections	6660 (R_{int} = 0.0582)
Reflections with I>2σ(I)	5062
Absorption correction	semi-empirical from ψ-scans
Max. and min. transmission	0.516 and 0.436
Structure solution	direct methods
Refinement method	full-matrix least-squares on F^2
Weighting parameters a, b	0.0346, 35.5110
Data / restraints / parameters	6646 / 0 / 735
Goodness-of-fit on F^2	1.117
Final R indices [I>2σ(I)]	R1 = 0.0425, wR2 = 0.1024
R indices (all data)	R1 = 0.0657, wR2 = 0.1220
Largest and mean shift/esd	0.001 and 0.000
Largest diff. peak and hole	.542 and -.699 $eÅ^{-3}$

Table 3.3.5. Atomic coordinates (x 10^4) and equivalent isotropic displacement parameters ($Å^2$ x 10^3) for 2. U(eq) is defined as one third of the trace of the orthogonalized U_{ij} tensor.

	x	y	z	U(eq)
As(1)	3270.4(3)	-4062.1(9)	4685.3(3)	24.6(2)
F(1)	2638(2)	-3067(5)	4279(2)	40.7(11)
F(2)	3252(2)	-3195(5)	5256(2)	38.9(11)
F(3)	2885(2)	-5737(5)	4731(2)	38.6(10)
F(4)	3292(2)	-4903(5)	4117(2)	40.3(11)
F(5)	3657(2)	-2378(5)	4638(2)	36.0(10)
F(6)	3901(2)	-5051(5)	5104(2)	42.9(11)
As(2)	5974.2(3)	108.0(10)	3148.8(3)	34.8(2)
F(7)	6206(5)	1051(9)	2726(5)	116(4)
F(8)	6592(3)	-900(9)	3481(5)	123(4)
F(9)	6229(4)	1743(8)	3597(3)	94(3)
F(10)	5722(4)	-795(9)	3566(3)	97(3)
F(11)	5339(2)	1180(8)	2840(3)	73(2)
F(12)	5681(3)	-1460(7)	2706(2)	70(2)
F(7A)	5619(12)	637(36)	2526(11)	45(8)
F(8A)	6284(13)	-1547(37)	2905(12)	48(8)
F(9A)	6525(10)	1252(33)	3197(11)	32(7)
F(10A)	6390(12)	-678(33)	3776(10)	29(7)
F(11A)	5725(18)	1539(50)	3390(17)	79(12)
F(12A)	5488(13)	-1295(41)	3119(14)	57(9)
As(3)	8921.2(3)	621.8(10)	6784.2(3)	32.4(2)
F(13)	9487(2)	1828(8)	6848(3)	77(2)
F(14)	9159(4)	-931(8)	6526(3)	93(3)
F(15)	8338(3)	-543(8)	6710(3)	77(2)
F(16)	8653(3)	2213(6)	7026(2)	62(2)
F(17)	8529(2)	1409(7)	6136(2)	57(2)
F(18)	9295(3)	-140(8)	7424(2)	84(2)
F(13A)	9341(21)	2002(62)	7227(20)	28(14)
F(14A)	9506(22)	-818(68)	6966(23)	32(14)
F(15A)	8558(26)	-998(75)	6393(24)	46(17)
F(16A)	8405(38)	1722(118)	6618(40)	90(28)
F(17A)	9173(25)	1471(72)	6352(24)	41(16)
F(18A)	8807(23)	-367(64)	7322(20)	29(14)
As(4)	6766.4(3)	1663.2(9)	331.4(3)	27.9(2)
F(19)	7224(2)	138(6)	331(2)	45.7(12)
F(20)	7344(2)	2807(7)	764(2)	63(2)
F(21)	6301(2)	3176(6)	333(2)	52.8(13)
F(22)	6192(2)	520(6)	-111(2)	45.9(12)
F(23)	6726(2)	754(5)	883(2)	44.4(11)
F(24)	6806(2)	2589(6)	-221(2)	45.6(12)
Cl(1)	4900.1(8)	2026(3)	5268.6(8)	49.8(6)
S(1)	2660.9(8)	655(2)	4433.6(8)	32.6(4)
S(2)	3763.9(8)	1060(2)	5153.7(7)	31.8(4)
N(1)	3044(2)	1152(7)	4125(2)	26.0(13)
N(2)	3115(3)	604(8)	5057(2)	34(2)
C(1)	3599(3)	1385(8)	4461(3)	25(2)
C(2)	4003(3)	1861(8)	4242(3)	27(2)
C(3)	4589(3)	2165(10)	4557(3)	35(2)
C(4)	4936(3)	2667(12)	4313(4)	52(2)
C(5)	4710(4)	2820(12)	3754(4)	52(2)
C(6)	4134(4)	2498(11)	3433(3)	45(2)

C(7)	3779(3)	2012(10)	3669(3)	34(2)
Cl(2)	5611.6(10)	-6335(4)	1732.0(8)	62.8(7)
S(3)	5659.7(8)	-5187(3)	2760.0(8)	36.0(5)
S(4)	6386.6(9)	-4445(3)	3793.4(8)	40.6(5)
N(3)	5735(3)	-4715(8)	3368(3)	41(2)
N(4)	6733(3)	-4763(8)	3440(2)	33(2)
C(8)	6397(3)	-5137(9)	2924(3)	30(2)
C(9)	6657(3)	-5428(9)	2549(3)	31(2)
C(10)	6351(4)	-6015(10)	2006(3)	40(2)
C(11)	6635(4)	-6314(11)	1685(3)	49(2)
C(12)	7211(4)	-5995(11)	1887(4)	52(2)
C(13)	7523(4)	-5370(12)	2408(4)	53(2)
C(14)	7246(3)	-5111(9)	2738(3)	36(2)
Cl(3)	9385.8(9)	-3085(3)	8239.5(8)	52.3(6)
S(5)	9261.9(8)	-4203(3)	7176.5(8)	34.7(5)
S(6)	8490.3(9)	-4782(3)	6147.7(7)	35.8(5)
N(5)	9153(3)	-4641(8)	6554(3)	40(2)
N(6)	8169(2)	-4408(7)	6524(2)	30.4(14)
C(15)	8536(3)	-4115(9)	7042(3)	29(2)
C(16)	8302(3)	-3793(9)	7437(3)	28(2)
C(17)	8642(3)	-3274(10)	7981(3)	35(2)
C(18)	8386(4)	-2941(11)	8326(3)	46(2)
C(19)	7805(4)	-3175(10)	8144(3)	45(2)
C(20)	7458(4)	-3723(11)	7614(3)	44(2)
C(21)	7711(3)	-4012(10)	7263(3)	39(2)
Cl(4)	5205.6(10)	-3011(5)	-261.1(10)	92.4(11)
S(7)	6392.7(8)	-3377(2)	-88.0(7)	31.3(4)
S(8)	7482.9(8)	-3480(3)	672.6(8)	37.2(5)
N(7)	7059(3)	-3631(8)	42(2)	36(2)
N(8)	7063(2)	-3082(7)	948(2)	27.1(14)
C(22)	6509(3)	-3012(9)	588(3)	27(2)
C(23)	6067(3)	-2607(10)	773(3)	35(2)
C(24)	5485(3)	-2579(14)	434(3)	60(3)
C(25)	5088(4)	-2141(20)	636(5)	101(5)
C(26)	5291(5)	-1797(18)	1189(5)	91(4)
C(27)	5876(4)	-1828(13)	1536(4)	62(3)
C(28)	6258(4)	-2224(9)	1324(3)	38(2)

Table 3.3.6. Bond lengths (Å) and angles (°) for 2

As(1)-F(4)	1.711(4)	As(1)-F(1)	1.715(4)
As(1)-F(6)	1.717(4)	As(1)-F(2)	1.724(4)
As(1)-F(3)	1.726(4)	As(1)-F(5)	1.735(4)
As(2)-F(7A)	1.59(3)	As(2)-F(11A)	1.60(4)
As(2)-F(9A)	1.65(3)	As(2)-F(8)	1.660(6)
As(2)-F(12A)	1.67(3)	As(2)-F(10A)	1.69(2)
As(2)-F(12)	1.688(5)	As(2)-F(7)	1.694(7)
As(2)-F(10)	1.703(6)	As(2)-F(11)	1.712(6)
As(2)-F(9)	1.727(6)	As(2)-F(8A)	1.83(3)
As(3)-F(16A)	1.50(9)	As(3)-F(13A)	1.65(5)
As(3)-F(14)	1.689(6)	As(3)-F(18)	1.689(5)
As(3)-F(15A)	1.69(6)	As(3)-F(13)	1.702(5)
As(3)-F(15)	1.711(6)	As(3)-F(17A)	1.72(6)
As(3)-F(17)	1.720(5)	As(3)-F(16)	1.730(5)
As(3)-F(14A)	1.80(5)	As(3)-F(18A)	1.80(5)
As(4)-F(20)	1.708(5)	As(4)-F(22)	1.712(4)
As(4)-F(23)	1.714(4)	As(4)-F(19)	1.714(4)
As(4)-F(21)	1.722(4)	As(4)-F(24)	1.722(4)
Cl(1)-C(3)	1.738(7)	S(1)-N(2)	1.577(6)
S(1)-N(1)	1.604(6)	S(2)-N(2)	1.617(6)
S(2)-C(1)	1.756(7)	N(1)-C(1)	1.326(8)
C(1)-C(2)	1.462(9)	C(2)-C(3)	1.389(10)
C(2)-C(7)	1.404(9)	C(3)-C(4)	1.389(11)
C(4)-C(5)	1.370(12)	C(5)-C(6)	1.374(11)
C(6)-C(7)	1.387(10)	Cl(2)-C(10)	1.730(9)
S(3)-N(3)	1.621(7)	S(3)-C(8)	1.748(8)
S(4)-N(3)	1.576(7)	S(4)-N(4)	1.594(6)
N(4)-C(8)	1.315(9)	C(8)-C(9)	1.467(10)
C(9)-C(14)	1.393(10)	C(9)-C(10)	1.413(10)
C(10)-C(11)	1.385(11)	C(11)-C(12)	1.362(12)
C(12)-C(13)	1.380(13)	C(13)-C(14)	1.388(11)
Cl(3)-C(17)	1.731(8)	S(5)-N(5)	1.626(7)
S(5)-C(15)	1.742(7)	S(6)-N(5)	1.575(7)
S(6)-N(6)	1.602(6)	N(6)-C(15)	1.325(9)
C(15)-C(16)	1.468(10)	C(16)-C(21)	1.391(10)
C(16)-C(17)	1.408(10)	C(17)-C(18)	1.390(11)
C(18)-C(19)	1.367(12)	C(19)-C(20)	1.392(12)
C(20)-C(21)	1.393(10)	Cl(4)-C(24)	1.733(9)
S(7)-N(7)	1.606(6)	S(7)-C(22)	1.749(7)
S(8)-N(7)	1.576(6)	S(8)-N(8)	1.597(6)
N(8)-C(22)	1.325(9)	C(22)-C(23)	1.472(10)
C(23)-C(24)	1.370(11)	C(23)-C(28)	1.388(10)
C(24)-C(25)	1.402(12)	C(25)-C(26)	1.38(2)
C(26)-C(27)	1.379(14)	C(27)-C(28)	1.380(11)

F(4)-As(1)-F(1)	90.6(2)	F(4)-As(1)-F(6)	90.6(2)
F(1)-As(1)-F(6)	178.8(2)	F(4)-As(1)-F(2)	179.4(2)
F(1)-As(1)-F(2)	89.3(2)	F(6)-As(1)-F(2)	89.5(2)
F(4)-As(1)-F(3)	89.8(2)	F(1)-As(1)-F(3)	90.4(2)
F(6)-As(1)-F(3)	89.2(2)	F(2)-As(1)-F(3)	90.8(2)
F(4)-As(1)-F(5)	90.1(2)	F(1)-As(1)-F(5)	89.5(2)
F(6)-As(1)-F(5)	90.9(2)	F(2)-As(1)-F(5)	89.2(2)
F(3)-As(1)-F(5)	179.9(2)	F(7A)-As(2)-F(11A)	95(2)
F(7A)-As(2)-F(9A)	90.0(14)	F(11A)-As(2)-F(9A)	92(2)
F(7A)-As(2)-F(12A)	94(2)	F(11A)-As(2)-F(12A)	95(2)
F(9A)-As(2)-F(12A)	171.1(14)	F(7A)-As(2)-F(10A)	171.6(14)
F(11A)-As(2)-F(10A)	93(2)	F(9A)-As(2)-F(10A)	89.8(12)
F(12A)-As(2)-F(10A)	85.2(14)	F(8)-As(2)-F(12)	91.8(4)

F(8)-As(2)-F(7)	93.1(6)	F(12)-As(2)-F(7)	92.4(4)
F(8)-As(2)-F(10)	88.8(5)	F(12)-As(2)-F(10)	87.9(4)
F(7)-As(2)-F(10)	178.1(4)	F(8)-As(2)-F(11)	176.8(5)
F(12)-As(2)-F(11)	90.5(3)	F(7)-As(2)-F(11)	89.0(4)
F(10)-As(2)-F(11)	89.1(4)	F(8)-As(2)-F(9)	91.5(4)
F(12)-As(2)-F(9)	176.2(4)	F(7)-As(2)-F(9)	89.4(4)
F(10)-As(2)-F(9)	90.2(4)	F(11)-As(2)-F(9)	86.2(3)
F(7A)-As(2)-F(8A)	87.3(14)	F(11A)-As(2)-F(8A)	177(2)
F(9A)-As(2)-F(8A)	87.1(13)	F(12A)-As(2)-F(8A)	85(2)
F(10A)-As(2)-F(8A)	84.3(13)	F(16A)-As(3)-F(13A)	91(4)
F(14)-As(3)-F(18)	90.3(4)	F(16A)-As(3)-F(15A)	96(4)
F(13A)-As(3)-F(15A)	172(3)	F(14)-As(3)-F(13)	91.4(4)
F(18)-As(3)-F(13)	92.1(3)	F(14)-As(3)-F(15)	89.7(4)
F(18)-As(3)-F(15)	89.3(3)	F(13)-As(3)-F(15)	178.2(3)
F(16A)-As(3)-F(17A)	96(4)	F(13A)-As(3)-F(17A)	84(3)
F(15A)-As(3)-F(17A)	99(3)	F(14)-As(3)-F(17)	90.7(3)
F(18)-As(3)-F(17)	178.7(3)	F(13)-As(3)-F(17)	88.7(3)
F(15)-As(3)-F(17)	89.9(3)	F(14)-As(3)-F(16)	177.8(4)
F(18)-As(3)-F(16)	91.5(3)	F(13)-As(3)-F(16)	89.7(3)
F(15)-As(3)-F(16)	89.2(3)	F(17)-As(3)-F(16)	87.5(3)
F(16A)-As(3)-F(14A)	176(4)	F(13A)-As(3)-F(14A)	93(3)
F(15A)-As(3)-F(14A)	80(3)	F(17A)-As(3)-F(14A)	86(3)
F(16A)-As(3)-F(18A)	94(4)	F(13A)-As(3)-F(18A)	90(2)
F(15A)-As(3)-F(18A)	85(3)	F(17A)-As(3)-F(18A)	168(3)
F(14A)-As(3)-F(18A)	84(2)	F(20)-As(4)-F(22)	179.0(2)
F(20)-As(4)-F(23)	90.4(2)	F(22)-As(4)-F(23)	90.6(2)
F(20)-As(4)-F(19)	90.4(3)	F(22)-As(4)-F(19)	89.2(2)
F(23)-As(4)-F(19)	89.6(2)	F(20)-As(4)-F(21)	90.2(3)
F(22)-As(4)-F(21)	90.3(2)	F(23)-As(4)-F(21)	89.9(2)
F(19)-As(4)-F(21)	179.3(2)	F(20)-As(4)-F(24)	89.5(2)
F(22)-As(4)-F(24)	89.6(2)	F(23)-As(4)-F(24)	179.6(2)
F(19)-As(4)-F(24)	90.7(2)	F(21)-As(4)-F(24)	89.8(2)
N(2)-S(1)-N(1)	103.5(3)	N(2)-S(2)-C(1)	96.8(3)
C(1)-N(1)-S(1)	113.7(5)	S(1)-N(2)-S(2)	113.0(3)
N(1)-C(1)-C(2)	120.2(6)	N(1)-C(1)-S(2)	113.1(5)
C(2)-C(1)-S(2)	126.7(5)	C(3)-C(2)-C(7)	118.0(6)
C(3)-C(2)-C(1)	124.9(6)	C(7)-C(2)-C(1)	117.1(6)
C(2)-C(3)-C(4)	120.8(7)	C(2)-C(3)-Cl(1)	121.0(5)
C(4)-C(3)-Cl(1)	118.2(6)	C(5)-C(4)-C(3)	120.5(7)
C(4)-C(5)-C(6)	119.7(7)	C(5)-C(6)-C(7)	120.6(7)
C(6)-C(7)-C(2)	120.3(7)	N(3)-S(3)-C(8)	96.2(3)
N(3)-S(4)-N(4)	103.5(3)	S(4)-N(3)-S(3)	112.9(4)
C(8)-N(4)-S(4)	113.5(5)	N(4)-C(8)-C(9)	119.3(7)
N(4)-C(8)-S(3)	113.9(5)	C(9)-C(8)-S(3)	126.7(5)
C(14)-C(9)-C(10)	117.6(7)	C(14)-C(9)-C(8)	118.1(6)
C(10)-C(9)-C(8)	124.3(7)	C(11)-C(10)-C(9)	120.6(8)
C(11)-C(10)-Cl(2)	119.4(6)	C(9)-C(10)-Cl(2)	120.0(6)
C(12)-C(11)-C(10)	119.9(8)	C(11)-C(12)-C(13)	121.3(8)
C(12)-C(13)-C(14)	119.2(8)	C(13)-C(14)-C(9)	121.3(8)
N(5)-S(5)-C(15)	96.7(3)	N(5)-S(6)-N(6)	104.2(3)
S(6)-N(5)-S(5)	112.3(4)	C(15)-N(6)-S(6)	112.7(5)
N(6)-C(15)-C(16)	118.6(6)	N(6)-C(15)-S(5)	114.2(5)
C(16)-C(15)-S(5)	127.2(5)	C(21)-C(16)-C(17)	118.4(6)
C(21)-C(16)-C(15)	117.9(6)	C(17)-C(16)-C(15)	123.7(6)
C(18)-C(17)-C(16)	120.3(7)	C(18)-C(17)-Cl(3)	118.6(6)
C(16)-C(17)-Cl(3)	121.0(6)	C(19)-C(18)-C(17)	120.0(7)
C(18)-C(19)-C(20)	121.3(7)	C(19)-C(20)-C(21)	118.7(7)
C(16)-C(21)-C(20)	121.3(7)	N(7)-S(7)-C(22)	96.9(3)
N(7)-S(8)-N(8)	103.7(3)	S(8)-N(7)-S(7)	112.9(4)
C(22)-N(8)-S(8)	113.2(5)	N(8)-C(22)-C(23)	120.0(6)
N(8)-C(22)-S(7)	113.3(5)	C(23)-C(22)-S(7)	126.6(5)
C(24)-C(23)-C(28)	118.8(7)	C(24)-C(23)-C(22)	123.9(7)

-C(23)-C(22)	117.4(6)	C(23)-C(24)-C(25)	120.8(8)
-C(24)-Cl(4)	122.1(6)	C(25)-C(24)-Cl(4)	117.1(7)
-C(25)-C(24)	119.0(9)	C(27)-C(26)-C(25)	120.8(9)
-C(27)-C(28)	119.0(9)	C(27)-C(28)-C(23)	121.6(8)

heme

Figure 3.3.6. The unit cell of 2, containing four molecules

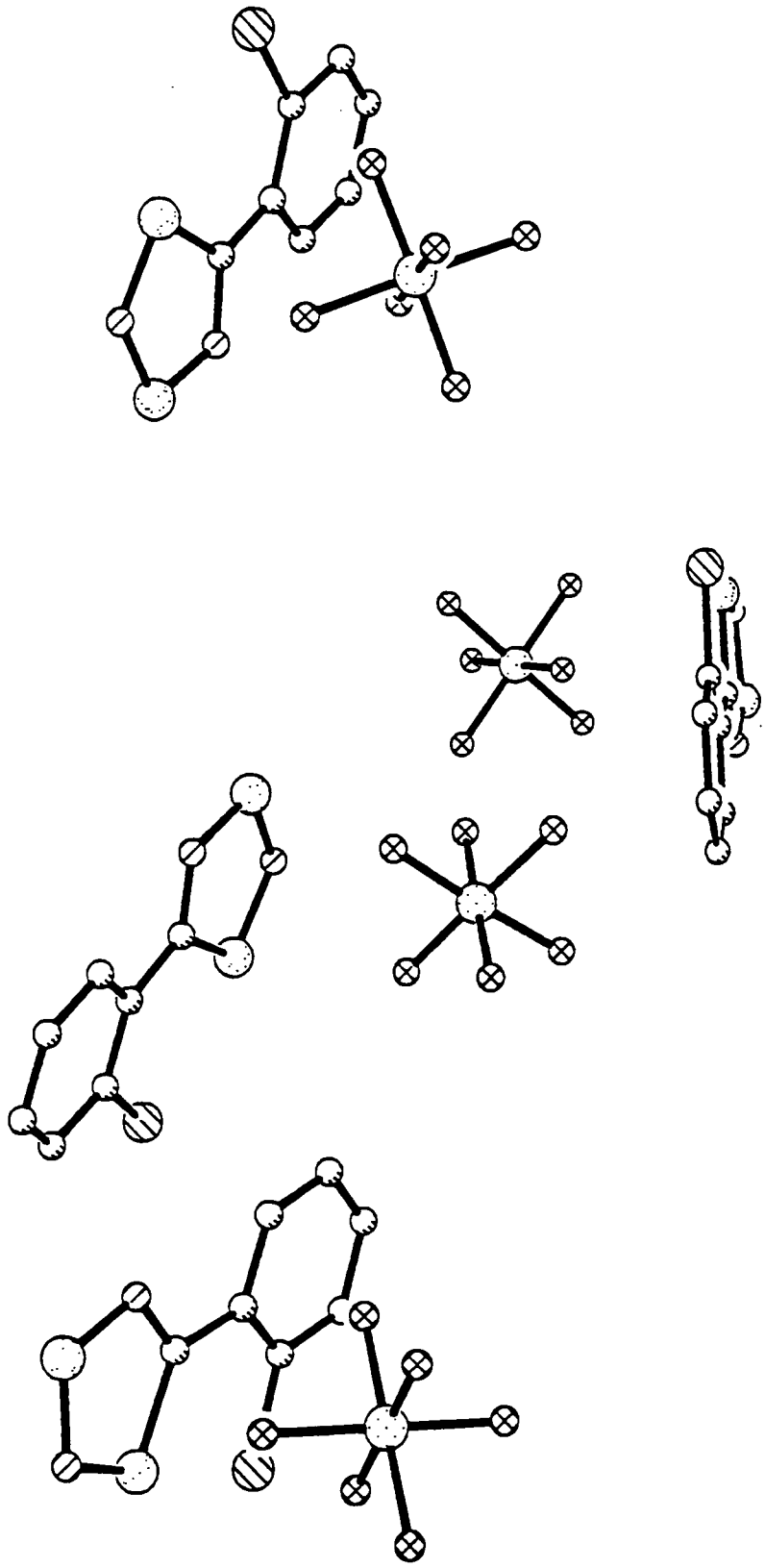

Figure 3.3.7. The packing in **2**

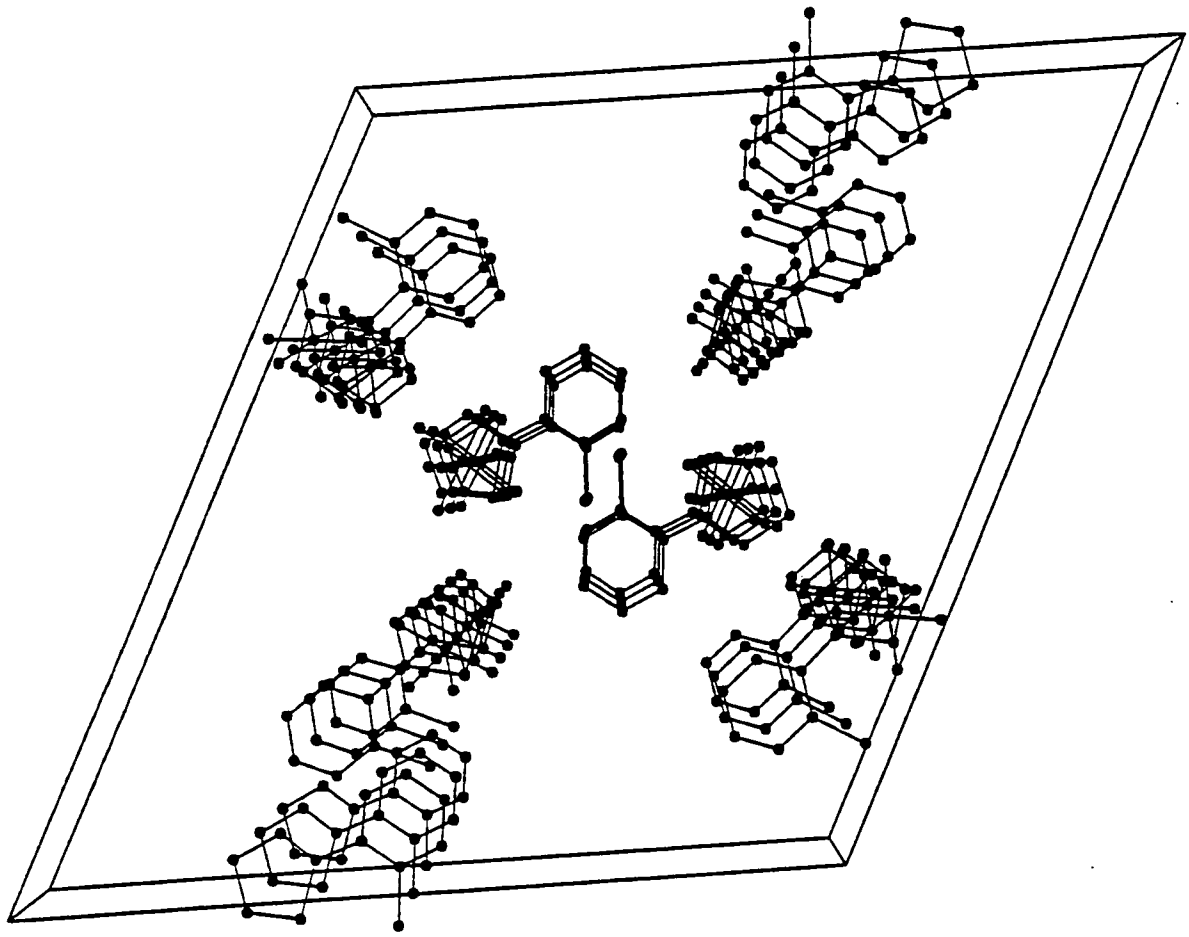

3.4 Reduction data

Esr experiments were carried out on the radical derivatives of all five *ortho*-substitued dithiadiazolium $[AsF_6]^-$ salts discussed in this chapter, the radicals being created *in situ* in the esr tube from a mixture of the $[AsF_6]^-$ salt, $[Et_4N][Cl]$, and Zn/Cu couple. Each radical gave a triplet of 1:1:1 relative intensity, typical of a dithiadiazolyl radical, thus indicating that the ortho-substituents had little effect on the unpaired electron in the radical. These esr experiments were carried out by Dr J.M. Rawson in the Department of Chemistry at the University of Edinburgh.

Cyclic voltammagrams of all five *ortho*-substitued dithiadiazolium $[AsF_6]^-$ salts discussed in this chapter were also run, by Miss C.M. Aherne. These CVs are shown in figures **3.4.1.**, **3.4.2.**, **3.4.3.**, **3.4.4.** and **3.4.5.**

Figure 3.4.1. CV of *ortho*-$[BrC_6H_4CNSNS][AsF_6]$

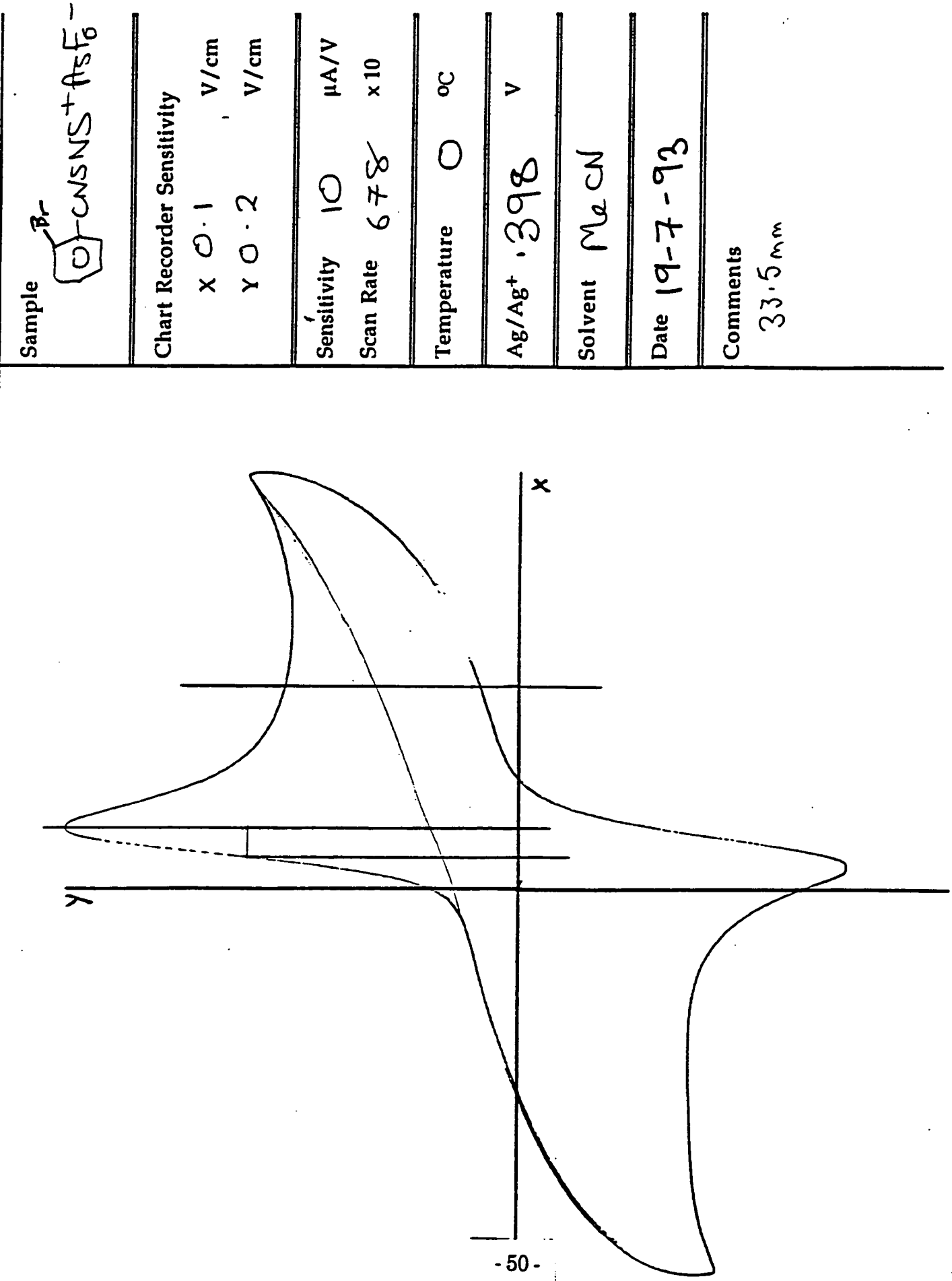

Figure 3.4.2. CV of *ortho*-[ClC_6H_4CNSNS][AsF_6]

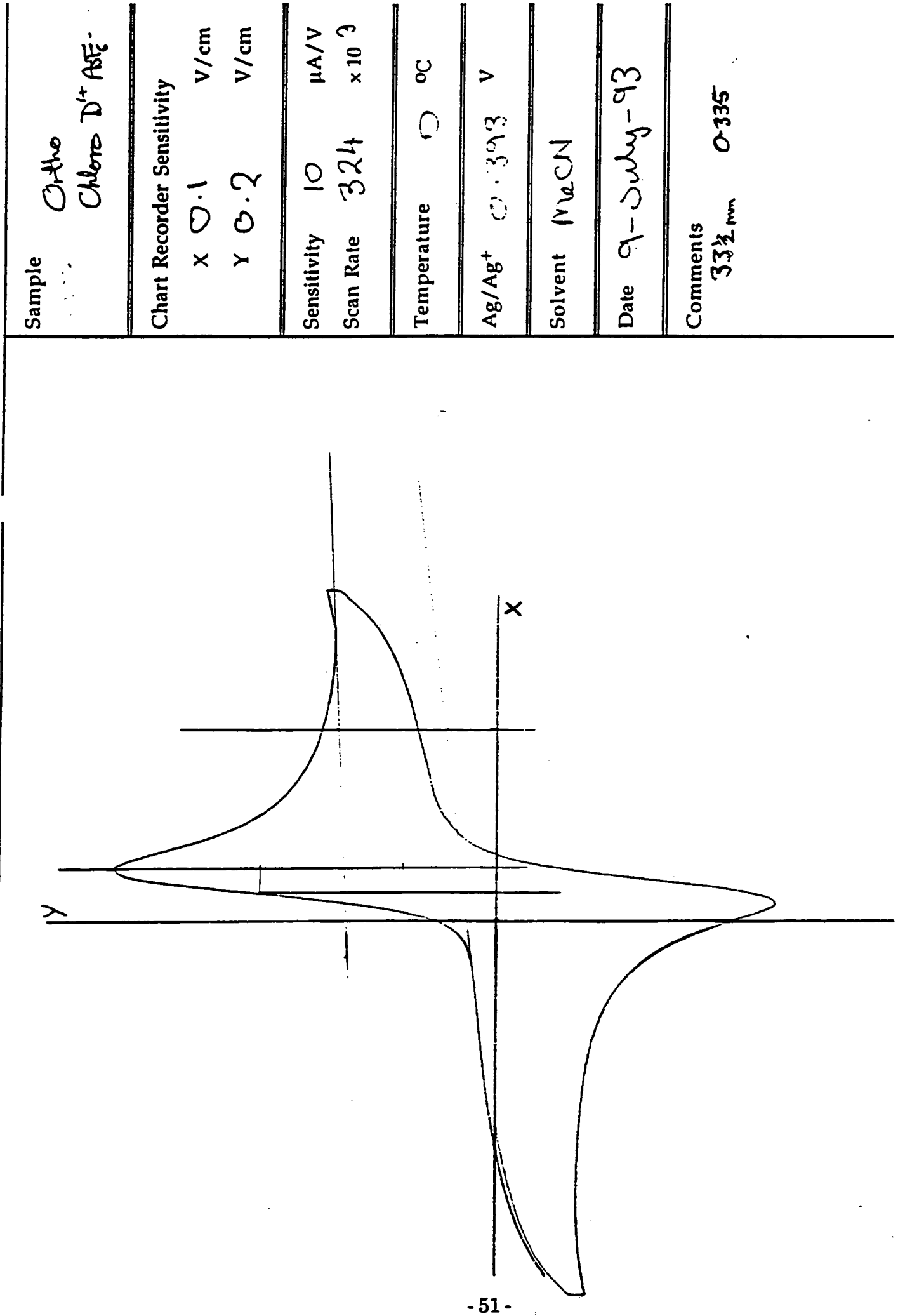

Figure 3.4.3. CV of *ortho*-$[FC_6H_4CNSNS][AsF_6]$

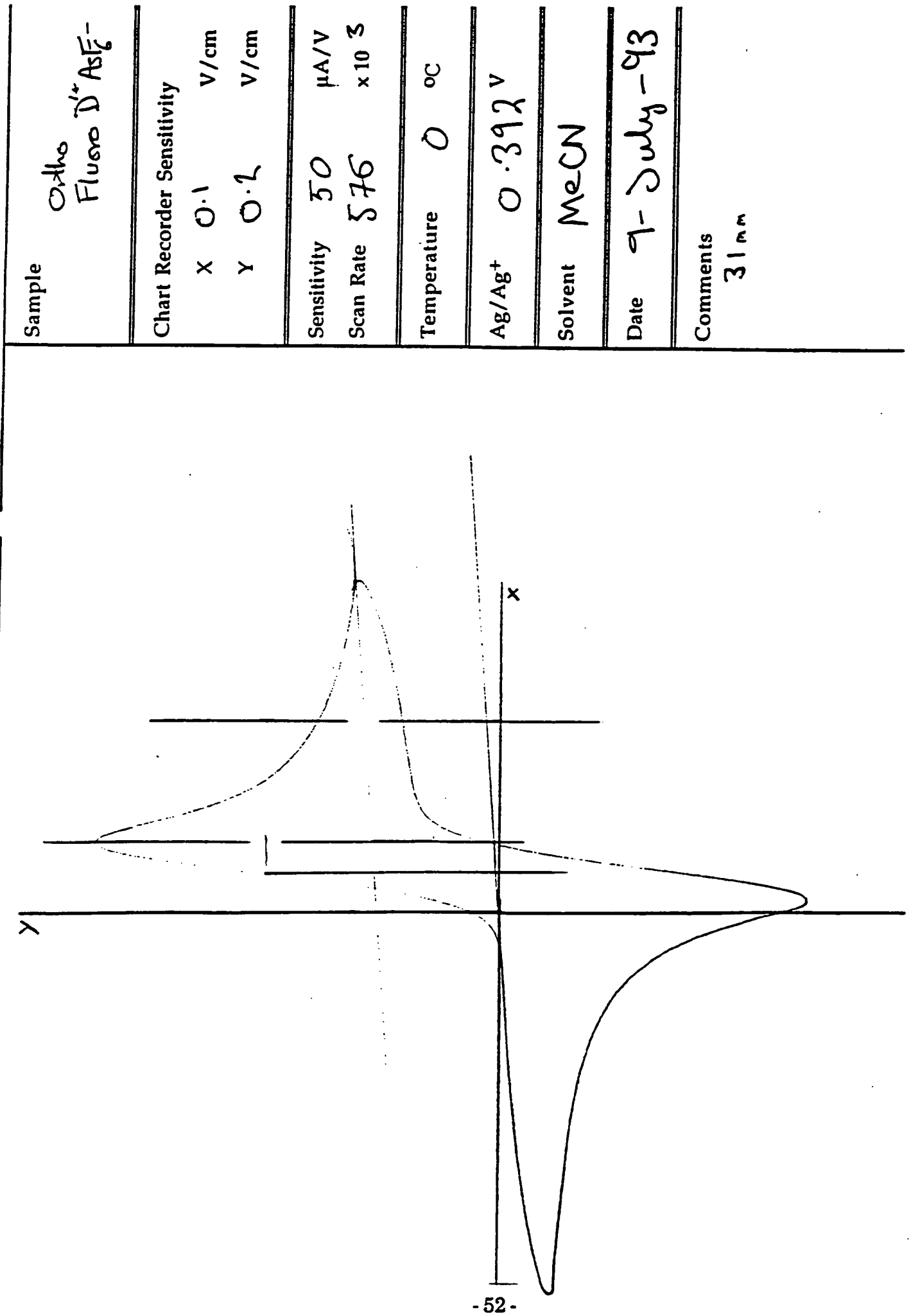

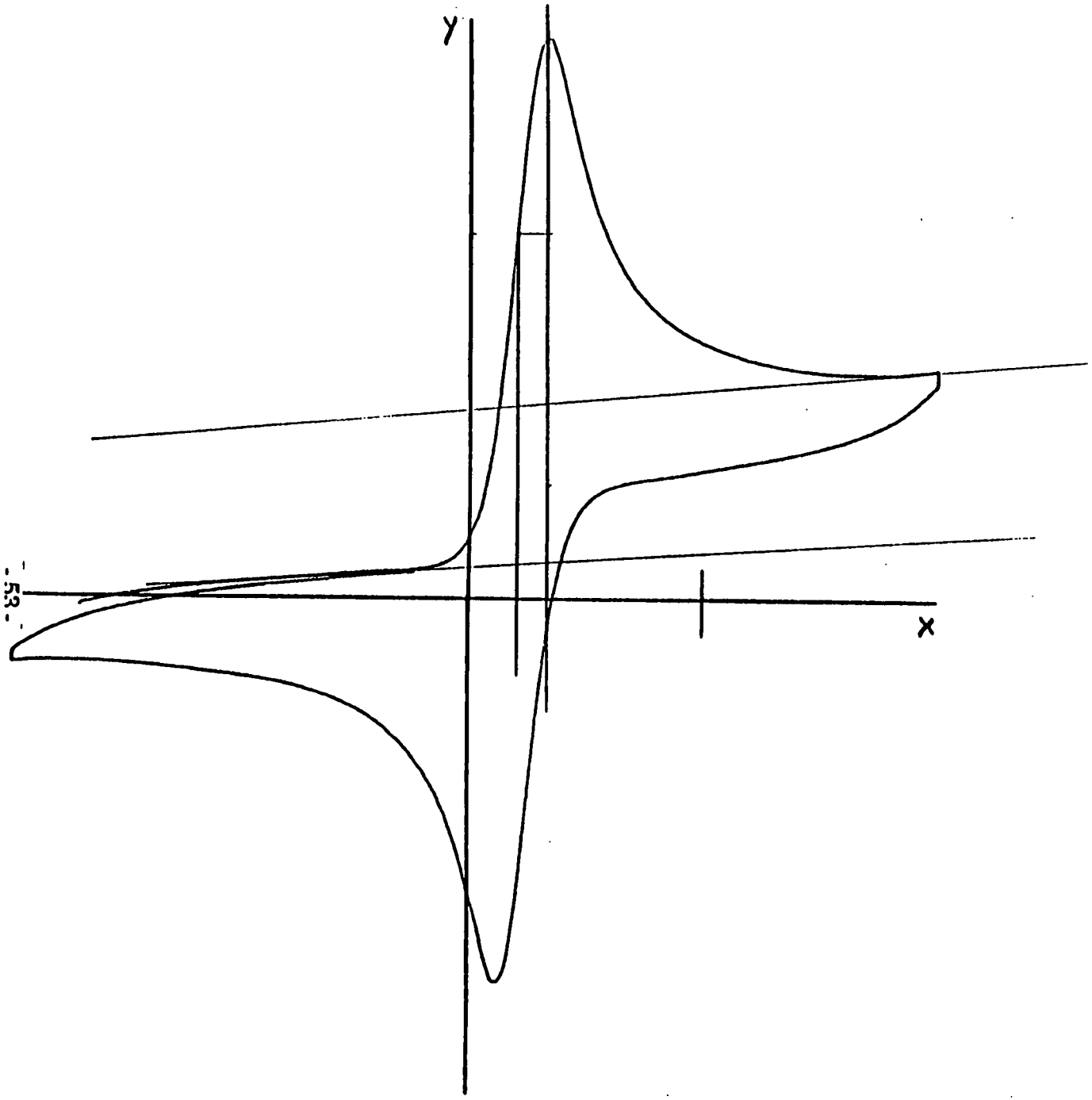

Sample	*o*-Me-C_6H_4-CNSNS$^+$ AsF_6^-	
Chart Recorder Sensitivity		
X	0·1	V/cm
Y	0·2	V/cm
Sensitivity	20	µA/V
Scan Rate	226	x 10
Temperature	0	°C
Ag/Ag$^+$	0·389	V
Solvent	MeCN	
Date	29-7-93	
Comments	31mm	

Figure 3.4.4. CV of *ortho*-[$CH_3C_6H_4CNSNS$][AsF_6]

Figure 3.4.5. CV of *ortho*-$[CF_3C_6H_4CNSNS][AsF_6]$

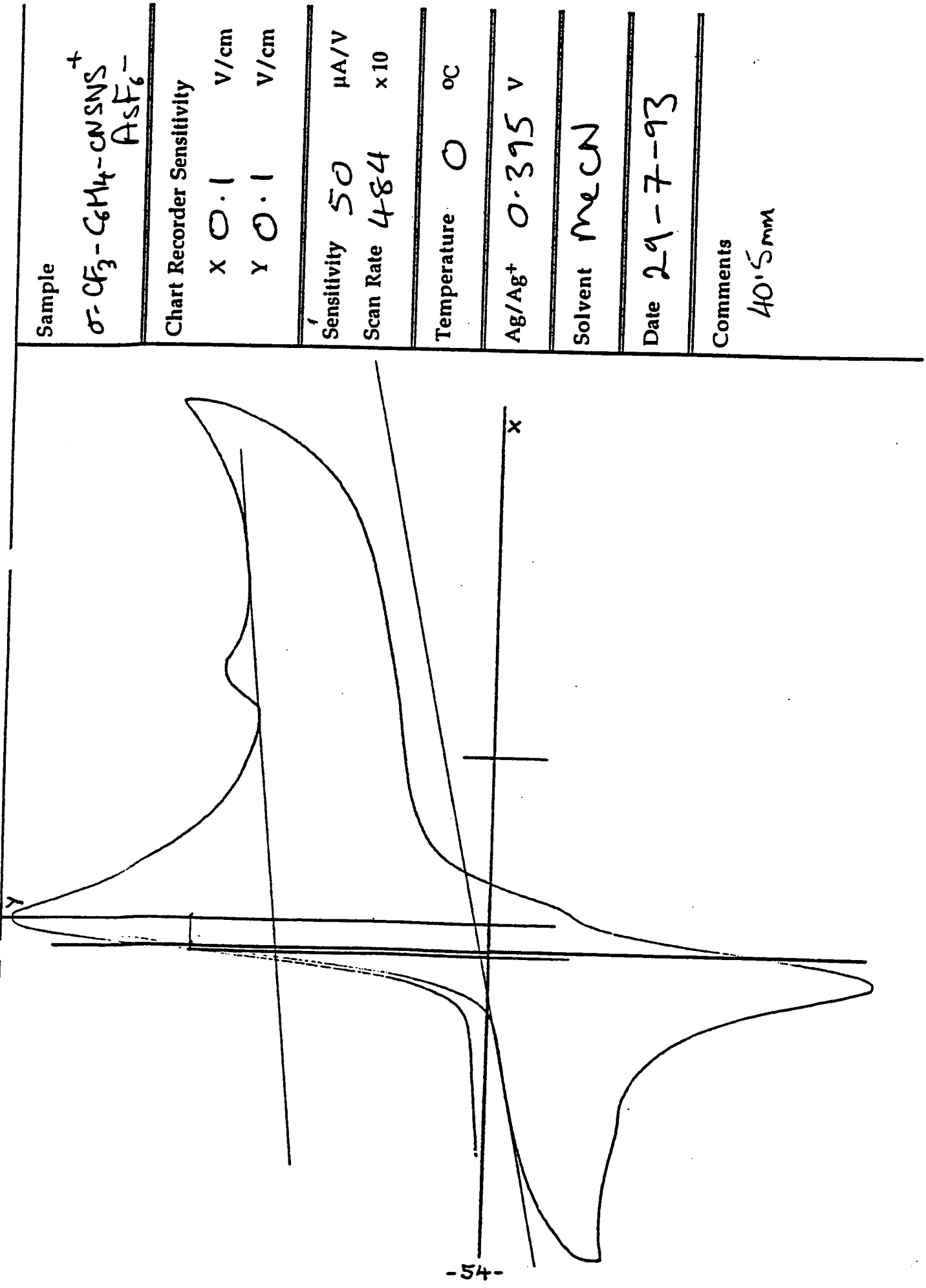

3.5. Experimental

3.5.1. Preparation of *ortho*-[BrC_6H_4CNSNS][AsF_6]

Beige [SNS][AsF_6] (269 mg, 1.01 mmol) was placed, along with white *ortho*-bromobenzonitrile (249 mg, excess) in the rear leg of a 'dog' containing a magnetic follower. SO_2 was condensed into the leg sufficient to dissolve both reagents, giving a red-brown solution. After stirring (18 h, room temperature) the solution was observed to have become darker. Following removal of the solvent, the crude solid was washed with hexane (3 x 10 ml) to remove the unreacted *ortho*-bromobenzonitrile and impurities. The purified product was dried *in vacuo,* and proved to be highly moisture-sensitive.

Appearance: Yellow-green solid
Yield: 338 mg, 0.769 mmol, 76.2%
IR (Nujol mull, KBr plates) ν_{max}: 1734 w; 1646 vw,br; 1584 vw,br; 1559 s; 1308 w; 1292w; 1276 m; 1213 vw; 1170 w; 1126 vw,sh; 1082 vw; 1059 w; 1029 s; 983 s; 915 m; 903 w; 794 s; 780 m; 771 s; 755 vw; 701 vs,br; 669 w,sh; 577 m; 484 vw; 451 vw,sh; 440 w; 428 vw,sh. cm^{-1}
Mass Spectra (E.I.): 181 (M^+-Br), 141 ($C_6H_4S_2^+$), 115 ($C_6H_4CN_2^+$), 102 ($C_6H_4CN^+$), 77 ($C_6H_4^+$), 64 (S_2^+), 46 (SN^+). See scheme **3.2.1.** (C.I.): 199, 184, 140, 106, 88, 78.
Chemical Analysis: Found (%) C: 18.87 H: 0.98 N: 6.35
Required (%) C: 18.72 H: 0.90 N: 6.24

3.5.2. Preparation of *ortho*-[ClC_6H_4CNSNS][AsF_6]

Beige [SNS][AsF_6] (180 mg, 0.67 mmol) was placed, along with white *ortho*-chlorobenzonitrile (105 mg, excess) into the rear leg of a 'dog' containing a magnetic follower. Sufficient SO_2 was condensed into the leg to dissolve both reagents, giving a red-brown solution. After stirring (18 h, room temperature) the solution had darkened. The solvent was removed and the crude product was washed with hexane (3 x 10 ml) to remove the unreacted *ortho*-chlorobenzonitrile and impurities. The purified product, dried *in vacuo* was highly moisture-sensitive.

Appearance: Yellow solid
Yield: 296 mg, 0.490 mmol, 74.7%

IR (Nujol mull, KBr plates) ν_{max}: 1660 s; 1592 w,sh; 1133 m; 1059 s; 1035 w; 984 m,br; 717 w; 756 w; 721 vs,br; 630 m,sh; 575 m;556 s; 490w cm^{-1}

Mass Spectra (E.I.): 169 (M^+-SN), 160 (?), 137 ($ClC_6H_4CN^+$), 102 ($C_6H_4CN^+$), 64 (S_2^+). See scheme **3.2.3.**

Chemical Analysis. Found (%) C 17.92 H 2.48 N 3.80

Required (%) C 19.84 H 2.22 N 3.86

3.5.3. Preparation of ortho-[FC_6H_4CNSNS][AsF_6]

Beige [SNS][AsF_6] (259 mg, 0.97 mmol) was placed in one leg of a 'dog' along with a magnetic follower, and colourless *ortho*-fluorobenzonitrile (0.3 ml, excess) was syringed into the other leg against a dry nitrogen counterflow. Sufficient SO_2 was condensed into each leg to dissolve the reagents. The [SNS][AsF_6] solution was red-brown, whilst the *ortho*-fluorobenzonitrile solution remained colourless. The *ortho*-fluorobenzonitrile solution was then added to the [SNS][AsF_6] solution and stirred (18 h, room temperature). After this time the solution was observed to have darkened. The solvent was removed and the crude product was washed with hexane (3 x 10 ml) to remove unreacted *ortho*-fluorobenzonitrile and impurities. The purified product was dried *in vacuo* and was highly moisture-sensitive.

Appearance: Yellow solid

Yield: 265 mg, 0.697 mmol, 71.8%

IR (Nujol mull, KBr plates) ν_{max}: 1648 w; 1612 s,br; 1514 vw,br,sh; 1486 m; 1403 s; 1318 w; 1287 m; 1270 w; 1237 m; 1224 w; 1200w; 1162 m; 1157 w; 1109 m; 1100 w,sh; 1028 vw,br; 990 s; 968 w; 923 m; 917 w; 898 m; 875 w; 860 vw,br; 815 m; 792 s; 779 s; 770 m,sh; 758 vw; 737 w,sh; 700 vs,br; 670 m,sh; 630 w; 585 w; 540 w; 524 vw,br; 456 vw,br; 438 m; 400 vs; 363 w,br; 276 w,br. cm^{-1}

Mass Spectra (E.I.): 121 ($C_6H_4CS^+$) 94 ($C_6H_4F^+$), 78 ($C_6H_4^+$), 64 (S_2^+), 46 (SN^+). See scheme **3.2.4.**

Chemical Analysis: Found (%) C 21.58 H 1.06 N 7.16

Required (%) C 21.30 H 1.29 N 7.20

3.5.4. Preparation of *ortho*-[$CH_3C_6H_4CNSNS$][AsF_6]

Beige [SNS][AsF_6] (236 mg, 0.88 mmol) was placed, together with a magnetic follower, in one leg of a 'dog', and colourless *ortho*-

methylbenzonitrile (0.3, excess) was syringed into the other leg against a dry nitrogen counterflow. Sufficient SO_2 was condensed into each leg to dissolve both reagents. The [SNS][AsF_6] solution was red-brown, whilst the *ortho*-methylbenzonitrile solution remained colourless. The *ortho*-methylbenzonitrile solution was then transferred to the [SNS][AsF_6] and stirred (24 h, room temperature). After stirring the solution had darkened. The solvent was removed and the crude product washed with pentane (3 x 10 ml) to remove unreacted *ortho*-methylbenzonitrile and impurities, before being dried *in vacuo*.

Appearance: Bright yellow solid
Yield: 238 mg, 0.618 mmol, 70.2%
IR (Nujol mull, KBr plates) ν_{max}: 2360 w; 1600 w; 1402 s; 1294 m; 1212 w; 1172 w; 1116 vw; 980 w; 911 vw; 806 m; 772 s; 760 w,sh; 692 vs,br; 636 m; 588 vw; 444 m,sh. cm^{-1}
Mass Spectra (E.I.): 149 (M^+-SN), 117 (M^+-S_2N), 90 ($C_6H_4CH_3^+$), 71 ($CNSN^+$), 64 (S_2^+), 57 (CSN^+), 51 (?). See scheme **3.2.5.**
(C.I.): 152, 135, 52.
Chemical Analysis : Found (%) C 24.42 H 1.83 N 7.30
Required (%) C 25.01 H 1.84 N 7.29

3.5.5. Preparation of ortho-[$CF_3C_6H_4CNSNS$][AsF_6]

Beige [SNS][AsF_6] (236 mg, 0.88 mmol.).was placed, along with a magnetic follower, in one leg of a 'dog' and colourless *ortho*-(trifluoromethyl)benzonitrile (0.5 ml, excess) was syringed into the other leg against a dry nitrogen counterflow. Sufficient SO_2 was condensed into each leg to dissolve the reagents. The [SNS][AsF_6] solution was red-brown, whilst the *ortho*-(trifluoromethyl)benzonitrile solution remained colourless. This solution was then added to the [SNS][AsF_6] solution and stirred (24 h, room temperature). After this time the solvent was removed and the crude product was washed with pentane (3 x 10 ml) to remove unreacted *ortho*-(trifluoromethyl)benzonitrile and impurities. The product was then dried *in vacuo*.

Appearance: Pale beige solid
Yield: 293 mg, 0.681 mmol, 77.4%
IR (Nujol mull, KBr plates) ν_{max}: 1984 vw; 1676 vw; 1597 m; 1580 m; 1419 m,sh; 1318 m; 1302 m,sh; 1160 w; 1121 s,br; 1067 m; 1041 m; 985

m; 908 w; 879 w; 803 s; 784 s; 704 vs,br; 662 m,sh; 639 m,sh; 596 m,sh; 589 m; 570 m; 452 s cm^{-1}

Mass Spectra (E.I.): 203 (M^+-SN), 171 (M^+-S_2N), 152 (M^+-S_2NF), 121 ($C_6H_4CSN^+$), 102 ($C_6H_4CN^+$), 96 ($C_6H_4F^+$) 75 ($C_6H_4^+$), 64 (S_2^+), 50 (SF^+), 46 (SN^+). See scheme **3.2.6.**

(C.I.): 189, 140, 100, 78, 46.

Chemical Analysis : Found (%) C 20.93 H 0.85 N 6.34

Required (%) C 20.06 H 0.92 N 6.39

3.5.6. Attempted Preparation of *ortho*-[(NC)C_6H_4CNSNS][AsF_6]

Beige [SNS][AsF_6] (267 mg, 1.00 mmol.). and white 1,2-dicyanobenzene (128 mg, 1.00mmol) were placed in one leg of a 'dog', along with a magnetic follower. Sufficient SO_2 was condensed into the leg to dissolve both reagents, the solution being a red-brown colour. The solution was stirred (18 h, room temperature) and the solvent was removed leaving a straw coloured microcrystalline solid. An IR spectrum of this solid was run, and is shown below.

IR (Nujol mull, KBr plates) ν_{max}: 2227 m; 1732 w,br; 1580 m,br; 1421 m; 1400 s; 1302 m; 1290 m; 1283 vw,sh; 1220 m; 1202 vw;1170 w,br; 1152 vw; 1097 w; 1074 vw; 1050 w; 1017 w,br; 990 s; 966 w,sh; 918 m; 901 m; 890 m; 877 w; 864 vw,sh; 801 s; 784 s;764 m; 700 vs,br; 642 vw; 634 m; 595 m; 588 m; 576 m; 552 s; 528 vw; 489 w; 470 w; 455 m; 440 s; 398 vs; 348 vw cm^{-1}.

3.5.7. Preparation of *ortho*-[BrC_6H_4CNSNS][Cl]

Yellow-green ortho-[BrC_6H_4CNSNS][AsF_6] (157 mg, 0.35 mmol).and white [Bu_4N][Cl] (100 mg, excess) were placed, together with a magnetic follower, in one leg of a 'dog'. Dry CH_2Cl_2 (10 ml) was syringed onto the reactants against a dry nitrogen counterflow. Both reactants dissolved yielding a dull green solution. After stirring (24 h, room temperature) an off-white solid ([Bu_4N][AsF_6]) was observed to have formed below a red-brown solution. The solution was decanted and the solvent removed leaving a yellow solid, which was washed with pentane (3 x 10 ml) before being dried *in vacuo*.

Appearance: Bright yellow solid

Yield: 68 mg, 0.23 mmol, 66%

IR (Nujol mull, KBr plates) ν_{max}: 2361 w; 1733 vw; 1578 m; 1408 m,sh; 1304 m; 1288 m; 1267 m; 1212 w; 1164 m; 1056 vw; 1028 w; 970 w; 936 w; 851 w; 770 s; 758 s; 722 s; 710 m; 664 vw; 631 vw; 622 vw; 574 m. cm^{-1}

Mass Spectra (E.I.): 397 ($C_6H_4(CNSNS)_2Cl^+$), 260 (M^+), 199 (M^+-SN_2), 78 (S_2N^+), 64 (S_2^+). See scheme **3.2.7.**

Chemical Analysis: Found (%) C 27.21 H 1.28 N 9.84

Required (%) C 28.44 H 1.37 N 9.48

3.6. References

1. A.J. Banister and J.M. Rawson, in *The Chemistry of Inorganic Ring Systems.*, R. Steudel (Ed.), Elsevier, Amsterdam, 1992, p 323.

2. A.J. Banister and J.M. Rawson, *Chem. Br.*, **1991**, 148.

3. G.G. Alange, A.J. Banister, B. Bell and P.W. Millen, *J. Chem. Soc., Perkin Trans. 1*, **1979**, 1192.

4. J.M. Rawson, PhD Thesis, Durham University, 1990.

5. G.K. MacLean, J. Passmore, M.N.S. Rao, M.J. Schriver, P.S. White, D. Bethell, R.S. Pilkington and L.H. Sutcliffe, *J. Chem. Soc., Dalton Trans.*, **1985**, 1405.

6. G.G. Alange, A.J. Banister and P.J. Dainty, *Inorg. Nucl. Chem. Lett.*, **15**, 1979, 175.

7. A.J. Banister, N.R.M. Smith and R.G. Hey, *J. Chem. Soc., Perkin Trans.*, **1983**, 1181.

8. N. Burford, J. Passmore and M.J. Schriver, *J. Chem. Soc., Chem. Commun.*, **1986**, 110.

9. P.D.B. Belluz, A.W. Cordes, E.M. Kristof, S.W. Liblong and R.T. Oakley, *J. Am. Chem. Soc.*, **111**, 1989, 9276.

10. A.W. Cordes, S.H. Glarum, R.C. Haddon, R. Halford, R.G. Hicks, D.K. Kennepohl, R.T. Oakley, T.T.M. Palstra and S.R. Scott, *J. Chem. Soc., Chem. Commun.*, **1992**, 1265.

11. I. Lavender, personal communication.

12. A.J. Banister, A.W. Luke, J.M. Rawson, R.J. Whitehead and R. Singer, **1993**, manuscript in preparation.

13. A.J. Banister, I. Lavender, J.M. Rawson and R.J. Whitehead, *J. Chem. Soc., Dalton Commun.*, **1992**, 1499.

14. A.J. Banister, I. Lavender, J.M. Rawson, W. Clegg, B.K. Tanner and R.J. Whitehead, *J. Chem. Soc., Dalton Trans.*, **1993**, 1421.

15. C.M. Aherne, A.J. Banister, A.W. Luke, J.M. Rawson and R.J. Whitehead, *J. Chem. Soc., Dalton Trans.*, **1992**, 1277.

16. A.W. Cordes, R.C. Haddon, R.T. Oakley, L.F. Schneemeyer, J.V. Waszczak, K.M. Young and N.M. Zimmerman, *J. Am. Chem. Soc.*, 113, **1991**, 582.

17. A.J. Banister, I. Lavender, J.M. Rawson and D.B. Lambrick, *J. Chem. Soc., Dalton Trans.*, **1993**, manuscript in preparation.

18. C.M. Aherne, personal communication.

19. A.W. Luke, PhD Thesis, Durham University, 1992.

20. W. Clegg, personal communication.

Chapter 4 Novel reactions of [SNS][AsF_6] with double bonds

4.1. Introduction

In contrast to the large amount of work carried out on the reactions of [SNS][AsF_6] with triple bonds, the only double bond reactions that have been extensively studied are with C=C[1,2]. In this chapter the reactions of [SNS][AsF_6] with N=N, C=N, P=N and P=P moieties are described, all of which yield 1:1 addition products. The failure to grow single crystals of these compounds suitable for x-ray diffraction means that they have yet to have their structures definitively characterised, but nmr studies of the P=N and P=P addition products suggest that they, at least, possess acyclic structues (see figure **4.1.1.**). This is in contrast to known C=C product structures[1,2] which are cyclic. ^{31}P nmr studies of [Ph_3P=S=N-S=PPh_3][AsF_6] gave a signal at 36.57 ppm which is in the correct spectral region for 4-coordinate phosphorus(V) (*i.e.* the acyclic form) but outside the region for 5-coordinate phosphorus(V) (*i.e.* the cyclic form). ^{19}F and ^{31}P nmr spectra of the diphosphene product also indicate an acyclic structure (see section **4.2.5.**).

The P-N single bond (at 298 kJmol-1 [4]) is comparable in strength to the C-N sinle bond (305 kJmol-1 3), and is considerably stronger than the N-N single bond (167 kJmol-1 3), but there is no direct evidence for the structures of the C=N and N=N addition products. For simplicity, all addition products in this chapter are illustrated as having acyclic structures.

Figure 4.1.1. Generalised cyclic and acyclic structures

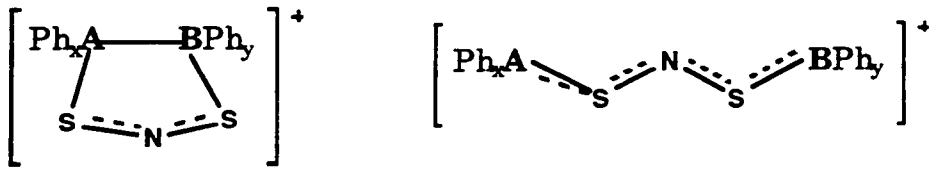

CYCLIC FORM ACYCLIC FORM

No work directly analogous to the work described in this chapter has, to the authors knowledge, been undertaken previously. The related products [PhSNSNSNSPh][AsF_6] (synthesised by Dr I. Lavender[5]) and many neutral acyclic azathienes (prepared by Zibarev and co-workers[6-9]) were obtained by quite different routes.

4.2. Results and Discussions

4.2.1. The reaction of azobenzene with [SNS][AsF_6]

Reaction of azobenzene with [SNS][AsF_6] in liquid SO_2 over 24 hours gave 1,5-diphenyl-2,4,1,3,5-dithiatriazonium hexafluoroarsenate(V), **1**, (see figure **4.2.1.**) in 72.8 % yield. The product, a black solid, was soluble in SO_2 and CH_3CN but insoluble in CH_2Cl_2. The IR spectrum of **1** was compared with spectra of the starting materials, showing that **1** was not simply a mixture of [SNS][AsF_6] and azobenzene. [SNS][AsF_6] has IR active resonances[1] at 1488 and 1030 cm^{-1} (corresponding to $[SNS]^+$) and at 695 and 398 cm^{-1} (due to $[AsF_6]^-$). As expected, the $[SNS]^+$ resonances are not present in **1**, and the $[AsF_6]^-$ resonances have shifted to 702 and 399 cm^{-1} respectively. The spectrum of **1** bears a superficial resemblance to a spectrum of azobenzene, but most of the peaks are displaced. The Ph-N peak in azobenzene, at 1584 cm^{-1}, moves to 1580 cm^{-1} in **1**, and the phenyl out-of-plane deformations in azobenzene (at 761, 722 and 688 cm^{-1}) appear in **1** at 773 and 690 cm^{-1} (the middle peak is masked by the strong, broad AsF_6^- peak at 702 cm^{-1}). The peaks in **1** at 1070 and 976 cm^{-1}, absent in azobenzene, have been tentatively assigned to dithiatriazonium S-N bending modes[10].

Figure 4.2.1. 1,5-diphenyl-2,4,1,3,5-dithiatriazonium hexafluoroarsenate(V)

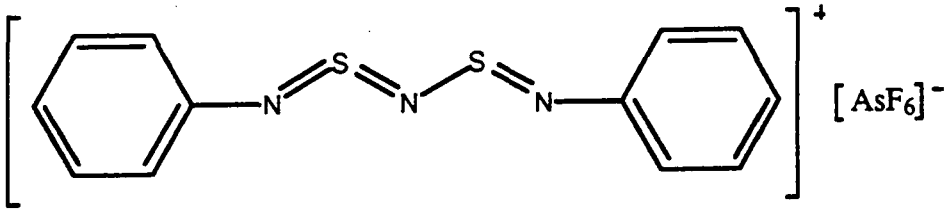

The mass spectrum (E.I.) of **1** showed an excellent breakdown pattern (see scheme **4.2.1.**) including, unusually for an AsF_6^- salt, the parent cation. Very good elemental analysis figures (C,H,N) were obtained for a sample of **1**. Differential scanning calorimetry measurements gave a sharp melting point for **1** of 252 °C +/- 1°C, compared to > 400 °C for [SNS][AsF6] and a literature value[11] of 69 °C for azobenzene. There was no sign of a peak at 69 °C in the DSC trace of **1**.

Numerous attempts to grow single crystals of **1** suitable for x-ray diffraction were ultimately unsuccessful.

Scheme 4.2.1. The mass spectrum (E.I.) of [PhN=S=N-S=NPh][AsF_6]

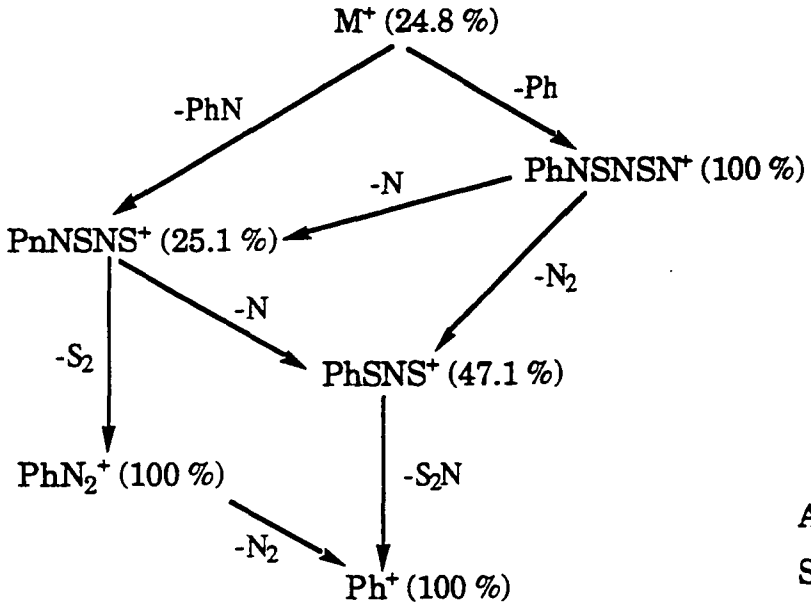

4.2.2. The reaction of triphenylenamine with [SNS][AsF_6]

Reaction of triphenylenamine (Ph_2C=NPh) with [SNS][AsF_6] in liquid SO_2 over 18 hours gave 1,1-diphenylmethylene-5-phenyl-2,4,3,5-dithiadiazonium hexafluoroarsenate(V), **2**, (see figure **4.2.2.**) in 82.9 % yield. The product, an olive green solid, was soluble in SO_2 and CH_3CN but insoluble in CH_2Cl_2. An IR spectrum of **2** was compared to spectra of the starting materials, illustrating that **2** was not simply a mixture of [SNS][AsF_6] and triphenylenamine. The $[SNS]^+$ IR peaks present in [SNS][AsF_6] (at 1488 and 1030 cm^{-1}) are absent in **2**, and the $[AsF_6]^-$ peaks in [SNS][AsF_6] (at 695 and 398 cm^{-1}) are shifted in **2** to 700 and 400 cm^{-1} respectively. The Ph-N peaks in Ph_2C=NPh (at 1597 and 1562 cm^{-1}) also appear in **2**, but displaced to 1589 and 1564 cm^{-1} respectively. The peaks in **2** at 1076 and 969 cm^{-1} have been tentatively assigned to S-N bending modes[10]. The fact that $[SNS]^+$ addition causes complete breaking of the reasonably strong C=N bond is perhaps worthy of note.

Figure 4.2.2. 1,1-diphenylmethylene-5-phenyl-2,4,3,5-dithiadiazonium hexafluoroarsenate(V)

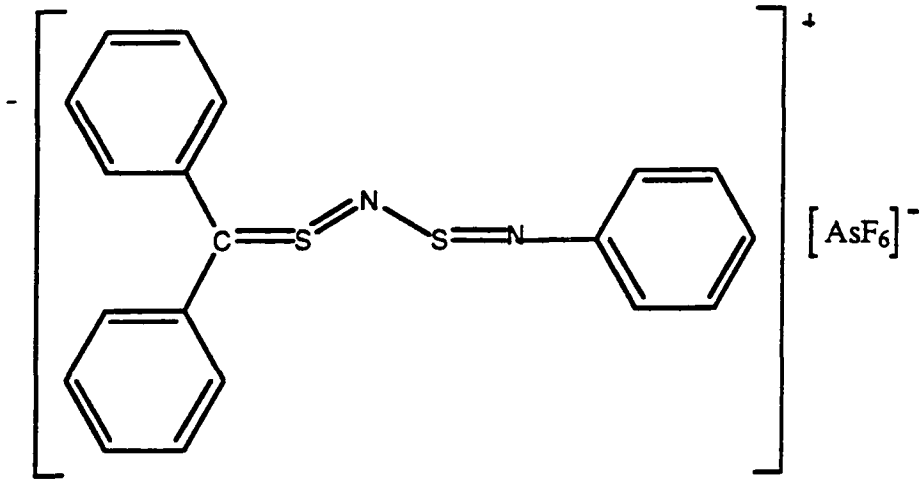

The mass spectrum (E.I.) of **2** showed a good breakdown pattern (see scheme **4.2.2.**). Reasonable chemical analysis figures (C,H,N) were obtained for a sample of **2**. Differential scanning calorimetry measurements gave a melting point for 2 of 148 °C +/- 2 °C, compared with > 400 °C for both [SNS][AsF_6] and Ph_2C=NPh. Attempts to grow single crytals of **2** suitable for x-ray difraction proved unsuccessful.

Scheme 4.2.2. The mass spectrum (E.I.) of [Ph_2C=S=N-S=NPh][AsF_6]

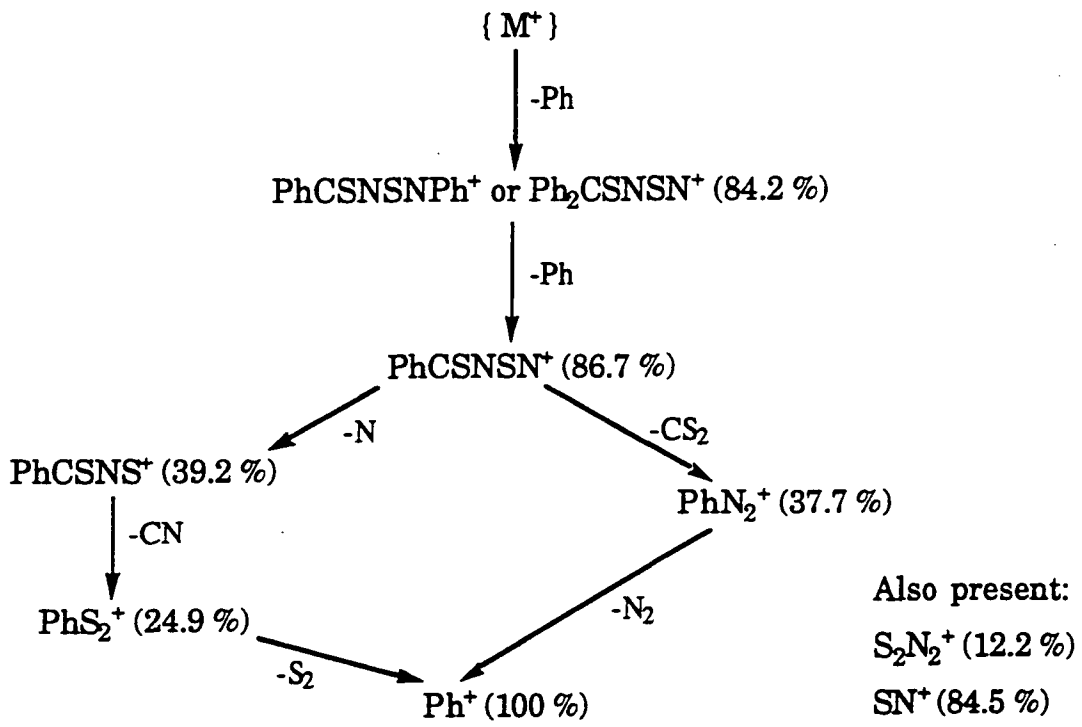

4.2.3. The reaction of tetraphenylphosphene imide with [SNS][AsF_6]

Reaction of tetraphenylphosphine imide (Ph_3P=NPh) with [SNS][AsF_6] in liquid SO_2 over 18 hours gave 1,1,1-triphenylphosphene-5-phenyl-2,4,3,5-dithiadiazonium hexafluoroarsenate(V), **3**, (see figure **4.2.3.**) in 89.8 % yield. The product, a black solid, was soluble in SO_2 and CH_3CN but insoluble in CH_2Cl_2. An IR spectrum of **3** was run and compared with spectra of the starting materials, showing that **3** was not simply a mixture of [SNS][AsF_6] and Ph_3P=NPh. The $[SNS]^+$ peaks present in [SNS][AsF_6] at 1488 and 1030 cm^{-1} were absent in **3**, and the $[AsF_6]^-$ peaks in [SNS][AsF_6] at 695 and 398 cm^{-1} are shifted in **3** to 701 and 400 cm^{-1} respectively. The Ph-N peak in Ph_3P=NPh (at 1584 cm^{-1}) is present in **3**, but shifted to 1588 cm^{-1}. The peak in **3** at 964 cm^{-1} has been tentatively assigned to an S-N bending mode[10].

Figure 4.2.3. 1,1,1-triphenylphosphene-5-phenyl-2,4,3,5-dithiadiazonium hexafluoroarsenate(V)

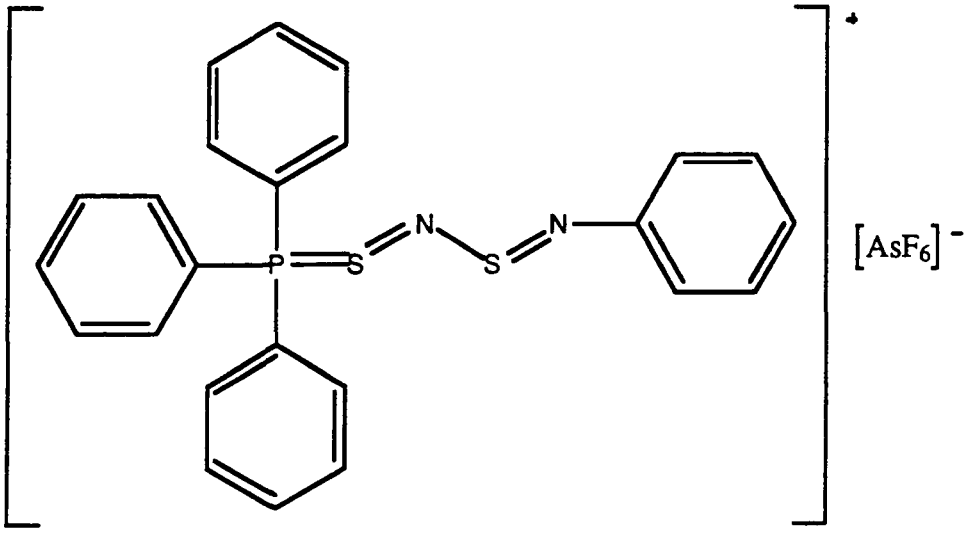

A ^{31}P nmr study of **3** (CD_3CN solvent) showed a strong signal at 36.57 ppm, attributable to $[Ph_3P$=S=N-S=NPh$]^+$. A smaller signal at 31.20 ppm is believed to correspond to the species ($[Ph_3P$=S=N-S=NPh$]_2)^{2+}$, supported by the fact that this signal diminishes in intensity at higher temperatures.

The mass spectrum (E.I.) of **3** showed a good breakdown pattern (see scheme **4.2.3.**) Acceptable elemental analysis figures (C,H,N) were obtained for a sample of **3**. Differential scanning calorimetry measurements gave a melting point for **3** of 338 °C +/- 2 °C, compared with

> 400 °C for both [SNS][AsF_6] and Ph_3P=NPh. Attempts to grow single crystals of **3** suitable for x-ray diffraction were unsuccessful.

Scheme 4.2.3. The mass spectrum (E.I.) of [Ph_3P=S=N-S=NPh][AsF_6]

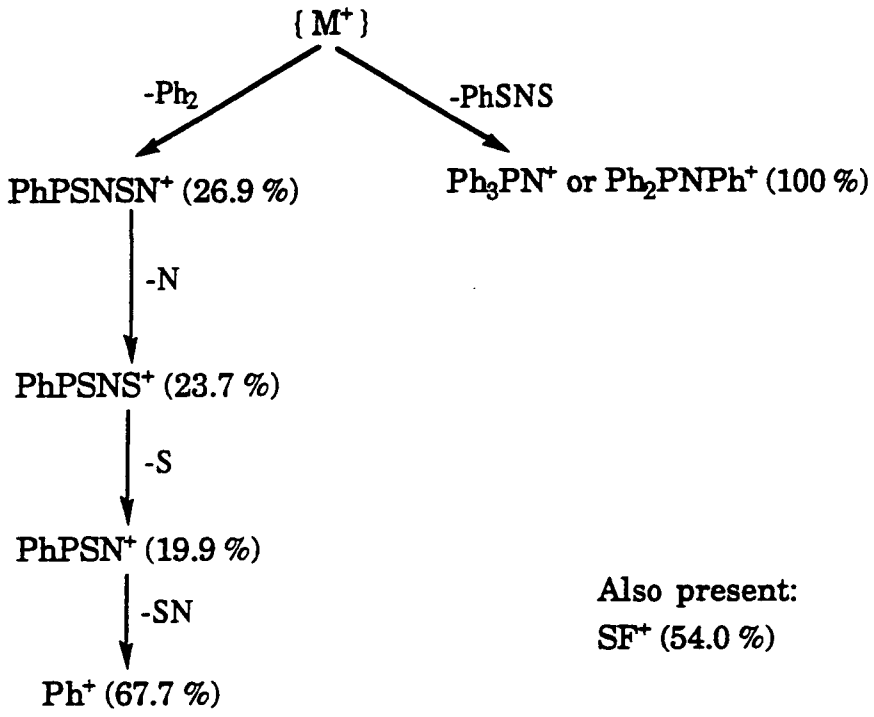

4.2.4. The reaction of 1,2-*bis*-tert-butyl-diazene with [SNS][AsF_6]

Reaction of 1,2-*bis*-tert-butyl-diazene ($^tBuN{=}N^tBu$) with [SNS][AsF_6] in liquid SO_2 over 24 hours gave 1,5-*bis*-tert-butyl-2,4,1,3,5-dithiatriazonium hexafluoroarsenate(V), **4**, (see figure **4.2.4.**) in 49.5 % yield. The product, a dark orange solid, was soluble in SO_2. An IR spectrum of **4** was run and compared with a spectrum of [SNS][AsF_6] (despite numerous attempts, a satisfactory spectrum of the liquid $^tBuN{=}N^tBu$ was not obtained). The $[SNS]^+$ peaks present in [SNS][AsF_6] (at 1488 and 1030 cm^{-1}) are absent in **4**, and the $[AsF_6]^-$ peaks in [SNS][AsF_6] at 695 and 398 cm^{-1} are shifted in **4** to 721 and 402 cm^{-1} respectively. The peak at 948 cm^{-1} in **4** has been tentatively assigned to an S-N bending mode[10].

Figure 4.2.4. 1,5-*bis*-tert-butyl-2,4,1,3,5-dithiatriazonium hexafluoroarsenate(V)

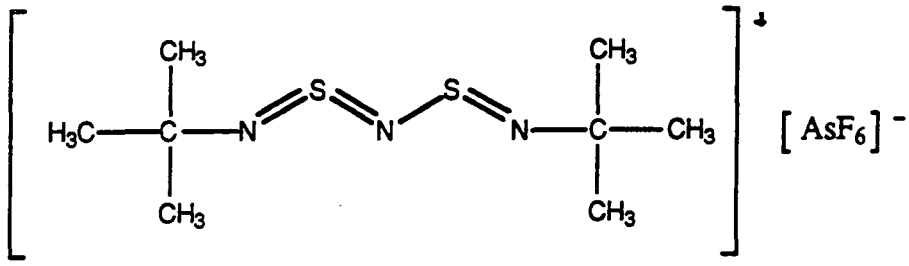

The mass spectrum (E.I.) of **4** showed a reasonable breakdown pattern (see scheme **4.2.4.**). Very good elemental analysis figures (C,H,N) were obtained for a sample of **4** Differential scanning calorimetry measurements gave a sharp melting point for **4** of 214 °C +/- 1 °C, compared with > 400 °C for [SNS][AsF_6] ($^tBuN{=}N^tBu$ is a liquid at room temperature).

Scheme 4.2.4. The mass spectrum (E.I.) of [$^tBuN{=}S{=}N{-}S{=}N^tBu$][$AsF_6$]

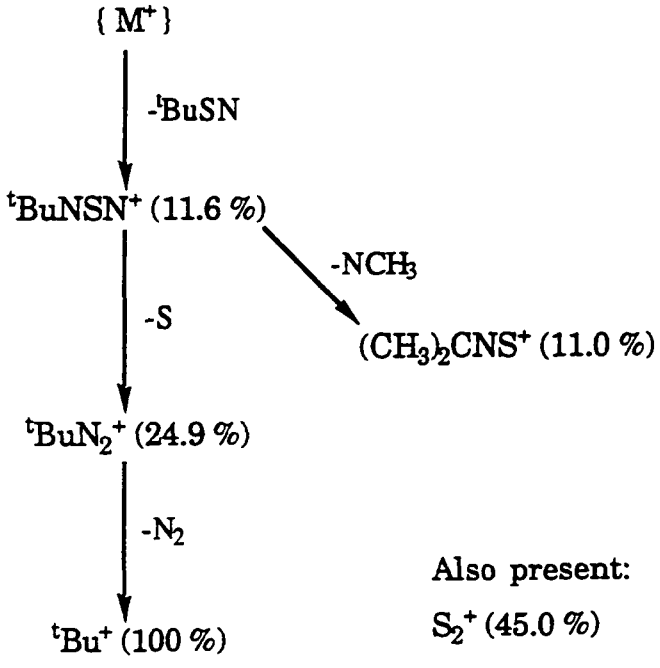

4.2.5. The reaction of [SNS][AsF_6] with ArP=PAr { Ar = $(CF_3)_3C_6H_2$ }

Reaction of ArP=PAr (see figure **4.2.5.**) with [SNS][AsF_6] in liquid SO_2 over 24 hours gave **5** (see figure **4.2.6.**) in an unspecified yield. The

product, a yellow solid, was insoluble in SO_2, CH_2Cl_2 and CH_3CN but soluble in DMSO.

Figure 4.2.5. The starting diphosphene, ArP=PAr

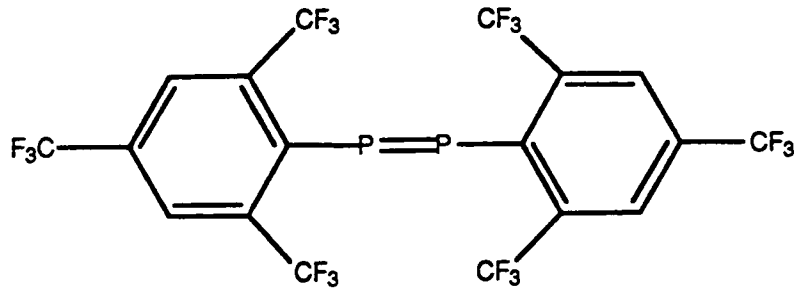

^{31}P and ^{19}F nmr spectra of **5** (both in d_6-DMSO) were recorded and proved crucial to the elucidation of the structure of **5**. The ^{31}P nmr study of **5** showed a doublet at δ = -0.73 ppm ($^{1}J_{PF}$ = 961.9 Hz) corresponding to the P-F bond. ^{19}F nmr spectra of **5** showed a doublet of multiplets at δ = -45.9 ppm ($^{1}J_{PF}$ = 962.2 Hz; $^{4}J_{PF}$ = 16.8 Hz) corresponding to the P-F bond (^{1}J), and coupling between the P and both the CF_2 and *ortho*-CF_3 groups (^{4}J). ^{19}F nmr analysis also showed a doublet at δ = -54.2 ppm ($^{4}J_{PF}$ = 16.6 Hz) corresponding to the CF_2 groups, a doublet at δ = -55.8 ppm ($^{4}J_{PF}$ = 16.6 Hz) corresponding to the *ortho*-CF_3 groups, a singlet at δ = -62.7 ppm corresponding to the *para*-CF_3 groups, and a 1:1:1:1 quartet at δ = -63.4 ppm ($^{1}J_{AsF}$ = 934.8 Hz) which corresponds to the $[AsF_6]^-$ anion (*cf.* literature value: $^{1}J_{AsF}$ = 933 Hz[12]).

Figure 4.2.6. The final product, **5**

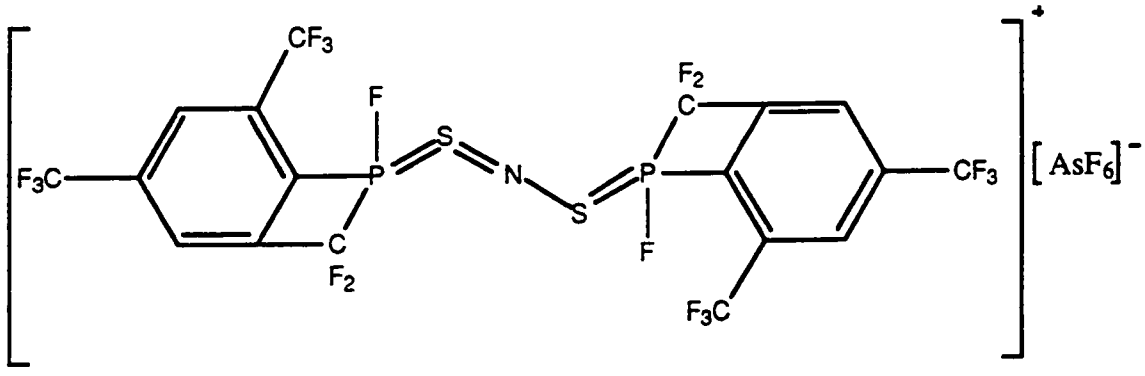

By analogy with earlier experiments, the addition of [SNS][AsF_6] to ArP=PAr is believed to initially proceed as shown in scheme **4.2.5.**.

Scheme 4.2.5. The initial reaction mechanism of [SNS][AsF_6] and ArP=PAr

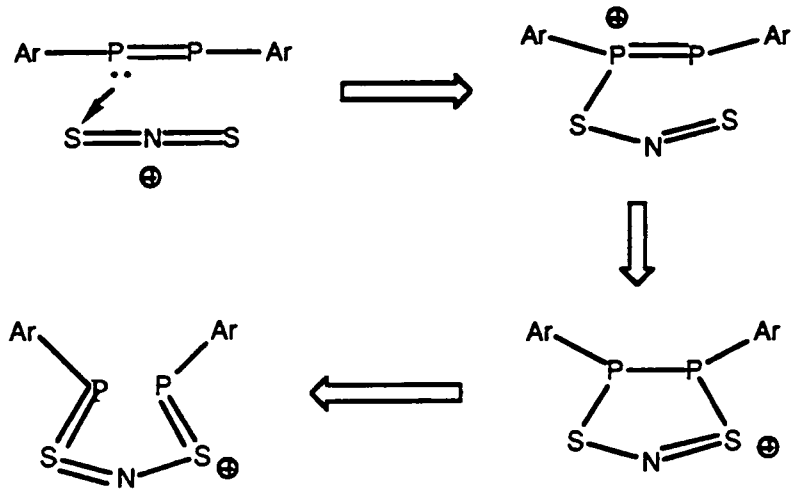

Each trivalent phosphorus atom can subsequently expand its valency via donation of its lone pair to the electrophilic carbon atom of an ortho-CF_3 group. This is illustrated in scheme **4.2.6.**.

Scheme 4.2.6. The rearrangement of [ArPSNSPAr][AsF_6]

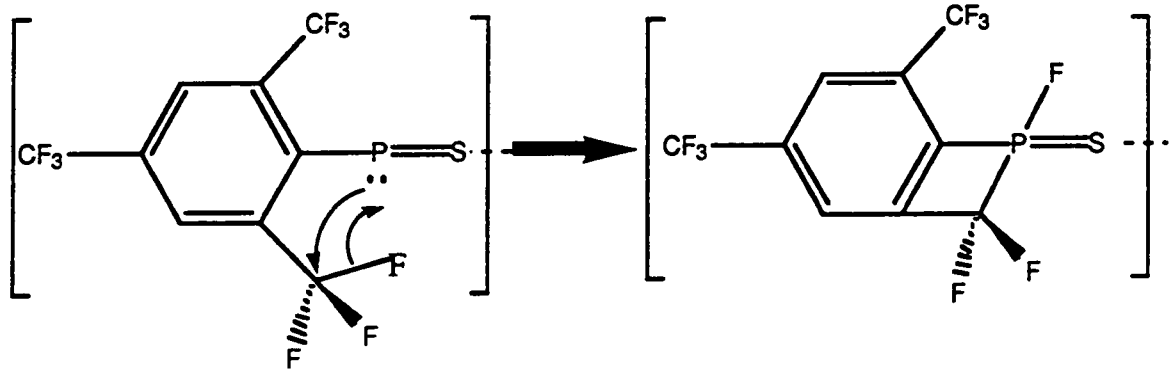

The reaction proceeds at room temperature via the abstraction of F from a CF_3 group to the adjacent phosphoros atom. Fluorine abstraction in this manner has been demonstrated by Chambers et al.[13] in flow pyrolysis reactions at 713 K, but the formation of a bond between the newly formed CF_2 and the phosphorus atom has not previously been observed.

4.3. Experimental

4.3.1. The preparation of [PhN=S=N=S-NPh][AsF_6]

As a preliminary to this reaction, the crude azobenzene (5.016 g. dull orange) was purified by vacuum sublimation (4 h, 65 °C, 0.01 mmHg) to give bright orange plates of pure azobenzene (4.581 g, 91.3 %).

Beige [SNS][AsF_6] (267 mg, 1.00 mmol) and orange azobenzene (188 mg, 1.03 mmol) were placed in the rear leg of a 'dog' containing a magnetic follower. Sufficient SO_2 was condensed into the leg to dissolve the reactants, creating a red-brown solution. After stirring (24 h, room temperature) the solution was observed to have become very dark green. Upon removal of the solvent, the crude solid was washed with pentane (3 x 15 ml) to remove unreacted azobenzene (the first washing was pale yellow). The product was then further purified by extraction with pentane (20 ml) in a sealed soxhlet extractor for 3 days before being dried *in vacuo*.

Appearance: Black Solid
Yield: 327 mg, 0.728 mmol, 72.8 %
IR (Nujol mull, KBr plates): 1580 m; 1342 w,sh; 1310 w; 1247 m; 1189 m; 1168 m; 1070 w; 1036 vw; 1024 w; 1000 w; 976 w; 933 w; 889w; 840 w; 827 vw,sh; 773 vs; 718 s,sh; 702 vs,b; 690 m,sh; 669 s; 547 vw; 533 m; 521 w; 512 vw,sh; 399 vs; 260 w cm^{-1}
Mass spectrum: (E.I.): 259 (M^+), 183 ($PhNSNSN^+$), 167 ($PhNSNS^+$), 153 ($PhSNS^+$), 128 (S_4^+), 105 (PhN_2^+), 77 (Ph^+), 64 (S_2^+), 51 (SF^+).
(C.I.): 184, 140, 105, 94, 46.
DSC: Sharp melting point peak at 252 +/- 1 °C
Chemical Analysis: Found(%) C 32.18 H 2.33 N 9.22 F 25.95 S 12.95
Required(%) C 32.08 H 2.25 N 9.36 F 25.37 S 14.27

4.3.2. The preparation of [Ph_2C=S=N=S-NPh][AsF_6]

Beige [SNS][AsF_6] (268 mg, 1.00 mmol) and white Ph_2C=NPh (290 mg, 1.13 mmol) were placed in the rear leg of a 'dog', along with a magnetic follower. Sufficient SO_2 was condensed onto the reactants to dissolve them, giving rise to a purple solution. After stirring (15 h, room

temperature) the solution was observed to have become dark green. The solvent was then removed and the crude product was washed with pentane (3 x 15 ml) to remove unreacted Ph_2C=NPh and impurities. The product was then further purified by extraction with pentane (20 ml) in a sealed soxhlet extractor for 3 days before being dried *in vacuo*.

Appearance: Olive green solid
Yield: 436 mg, 0.832 mmol, 82.9 %
IR (Nujol mull, KBr plates): 1589 m,b; 1564 m,b; 1346 vw,sh; 1300 w,b; 1226 vw,b; 1151 m; 1076 w; 1028 w,sh; 1017 m; 1000 w; 969 w; 843 m; 785 m; 762 m; 720 s,sh; 700 vs,b; 589 w; 557 w; 551 w; 500 vw,b; 470 vw; 454 w; 400 s cm^{-1}
Mass spectrum: (E.I.): 257 ($PhCSNSNPh^+$ or PH_2CSNSN^+), 180 ($PhCSNSN^+$), 165 ($PhCSNS^+$), 138 (PhS_2^+), 105 (PhN_2^+), 92 ($S_2N_2^+$), 77 (Ph^+), 69 (?), 46 (SN^+).
(C.I.): 258, 182.
DSC: Melting point peak at 148 +/- 2 °C
Chemical Analysis: Found (%) C 44.72 H 2.97 N 5.03
Required (%) C 43.51 H 2.89 N 5.34

4.3.3. The preparation of $[Ph_3P{=}S{=}N{=}S{-}NPh][AsF_6]$

Beige $[SNS][AsF_6]$ (267 mg, 1.00 mmol) and white Ph_3P=NPh (363 mg, 1.03 mmol) were placed in the rear leg of a 'dog' containing a magnetic follower. Sufficient SO_2 was condensed into the leg to dissolve the reactants, giving a red-brown solution. After stirring (18 h, room temperature) the solution was observed to have turned black. Removal of the solvent was followed by washing of the crude product with pentane (3 x 15 ml) to remove unreacted Ph_3P=NPh and impurities. The product was then dried *in vacuo*.

Appearance: Black solid
Yield: 546 mg, 0.880 mmol, 89.8 %
IR (Nujol mull, KBr plates): 1588 w,b; 1261 m; 1156 w; 1112 s; 1021 m; 964 m; 879 w; 803 m; 723 m,sh; 701 vs,b; 541 vw; 519 w; 399 vs cm^{-1}
Mass spectrum (E.I.): 277 (Ph_3PN^+ or Ph_2PNPh^+), 201 ($PhPSNSN^+$), 183 ($PhPSNS^+$), 152 ($PhPSN^+$), 77 (Ph^+), 51 (SF^+).
(C.I.): 279, 94.

NMR: ^{31}P (161.903 MHz, CD_3CN solvent) 36.57 ppm (with ^{13}C satellites at J = 5.18 Hz), 31.20 ppm.
DSC: Melting point peak at 338 +/- 2 °C
Chemical Analysis: Found (%) C 48.49 H 3.41 N 4.15
Required (%) C 46.46 H 3.26 N 4.52

4.3.4. The preparation of [^{t}BuN=S=N=S-N^{t}Bu][AsF_6]

Beige [SNS][AsF_6] (282 mg, 1.06 mmol) was placed in the rear leg of a 'dog' together with a magnetic follower. ^{t}BuN=N^{t}Bu (0.3 ml, excess), a gelatinous, pale yellow liquid, was syringed into the front leg of the 'dog' against a dry nitrogen counterflow. Sufficient SO_2 was condensed into each leg to dissolve the reactants, with the [SNS][AsF_6] solution being red-brown. The ^{t}BuN=N^{t}Bu solution was then transferred into the rear leg of the 'dog' and stirring was initiated. During stirring (24 h, room temperature) the solution was observed to have become redder in colour. After removal of the solvent, the crude solid was washed with pentane (3 x 10 ml) to remove unreacted ^{t}BuN=N^{t}Bu and impurities, before being dried *in vacuo*.

Appearance: Dark orange solid
Yield: 210 mg, 0.515 mmol, 49.5 %
IR (Nujol mull, KBr plates): 1610 s,b; 1299 s; 1206 w,b; 1107 s; 1019 w; 948 w; 721 vs,b; 634 s; 564 m; 486 vw; 402 vs cm^{-1}
Mass spectrum (E.I.): 119 (^{t}BuNSN$^+$), 99 ($(CH_3)_2CNS^+$), 87 (^{t}BuN$_2^+$), 64 (S_2^+), 57 (^{t}Bu$^+$).
(C.I.): 155, 143, 100, 88, 74, 58.
DSC: Sharp melting point peak at 214 +/- 1 °C
Chemical Analysis: Found (%) C 23.47 H 4.45 N 9.96
Required (%) C 23.47 H 4.44 N 10.27

4.3.5. The preparation of [ArP(F)=S=N-S=P(F)Ar][AsF_6]
{ where Ar = $(CF_3)_2C_6H_2CF_2$ }

Beige [SNS][AsF_6] (43 mg, 0.16 mmol) and lemon yellow ArP=PAr {where Ar = *sym*-$(CF_3)_3C_6H_2$ } (99 mg, 0.16 mmol) were placed in the rear leg of a 'dog' containing a magnetic follower. Sufficient SO_2 was condensed into the leg to dissolve the [SNS][AsF_6] , giving a red-brown solution standing over the yellow ArP=PAr. Stirring was commenced,

and the diphosphene slowly dissolved until no solid remained in the reaction vessel. After approximately 20 hours of stirring, the formation of a yellow solid (a different shade to the starting diphosphene) was observed, and reaction proceeded to completion after 24 hours. The yellow solid (see figure **4.3.1.**) was isolated by filtration, washed with back-condensed SO_2 until the washings were colourless, and dried *in vacuo*.

Figure 4.3.1. Product of the reaction of [SNS][AsF_6] with ArP=PAr

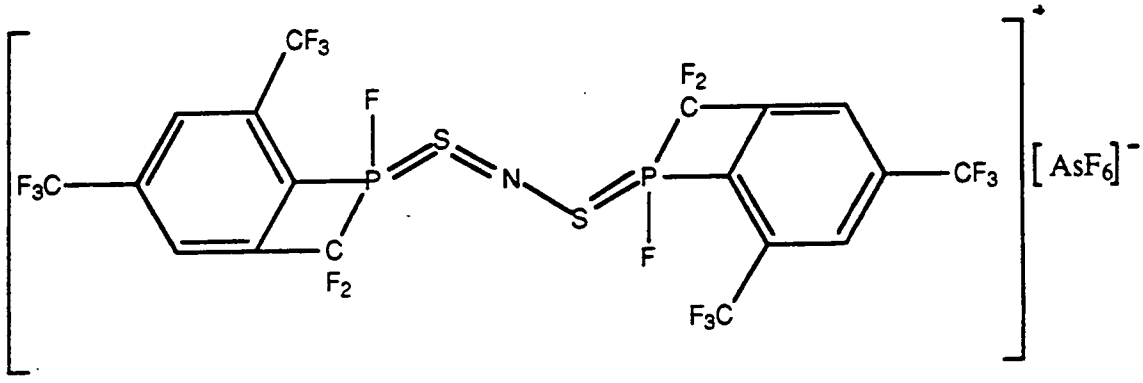

Appearance: Yellow solid

^{31}P NMR (161.903 MHz, CD_3CN solvent): δ = -0.73 ppm (doublet, $^1J_{PF}$ = 961.9 Hz).

^{19}F NMR (376.289 MHz, CD_3CN solvent): δ = -45.9 ppm (multiplet, $^1J_{PF}$ = 962.2 Hz, $^4J_{PF}$ = 16.8 Hz); δ = -54.2 ppm (doublet, $^4J_{PF}$ = 16.6 Hz); δ = 55.8 ppm (doublet, $^4J_{PF}$ = 16.6 Hz) δ = -62.7 ppm (singlet); δ = -63.4 ppm (1:1:1:1 quartet, $^1J_{AsF}$ = 934.8 Hz).

4.4. References

1. M. Schriver, PhD Thesis, University of New Brunswick, 1988.

2. N. Burford, J.P. Johnson, J. Passmore, M.J. Schriver and P.S. White, *J. Chem. Soc., Chem. Commun.*, **1986**, 966.

3. J.E. Huheey, E.A. Keiter and R.L Keiter,.*Inorganic Chemistry: Principles of Structure and Reactivity.*, 4th Edn., Harper Collins, New York, 1993.

4. R.T. Sanderson, *Polar Covalence*, Academic Press, New York, 1983.

5. I. Lavender, PhD Thesis, University of Durham, 1992.

6. A.O. Miller, A.V. Zibarev, M.A. Fedotov and G.G. Furin, *Zh. Obshch. Khim.*, **59**, No. 3, 586, (1989).

7. A.V. Zibarev, Y.V. Gotilov, and G.G. Furin, *Zh. Obshch. Khim.*, **60**, No. 12, 2710, (1990).

8. A.V. Zibarev, S.N. Konchenko, M.A. Fedotov and G.G. Furin, *Zh. Obshch. Khim.*, **58**, No. 2, 465, (1988).

9. A.V. Zibarev, A.O. Miller, M.M. Shakirov and G.G. Furin, *Zh. Obshch. Khim.*, **61**, No. 4, 951, (1991).

10. I.B. Gorrel, PhD Thesis, University of Durham, 1988.

11. *Handbook of Chemistry and Physics*, 70th Edn. Ed. R.C. Weast, CRC Press, Boca Raton, FL, 1989.

12. M.St.J. Arnold and K.J. Packer, *Mol. Phys.*, 1966, **10**, 141.

13. R.D. Chambers, K.B. Dillon and T.A. Straw, *J. Fluor. Chem.*, 1992, **56**, 385.

Chapter 5. Reaction of [SNS][AsF_6] with single bonds

5.1. Introduction

Reaction of [SNS][AsF_6] with single bonds has been a curiously neglected area of $[SNS]^+$ chemistry. The only single bonds with which [SNS][AsF_6] had been reacted previously are Xe-F, Cl-Cl and Br-Br[1]. These reactions are perhaps unsurprising considering the reactive nature of XeF_2, Cl_2 and Br_2. In this chapter the 1:1 addition reactions of [SNS][AsF_6] with N-N, O-O, P-P and C-O single bonds are studied. These single bonds were chosen as being liable to react with [SNS][AsF_6] because they are either strained (in the case of the epoxide C-O) or are relatively weak bonds (O-O, N-N and P-P are 142, 167 and 201 $kJmol^{-1}$ respectively[2]).

The N-N and O-O addition productsmust possess an acyclic structure (see figure **5.2.1.**), whereas the P-P addition product may be cyclic or acyclic, as in figure **5.1.1.**. A ^{31}P nmr study of the P-P addition product gave a spectrum whose interpretation is as yet unclear (see section 5.2.2.). Clearly more work is required (particularly ^{19}F nmr) to elucidate the structure of this compound.

At time of writing, attempts to grow single crystals of these compounds, suitable for x-ray diffraction, are underway, with the goal of definitively characterising the structures of these products.

Figure 5.1.1. Generalised cyclic and acyclic structures

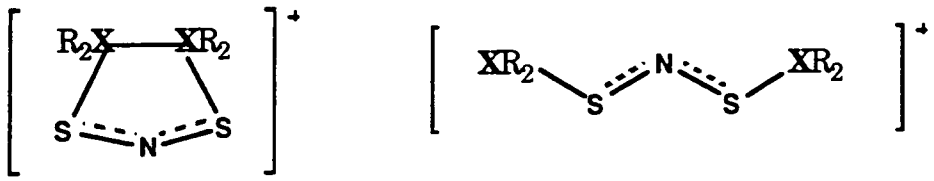

CYCLIC FORM ACYCLIC FORM

5.2. Results and Discussion

5.2.1. The reaction of tetraphenylhydrazine with [SNS][AsF_6]

Reaction of tetraphenylhydrazine (previously prepared by an established literature route[3], see section **5.3.1.**) with [SNS][AsF_6] in liquid SO_2 over 24 hours gave 1,1,5,5-tetraphenyl-2,4,1,3,5-dithiatriazonium hexafluoroarsenate(V),**1** (see figure **5.2.1.**) in 88.1 % yield. The product, a dark green solid, was soluble in SO_2.

The IR spectrum of **1** was compared with spectra of the starting materials. The $[SNS]^+$ peaks at 1488 and 1030 cm^{-1} in [SNS][AsF_6][4] are absent in **1**, and peaks corresponding to $[AsF_6]^-$ (at 695 and 398 cm^{-1} in [SNS][AsF_6]) appear in **1** at 721 and 398 cm^{-1}. The Ph-N stretch appears in Ph_2N-NPh_2 at 1589 cm^{-1} but this is shifted to 1565 cm^{-1} in **1**. Other peaks in Ph_2N-NPh_2, at 1153, 1079 and 993 cm^{-1}, are also present in **1** but displaced to 1150, 1080 and 999 cm^{-1} respectively. The new peak in **1** at 816 cm^{-1} has been tentatively assigned to an S-N bending mode[5].

The mass spectrum of **1** showed a good breakdown pattern (see scheme **5.2.1.**). Reasonable elemental analysis figures (C,H,N) were also obtained for a sample of **1**.

Scheme 5.2.1. The mass spectrum (E.I.) of [$Ph_2NSNSNPh_2$][AsF_6]

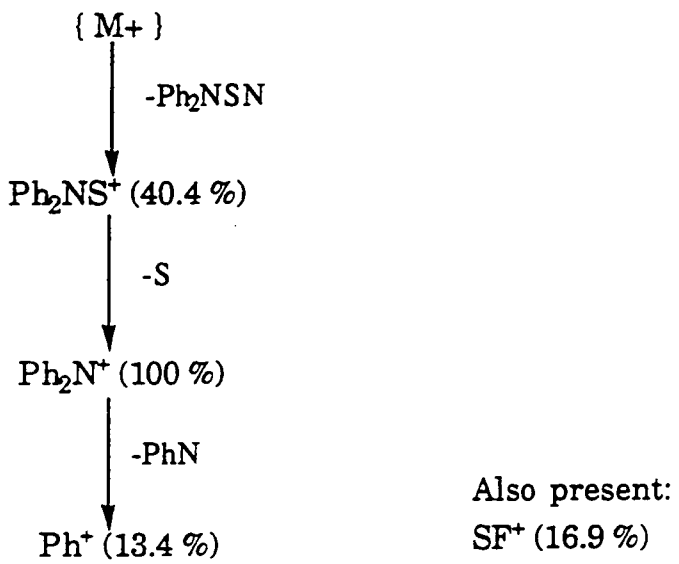

Figure 5.2.1. Postulated structures of the reaction products of $R_nX\text{-}XR_n$ with $[SNS][AsF_6]$

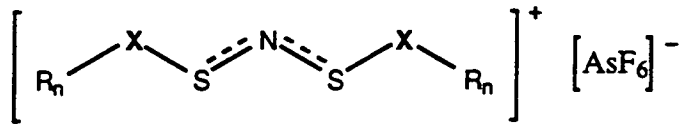

1: X = Nitrogen ; R = Ph ; n = 2

2: X = Oxygen ; R = $(CH_3)_3C$; n = 1

5.2.2. The reaction of tetraphenyl biphosphine with $[SNS][AsF_6]$

Reaction of tetraphenyl biphosphine ($Ph_2P\text{-}PPh_2$) with $[SNS][AsF_6]$ in liquid SO_2 over 24 hours gave 1,1,2,2-tetraphenyl-2,3-diphospha-1,4-dithiazyl hexafluoroarsenate(V), **2**, in 89.9 % yield. The product, a golden yellow solid, was soluble in SO_2 and CH_3CN, but insoluble in pentane.

The IR spectrum of **2** was compared with spectra of the starting materials. The $[SNS]^+$ peaks at 1488 and 1030 cm^{-1} in $[SNS][AsF_6]$ are absent in **2**, and the $[AsF_6]^-$ peaks (at 695 and 398 cm^{-1} in $[SNS][AsF_6]$) appear at 701 and 398 cm^{-1} respectively in **2**. Peaks present in the spectrum of $Ph_2P\text{-}PPh_2$, at 2359, 1566, 1025 and 498 cm^{-1} also appear in **2**, but displaced to 2356, 1568, 1027 and 500 cm^{-1} respectively. The new peaks in **2** at 1132 and 848 cm^{-1} have been tentatively assigned to S-N bending modes[5].

A ^{31}P nmr spectrum of **2** show a relatively strong doublet at δ = 43.62 ppm (J = 1012.2 Hz) which clearly indicates either direct P-P bonding or perhaps P-F bonding. A weaker doublet is also present at δ= 34.07 ppm (J = 902.8 Hz),as is a weak singlet (believed to be an impurity) at δ = 32.27 ppm.

The mass spectrum (E.I.) of **2** gave a reasonable breakdown pattern, showing in-flight recombination of fragments, giving rise to species such as $PhS_2NF_2^+$ inside the mass spectrometer (see scheme **5.2.2.**).Good elemental analysis figures (C,H,N) were obtained for a sample of **2**.

Scheme 5.2.2. The mass spectrum (E.I.) of 1,1,2,2-tetraphenyl-2,3-diphospha-1,4-dithiazyl hexafluoroarsenate(V)

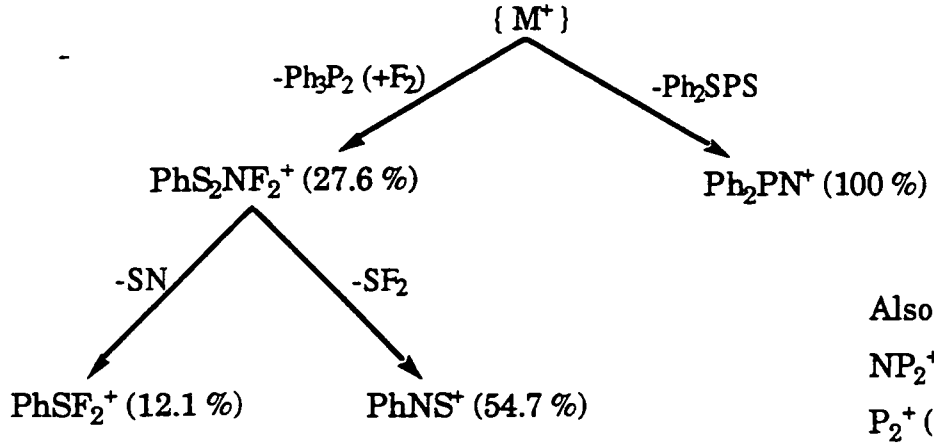

5.2.3. The reacion of t-butyl peroxide with [SNS][AsF6]

Reaction of t-butyl peroxide (^{t}BuO-O^{t}Bu) with [SNS][AsF$_6$] in liquid SO_2 over 24 hours gave [^{t}BuOSNSO^{t}Bu][AsF$_6$], **3** (see figure **5.2.1.**), in 42.2% recovered yield. Much of the product was lost in transfer and in recrystallisation, and the actual yield is believed to be considerably higher than this. The product, a peach coloured solid, is soluble in SO_2 and diethyl ether, but insoluble in hexane. Despite repeated attempts, no satiafactory IR spectrum of **3** has yet been obtained.

The mass spectrum of **3** proved to be very weak. Only the t-butyl peak (m^+/e = 57; intensity = 6.0 %) acheived an intensity of > 3 %, and as such the spectrum must be considered potentially unreliable, and is thus not reproduced in schematic form (the data is given in section **5.3.4.**). Reasonable elemental analysis figures (C,H,N) were obtained for **3**.

5.2.4. The reaction of cyclohexene oxide with [SNS][AsF6]

Reaction of cyclohexene oxide with [SNS][AsF$_6$] gave 4,5-cyclohexo-1,3,2-dithiazol-1-oxo-2-ylium hexafluoroarsenate(V), **4** (see figure **5.2.3.**), in 84.0 % yield. The product, a light brown solid, was soluble in SO_2 but insoluble in hexane. At the start of the reaction a

bright yellow, SO_2 insoluble precipitate was formed, which slowly redissolved. This yellow precipitate is believed to be the bicyclo-[6.6.0] intermediate, illustrated in figure **5.2.2.**, which then rearranges to the bicyclo-[6.5.0] final product (**4**). The proposed mechanism for this rearrangement is shown in scheme **5.2.3.**.

Figure 5.2.2. The bicyclo-[6.6.0] intermediate

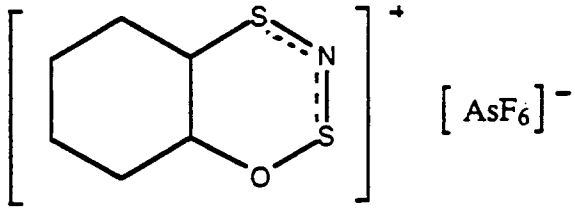

Figure 5.2.3. 4,5-cyclohexo-1,3,2-dithiazol-1-oxo-2-ylium hexafluoroarsenate(V)

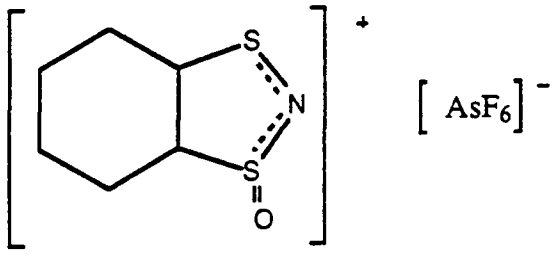

The IR spectrum of **4** was compared with spectra of the starting materials. The $[SNS]^+$ peaks in $[SNS][AsF_6]$ at 1488 and 1030 cm^{-1} are not present in **4**, and the $[AsF_6]^-$ peaks (at 695 and 398 cm^{-1} in $[SNS][AsF_6]$) apper at 700 and 398 cm^{-1} in **4**. The strong epoxide peaks in cyclohexene oxide, at 891 and 812 cm^{-1} [6], are notably absent in **4**, and the new peak in **4** at 1098 cm^{-1} is in the correct spectral region to correspond to the (N)S=O stretch[7]. The value of 1098 cm-1 for the S=O bond corresponds to an S=O bond distance of 1.478 Å (+/- 0.001 Å)[8]. Hence IR spectra have proved particulaly useful for characterising this reaction.

Scheme 5.2.3. The rearrangement of the bicyclo-[6.6.0] intermediate to the bicyclo-[6.5.0] final product (**4**)

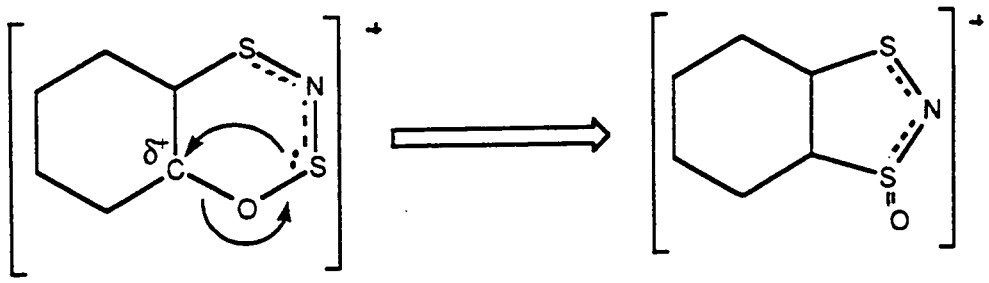

Unfortunately a mass spectrum of **4** has yet to be obtained due to a complex mechanical fault in the mass spectrometer. Good elemental analysis figures (C,H,N) were obtained for a sample of **4**.

5.3. Experimental

5.3.1. The preparation of Ph_2N-NPh_2

A sample of Ph_2N-NPh_2 was prepared[3] to provide starting material for the subsequent reaction of Ph_2N-NPh_2 with $[SNS][AsF_6]$. Off-white Ph_2NH (10.02 g, 59.3 mmol) was placed in a three-necked 500 ml round bottomed flask, containing a magnetic follower. The flask was then immersed in an ice bath and acetone (100 ml) was added to the Ph_2NH which dissolved, forming a pale, straw-coloured solution. A deep purple solution of $KMnO_4$ (4.67 g, 29.6 mmol) in acetone (150 ml) was then added dropwise to the Ph_2NH solution, with constant stirring, and reaction took place as shown in scheme **5.3.1.**, below.

Scheme 5.3.1. The reaction of $KMnO_4$ with diphenylamine

$$KMnO_4 + 2\,Ph_2NH \longrightarrow Ph_2N\text{-}NPh_2 + MnO_2 + KOH + H_2O$$

After all the $KMnO_4$ solution had been added, the reaction was stirred for a further hour, and then left to warm to room temperature. At this time the reaction vessel contained a colourless solution standing over a brown solid. This brown solid (MnO_2) was removed by filtration, leaving only a clear solution. Addition of ethanol (80 ml) to this solution precipitated a white solid (Ph_2N-NPh_2), which was

isolated by filtration and washed with ethanol (5 x 10 ml) to remove impurities before being dried *in vacuo*.

Appearance: White solid
Yield: 5.82 g, 17.3 mmol, 58.5 %
IR (Nujol mull, KBr plates): 2299 vw,b; 1731 w; 1709 vw; 1643 vw; 1589 s; 1337 vw; 1309 vw; 1292 w; 1271 vw; 1204 w; 1153 m,b; 1079 w; 1027 m; 993 vw; 972 w; 888 vw; 782 vw,sh; 743 vs; 722 vs; 680 s; 664 vw,sh; 636 m; 616 w; 606 m; 508 m; 492 m; 453 m; 418 vw,sh cm^{-1}
DSC: Melting point at 145.8 +/- 2 ^{0}C (cf. literature[9] value; 149 °C)

5.3.2. The preparation of $[Ph_2N\text{-}S\text{-}N{=}S\text{-}NPh_2][AsF_6]$

Beige [SNS][AsF_6] (107 mg, 0.401 mmol) and white $Ph_2N\text{-}NPh_2$ (145 mg, 0.432 mmol) were placed in the rear leg of a 'dog', together with a magnetic follower. Sufficient SO_2 was then condensed into the leg to dissolve the reagents, forming a red-brown solution. After stirring (24 h, room temperature) the solution was observed to have turned green. The solvent was removed, and the crude product was washed with hexane (3 x 10 ml) to remove unreacted $Ph_2N\text{-}NPh_2$ and impurities. This was followed by drying of the product *in vacuo*.

Appearance: Dark green solid
Yield: 213 mg, 0.353 mmol, 88.1 %
IR (Nujol mull, KBr plates): 1565 s; 1150 s,b; 1080 w; 999 vw; 816 m; 746 m,sh; 721 s,sh; 696 vs,b; 671 w,sh; 506 m; 398 vs cm^{-1}
Mass spectrum (E.I.): 199 (Ph_2NS^+), 169 (Ph_2N^+), 77 (Ph^+), 51 (SF^+).
(C.I.): 200, 170.
Chemical Analysis: Found (%) C 33.08 H 2.54 N 8.99
Required (%) C 32.74 H 2.29 N 9.55

5.3.3. The preparation of $[Ph_2P\text{-}S\text{-}N{=}S\text{-}PPh_2][AsF_6]$

Beige [SNS][AsF_6] (254 mg, 0.951 mmol) and white $Ph_2P\text{-}PPh_2$ (403 mg, 1.09 mmol) were placed, along with a magnetic follower, in the rear leg of 'dog'. Sufficient SO_2 was condensed into the leg to

dissolve the reagents, giving a red-brown solution. After stirring (24 h, room temperature) the solution was observed to have become slightly lighter in colour. Removal of the solvent was followed by extraction of the crude product in pentane (15 ml) for 3 days to remove unreacted Ph_2P-PPh_2 and impurities. The product was then dried *in vacuo*.

Appearance: Golden yellow solid
Yield: 578 mg, 0.838 mmol, 89.9 %
IR (Nujol mull,KBr plates): 2356 m; 1732 w; 1642 vw; 1587 m; 1568 m; 1305 w; 1132 m; 1027 w,sh; 998 w; 962 s,b; 848 vw,sh; 722 vs; 701 vs,b; 669 vw,sh; 614 vw,sh; 544 s; 500 s; 418 vw,sh; 398 vs cm^{-1}
Mass spectra:(E.I.): 199 (Ph_2PN^+); 193 ($PhS_2NF_2^+$); 147 ($PhSF_2^+$); 123 ($PhNS^+$); 74 (P_2N^+); 62 (P_2^+)
(C.I.): 419, 220
NMR: ^{31}P (161.903 MHz; CD_3CN solvent) δ = 43.62 ppm (doublet; $^1J_{PP}$ = 1012.2 Hz), δ = 34.07 ppm (doublet; $^1J_{PP}$ = 902.8 Hz), δ = 32.24 ppm (singlet; impurity)
Chemical Analysis: Found (%) C 43.94 H 3.17 N 2.09
Required (%) C 44.52 H 3.12 N 2.16

5.4. The preparation of [^{t}Bu-O-S=N-S-O-^{t}Bu][AsF_6]

Beige [SNS][AsF_6] (261 mg, 0.978 mmol) was placed in a 250 ml three-necked, round bottomed flask, together with a magnetic follower. Hexane (30 ml) was then syringed into the flask against a dry nitrogen counterflow, and a reflux condenser was fitted to the apparatus. A pressure-equilibrating dropping funnel containing colourless t-butyl peroxide (0.4 ml, excess) dissolved in hexane (20 ml) was also attached to the flask. The flask was then placed in an ice bath and after stirring was commenced, the t-butyl peroxide solution was added dropwise to the flask. Reaction proceeded slowly, producing a dull orange solid, and was complete after 24 hours, having warmed to room temperature. The hexane was then removed by cannulation and the crude solid was washed with hexane (3 x 20 ml) to ensure removal of all the unreacted peroxide. The product was further purified by recrystallisation from anhydrous diethyl ether (40 ml) and dried *in vacuo*, giving a peach-coloured product.

Appearance: Peach-coloured solid
Yield:
Mass spectrum (C.I.): 173 ($^tBuNS^tBu^+$); 156 ($^tBuS_2O^+$); 139 ($^tBuSNO^+$); 122 ($^tBuS_2^+$); 107 ($^tBuSF^+$); 96 ($S_2O_2^+$); 67 (SOF_2^+); 57 ($^tBu^+$)
(E.I.): 185, 154, 123, 109, 92, 62
Chemical Analysis: Found (%) C 23.67 H 4.22 N 4.00
Required (%) C 23.25 H 4.40 N 3.39

5.3.5. The preparation of [4,5-cyclohexo-1,3,2-dithiazol-1-oxo-2-ylium][AsF_6]

Beige [SNS][AsF_6] (255 mg, 0.955 mmol) was placed, along with a magnetic follower, in the rear leg of a 'dog'. Colourless cyclohexene oxide (vacuum distilled, 0.3 ml, excess) was syringed into the front leg against a dry nitrogen counterflow. Sufficient SO_2 was condensed into each leg to dissolve the reagents, the [SNS][AsF_6] solution being red-brown. The cyclohexene oxide was then transferred to the rear leg, and stirring (18 h, room temperature) was commenced. Immediately upon addition of the cyclohexene oxide to the [SNS][AsF_6] solution, a bright yellow precipitate was formed which slowly redissolved to give a deep red-brown solution. Removal of the solvent was followed by extraction of the crude solid in hexane (10 ml) in a sealed soxhlet extractor for 2 days. The product was then dried *in vacuo*.

Appearance: Light brown solid
Yield: 293 mg, 0.802 mmol, 84.0%
IR (Nujol mull,KBr plates): 2360 w; 1731 w; 1641 vw; 1567 s; 1303 m; 1155 w; 1098 m; 973 m; 847 vw; 778 w; 720 vs; 700 vs,b; 676 vw,sh; 398 vs cm^{-1}
Chemical Analysis: Found (%) C 20.14 H 2.73 N 3.55
Required (%) C 19.73 H 2.77 N 3.84

5.4 References

1. W.V.F. Brooks, G.K. MacLean, J. Passmore, P.S. White and C.M. Wong, *J. Chem. Soc., Dalton Trans.*, **1983**, 1961.

2. J.E. Huheey, E.A. Keiter and R.L. Keiter, *Inorganic Chemistry: Principles of Structure and Reactivity.*, 4th edn., Harper Collins, New York, 1993.

3. H. Wieland and S. Gambarjan, *Chem. Ber.*, 1906, 1499.

4. M.J. Schriver, PhD Thesis, University of New Brunswick, 1988.

5. I.B. Gorrell, PhD Thesis, University of Durham, 1989.

6. W.A. Patterson, *Anal. Chem.*, **26**, 823, 1954.

7. *The Aldrich Library of Infrared Spectra*, 3rd edn., ed. C.J. Pouchert, Aldrich Chemical Company Inc., Milwaukee, WI, 1981.

8. A.J. Banister, J.A. Durrant, I.B. Gorrell and R.S. Roberts, *J. Chem. Soc., Faraday Trans. 2*, 1985, **81**, 1771.

9. *Handbook of Chemistry and Physics*, 70th edn., ed. R.C. Weast, CRC Press, Boca Raton, FL, 1989.

Chapter 6. The plasma oxidation/reduction of silver

6.1. Introduction

6.1.1. General uses of plasma techniques

Over the past 25 years research into plasma techniques has concentrated on, amongst other things, the areas outlined below[1,2]:

(i) SURFACE DEPOSITION OF FILMS

Much lower temperatures (c. 100 °C) are required for plasma chemical vapour deposition than for thermal chemical vapour deposition, and plasma techniques produce cleaner products.

(ii) POLYMER SYNTHESIS

Supported or unsupported substrates can be used. Plasma induced polymer syntheses occur by mechanisms different from those in the solution state, hence many different products may be formed.

(iii) POLYMER MODIFICATION

Modifications may be obtained by cross-linking, adhesive bonding or by surface grafting to create reactive sites.

(iv) NUCLEAR FUSION RESEARCH

The chief difficulties in this field are in attaining the required temperatures, and keeping the hot plasmas in contact for sufficient time for fusion to occur.

(v) NOVEL SYNTHESES

The plasma synthesis of C_{60} has led to a considerable number of fullerenes being prepared via plasma routes. The chemistry of these compounds has excited much recent interest.

(vi) SURFACE MODIFICATION

The work described in this chapter falls under this broad heading.

6.1.2. Silver morphology alteration via plasma oxidation/reduction cycles

A.J. Banister and Z.V. Hauptman at Durham University have examined the use of a two stage plasma oxidation/reduction cycle to increase the surface area and alter the morphology of silver and silver alloys[3]. The four main conclusions of this work are set out below.

(i) Thermal decomposition vapours of several S/N/Cl compounds passed over a silver(I) selenide catalyst converted 50 μm thick silver wires into porous hollow tubes at 180 °C. The walls of these tubes were composed of a mixture of silver(I) sulphide and silver(I) chloride. Reduction of the tubes in a hydrogen plasma (c. 150 °C) produced porous silver tubes.

(ii) Reaction of S_4N_4 vapour with silver/copper alloy wire (*c.* 200 °C) produced a mixed silver/copper sulphide, and caused a tripling of the wire diameter. Reduction with plasma hydrogen gave an alloy of finely divided silver strands and largely unaltered copper.

(iii) Cycling between sulphochlorination of silver and hydrogen plasma reduction gave highly porous silver.

(iv) Cycling between oxygen plasma oxidation and hydrogen plasma reduction also gave highly porous silver[4].

The work described in this chapter was a partial continuation of section (iv), above, with a view to studying the morphologies of silver samples that have undergone several plasma oxidation/reduction cycles.

6.2. Results and discussions

6.2.1. A brief overview of the apparatus

All plasma experiments were carrried out using the same apparatus, illustrated in a simplified schematic form in figure **6.2.1.**, and the plasma disharge equipment used was of the A.C. glow, capacitance-coupled type. The key points of operation of the plasma apparatus are summarised below.

(i) Samples were be entered into the plasma chamber either in quartz boats or on a ceramic tray.

(ii) The displacement of the samples from the anode in the plasma chamber could be measured (+/- 0.5 mm) using a metal rule.

(iii) The entire apparatus was evacuated (c. 1 x 10^{-2} Torr) before plasma discharge was begun.

(iv) The oxygen was drawn from a BOC white spot cylinder and used without further purification. The hydrogen was also drawn from a BOC cylinder and purified by passage through a Pd/Ag hydrogen diffuser at 300 °C.

(v) Heating of the samples was provided solely by the plasma discharge (ie. no external heating source was employed).

(vi) In each cycle of each sample the duration of plasma discharge was three hours.

Samples were studied by electron microscopy, using a Cambridge Stereoscan 600 scanning electron microscope at the Applied Physics section of the School of Engineering and Applied Science at Durham University. This electron microscope is the source of all the photographs in this chapter.

Figure 6.2.1. Simplified schematic of the plasma apparatus

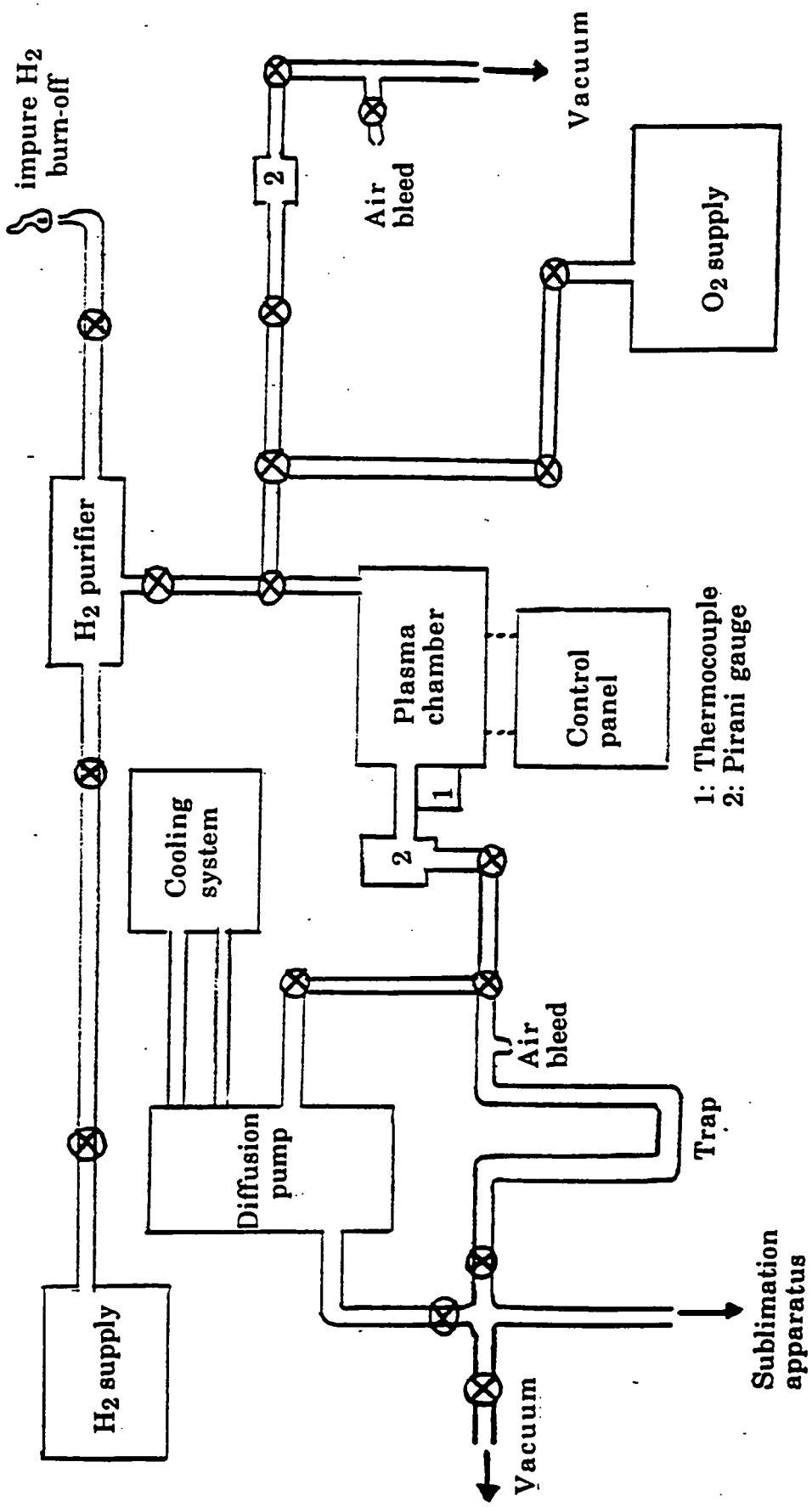

6.2.2. Plasma oxidation/reduction of 50 μm thick silver wire

Pure silver 50 μm thick wire was cut into three approximately 0.2 gram samples, which were shaped into rough spheres. The samples were degreased with a small amount of acetone and left to dry, prior to being placed in the discharge chamber of the plasma apparatus. The spheres were weighed accurately and their displacements from the anode in the plasma chamber were recorded.

Sphere **A**: initial mass = 0.19601 g; 13 mm from anode
Sphere **B**: initial mass = 0.19940 g; 66 mm from anode
Sphere **C**: initial mass = 0.19622 g; 145 mm from anode

The conditions of this experiment, in terms of temperature and pressure inside the plasma chamber, and the dial reading of the gas inlet valve (arbitary units), are given in table **6.2.1.**. After five complete oxidation/reduction cycles the spheres were removed from the plasma chamber and reweighed.

Sphere **A**: final mass = 0.19385 g (0.00216 g less than initial mass)
Sphere **B**: final mass = 0.19722 g (0.00218 g less than initial mass)
Sphere **C**: final mass = 0.19383 g (0.00239 g less than initial mass)

The mass lost by the spheres is assumed to be lost in the form of silver hydrides[4].

Table 6.2.1. Plasma oxidation/reduction of 50μm thick silver wire

Plasma	Pressure/Torr	Temp/°C	Inlet Dial
1st O_2	0.411	92	0.435
1st H_2	0.410	82	0.453
2nd O_2	0.385	92	0.436
2nd H_2	0.502	79	0.475
3rd O_2	0.485	91	0.438
3rd H_2	0.479	80	0.453
4th O_2	0.490	92	0.431
4th H_2	0.488	77	0.452
5th O_2	0.468	91	0.430
5th H_2	0.476	81	0.450

Figure 6.2.2. Treated 50 μm silver wire (50 times magnification).

Figure 6.2.3. Treated 50 μm silver wire (100 times magnification)

Figure 6.2.4. Treated 50 μm silver wire (200 times magnification).

Figure 6.2.5. Treated 50 μm silver wire (500 times magnification)

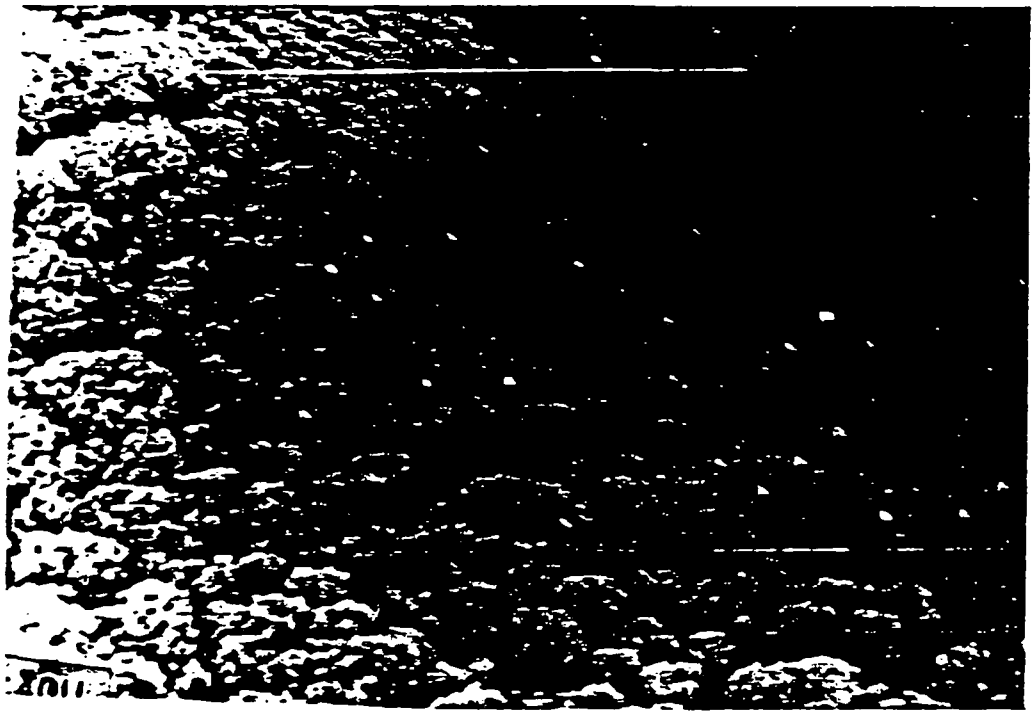

The spheres were then studied by scanning electron microscopy. Figure **6.2.2.** shows the treated wire at 50 times magnification, clearly illustrating the porous expansion of the silver and an area where mounting of the sample has caused removal of the porous fraction. Figure **6.2.3.** shows a similar section of wire at 100 times magnification. Figures **6.2.4.** and **6.2.5.** again show treated wire (at 200 and 500 times magnification respectively), with the highly irregular surface of the silver clearly visible. With these, as with all subsequent plasma experiments, the samples closest to the anode were the most thoroughly treated.

6.2.3. Plasma oxidation/reduction of silver ballotini

Samples of silver ballotini (tiny glass spheres coated with silver) were placed in quartz boats and underwent four complete oxidation/reduction cycles, as shown in table **6.2.2.**. A scanning electron microscope photograph of the ballotini before treatment (figure **6.2.6.**, 5000 times magnification) shows the smooth surfaces of the spheres, whereas after treatment (figure **6.2.7.**, 5000 times magnification) the surfaces of the spheres can be seen to be distinctly irregular. It can also be seen from figure **6.2.7.** that after treatment the ballotini remain as individual spheres, rather than being fused into much larger aggregations.

Table 6.2.2. Plasma oxidation/reduction of silver ballotini

Plasma	Pressure/Torr	Temp/°C	Inlet Dial
1st O_2	0.355	82	0.431
1st H_2	0.439	79	0.420
2nd O_2	0.371	76	0.433
2nd H_2	0.423	65	0.432
3rd O_2	0.436	79	0.434
3rd H_2	0.374	66	0.440
4th O_2	0.408	74	0.425
4th H_2	0.412	70	0.431

6.2.4. Plasma oxidation/reduction of 5 μm thick silver wire

Pure silver 5 μm thick wire was cut into three approximately 0.1 gram samples, which were shaped into rough spheres. The samples were degreased with a little acetone and left to dry, prior to being placed in the discharge chamber of the plasma apparatus. The samples underwent four complete oxidation/reduction cycles as shown in table **6.2.3.**.

Table 6.2.3. Plasma oxidation/reduction of 5μm thick silver wire

Plasma	Pressure/Torr	Temp/°C	Inlet Dial
1st O_2	0.410	86	0.415
1st H_2	0.411	76	0.439
2nd O_2	0.411	86	0.442
2nd H_2	0.438	77	0.463
3rd O_2	0.442	89	0.460
3rd H_2	0.459	80	0.427
4th O_2	0.420	85	0.437
4th H_2	0.437	78	0.435

6.2.5. Plasma oxidation/reduction of silver powder

Samples of silver powder (average particle size of roughly 5 μm diameter) were placed in quartz boats and underwent four complete plasma oxidation/reduction cycles, as shown in table **6.2.4.**.

The treated samples were then viewed using a scanning electron microscope. Figure **6.2.8.** shows a sample of the wire (200 times magnification) before treatment, illustrating the generally smooth surface of the wire. Figure **6.2.9.**, on the other hand, shows a sample of the wire (1000 times magnification) after treatment, with the expansion of surface area clearly visible.

Figure 6.2.6. Untreated silver ballotini (5000 times magnification).

Figure 6.2.7. Treated silver ballotini (5000 times magnification)

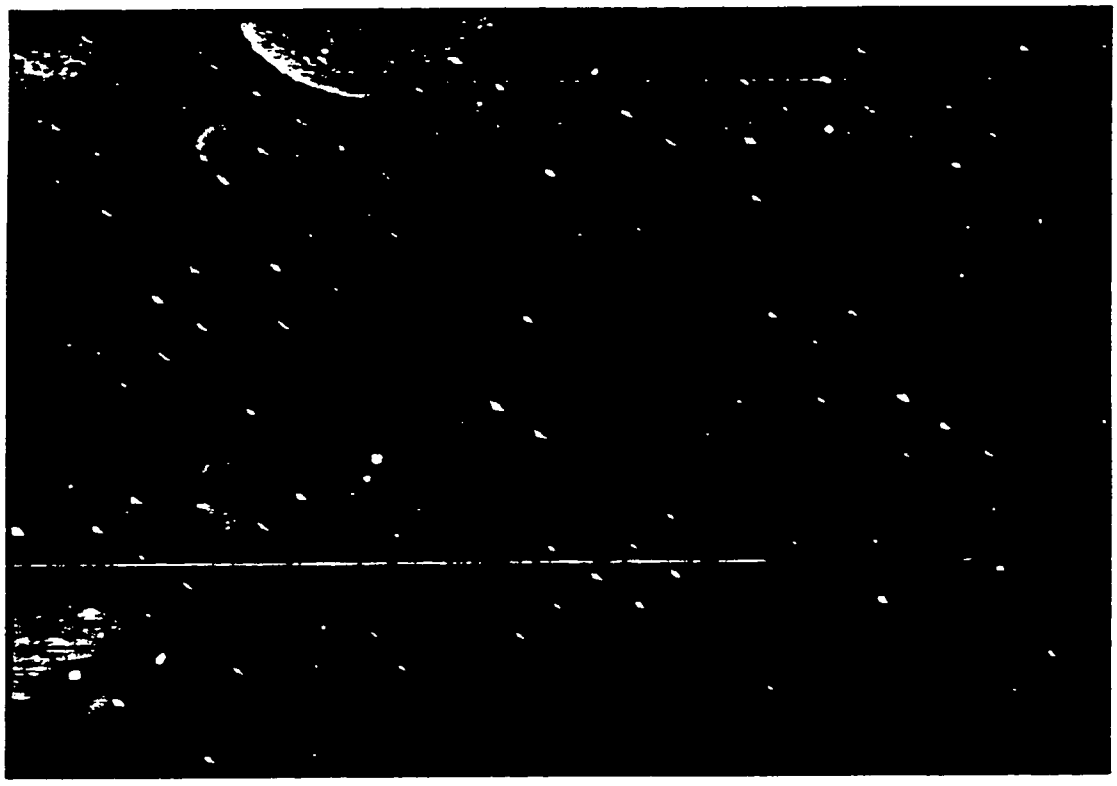

Figure 6.2.8. Untreated 5 μm silver wire (200 times magnification).

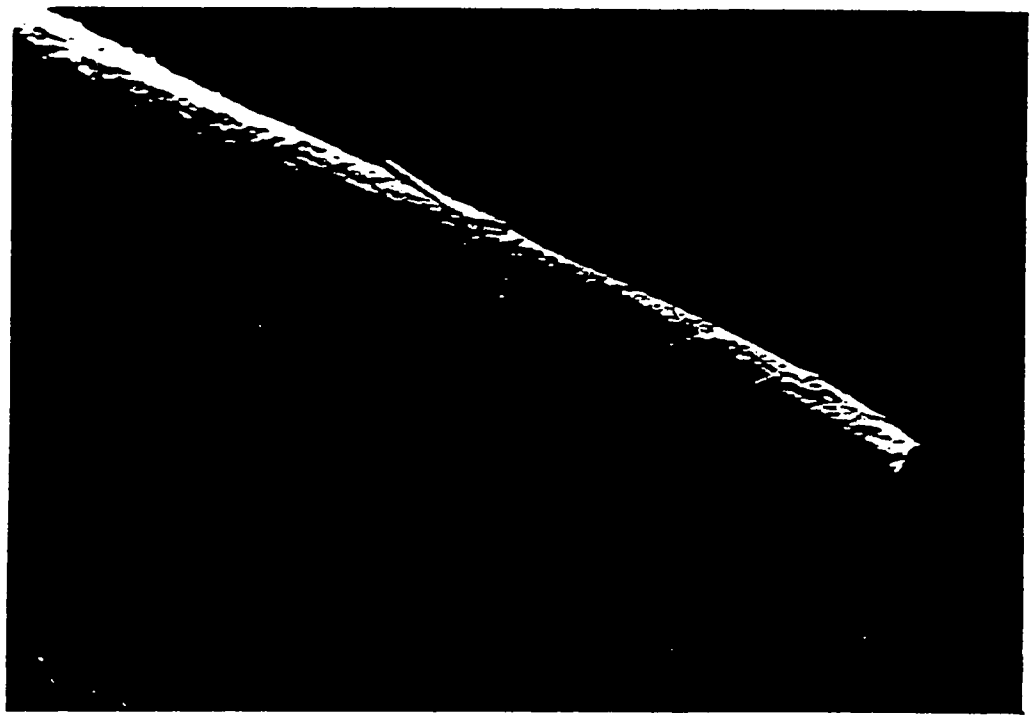

Figure 6.2.9. Treated 5 μm silver wire (1000 times magnification)

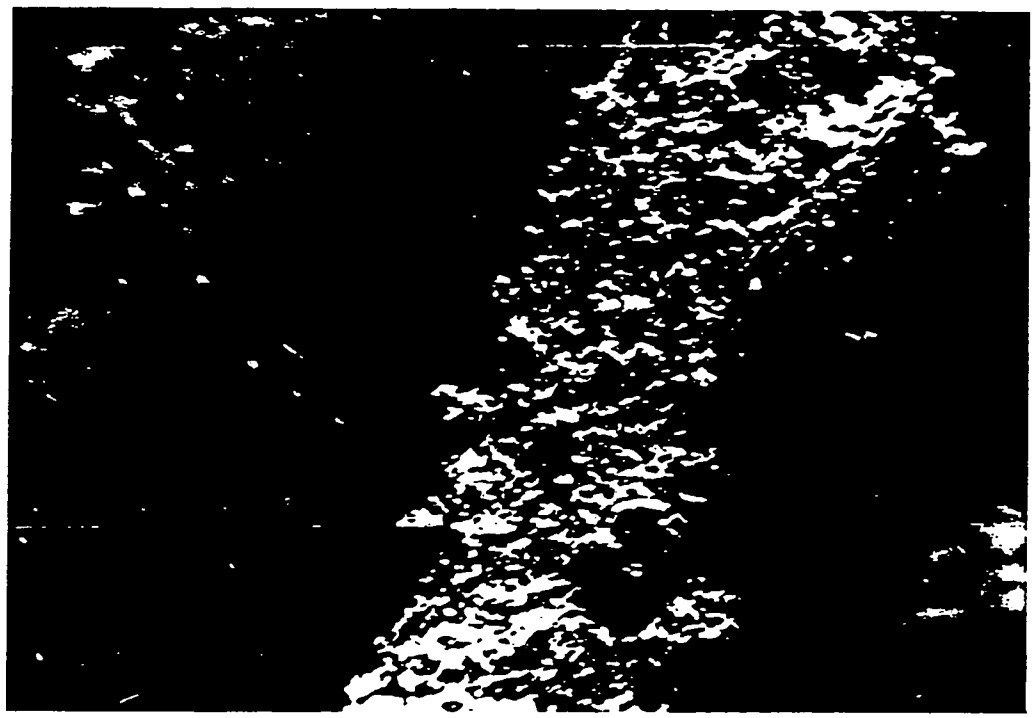

Figure 6.2.10. Untreated silver powder (1000 times magnification).

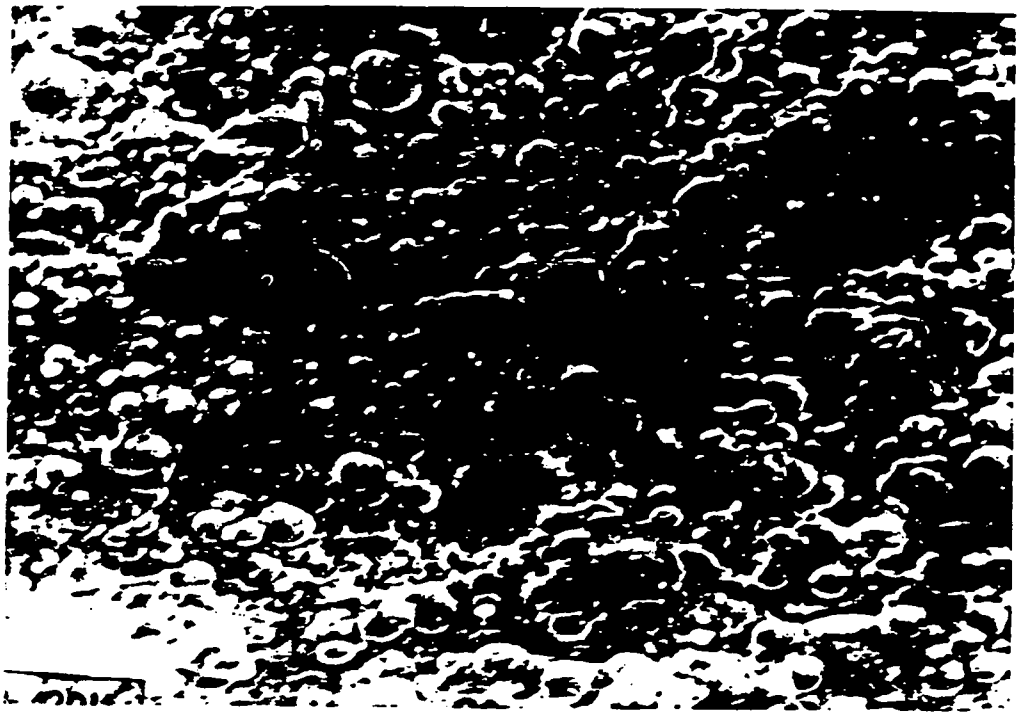

Figure 6.2.11. Treated silver powder (2000 times magnification)

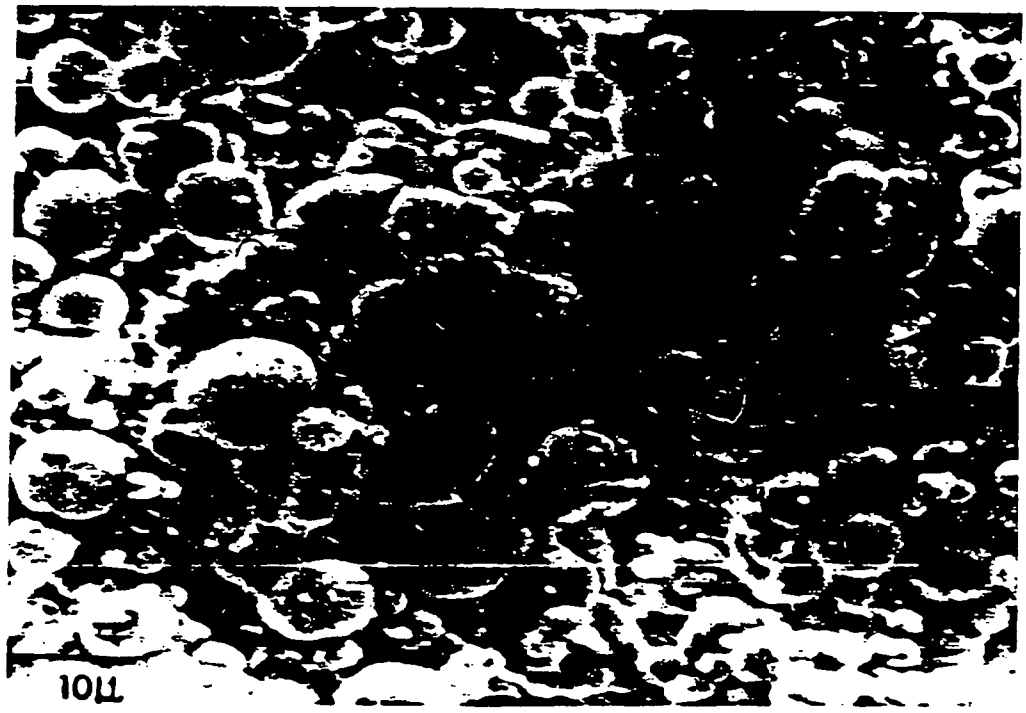

Table 6.2.4. Plasma oxidation/reduction of silver powder

Plasma	Pressure/Torr	Temp/°C	Inlet Dial
1st O_2	0.423	86	0.416
1st H_2	0.426	82	0.474
2nd O_2	0.402	92	0.469
2nd H_2	0.427	81	0.451
3rd O_2	0.442	84	0.405
3rd H_2	0.391	69	0.405
4th O_2	0.418	86	0.416
4th H_2	0.399	70	0.430

Unfortunately, the scanning electron microscope photographs of the samples are somewhat indistinct. Figure **6.2.10.** shows the silver powder (1000 times magnification) before treatment, posessing smooth surfaces. Figure **6.2.11.** shows the powder (2000 times magnification) after treatment, with irregular surfaces visible on some of the central flakes of powder.

6.3. References

1. H.F. Winters, *Top. Curr. Chem.*, **94**, 1980, 69.

2. M. Wittmer, *J. Vac. Technol. A*, Vol. 2, **2**, 1984, 273.

3. A.J. Banister and Z.V. Hauptman, SERC grant final report No. GR/G16519, February 1993.

4. Z.V. Hauptman, personal communication.

Appendix I. Synthesis of *para*-$[NSSNCC_6H_4CNSNS]^{+\cdot}$ $[AsF_6]^-$

Introduction

Bis-dithiadiazolyl compounds are, like dithiadiazolyl dimers, essentially diamagnetic[1], but the radical cation (*para*-$[SNSNCC_6H_4CNSSN]^{+\cdot}$) is paramagnetic (S = 1/2)[2]. The radical cation chloride has been synthesised by Dr I. Lavender (as has its selenium analogue[3]) and the Weiss constant for this compound, θ = -7 K, indicates antiferromagnetic ordering of the radical centres. This result can be explained by the fact that the solid state packing in *para*-$[SNSNCC_6H_4CNSSN][Cl]$ is determined by the coulombic interactions of the ions, thus preventing the radical centres from aligning in 'spin pairs'.

The unusual magnetic behaviour arising from this property prompted further research. As the properties of the radical cation are highly dependant on the solid state packing, changing the anion may have important consequences for its magnetic behaviour. It was for this reason that the preparation of *para*-$[SNSNCC_6H_4CNSSN][AsF_6]$ was attempted.

Results and discussions

Synthesis of the starting materials

The starting materials for the preparation of the target radical cation (see figure **7.1.1.**) are *para*-$[SNSNCC_6H_4CNSSN]^{2+}[AsF_6^-]_2$ and *para*-$[SNSNCC_6H_4CNSSN]^{\cdot\cdot}$. The *para*-dication was prepared by the author by standard literature routes[2] (mentioned in the experimental section of this appendix). The *para*-diradical was prepared[1] by Dr I. Lavender from a sample of the *para*-dication.

Figure 7.1.1. The radical cation *para*-$[SNSCC_6H_4CNSSN][AsF_6]$

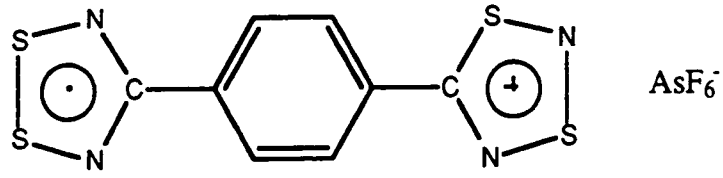

The reaction of *para*-$[SNSCC_6H_4CNSSN]^{2+}[AsF_6^-]_2$ and *para*-$[SNSNCC_6H_4CNSSN]$-

The reaction of *para*-$[SNSCC_6H_4CNSSN]^{2+}[AsF6^-]_2$ and *para*-$[SNSNCC_6H_4CNSSN]$.. in liquid SO_2 over 18 hours gave para-$[SN\bar{S}NCC_6H_4CNSSN]^{+\cdot}$ $[AsF_6]^-$, **a**, in 36.3 % yield. The product, a brown solid, was sparingly soluble in SO_2. An I.R. spectrum of **a** was run and compared with spectra of the starting materials, showing that **a** was <u>not</u> a mixture of the *para*-dication and *para*-diradical. The spectrum of **a** shows peaks that are present in the spectra of both the *para*-dication and *para*-diradical, but also other peaks (at 1423, 1092, 988 and 846 cm^{-1}) not present in the spectra of either the dication or diradical.

The mass spectrum of **a** showed a reasonably clear breakdown pattern, considering that AsF_6^- salts are notoriously involatile. Despite numerous attempts, fairly poor chemical analysis figures (C,H,N) were obtained for **a** .Differential scanning calorimetry measurements gave a melting point for **a** of 310 °C +/- 2 °C, compared with 253 °C +/- 2 °C for the diradical and > 330 °C for the dication. An esr study of **a** by Dr L.H. Sutcliffe of the Department of Chemistry, University of Sussex, showed a 1:1:1 triplet, typical of a dithiadiazolyl mono-radical. A cyclic voltammagram of **a** was also run (by Miss C.M. Aherne) as shown in figure **7.1.2.**, below.

Figure 7.1.2. Cyclic voltammagram of *para*-$[SNSNCC_6H_4CNSSN][AsF_6]$

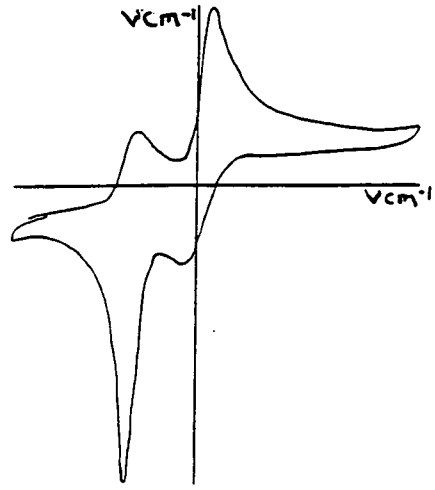

Experimental

Preparation of *para*-[NCC_6H_4CNSSN][Cl]

White $LiN(SiMe_3)_2$ (6.52g, 39 mmol) and white *para*-dicyanobenzene (5.00 g, 39 mmol) were placed, along with a magnetic follower, in a two-necked 250 ml round bottomed flask. Diethyl ether (30 ml) was added and the mixture was left to stir for 18 hours, at room temperature. An off-white precipitate ($[Li][NCC_6H_4C(NSiMe_3)_2]$) was observed to have formed, which was dried *in vacuo*. Yellow SCl_2 (6 ml, excess) was dissolved in CH_2Cl_2 (35 ml) and then added by cannulation to the $[Li][NCC_6H_4C(NSiMe_3)_2]$. An orange solid was formed, *para*-[NCC_6H_4CNSSN][Cl], which was purified by extraction with CH_2Cl_2 (10 ml) in a sealed soxhlet extractor for 2 days. The pure product was dried *in vacuo*.

Appearance: Bright orange solid
Yield: 8.05 g, 33.3 mmol, 85.4 %
IR (Nujol mull): 2100 s,b; 1285 vw,b; 1145 m; 1012 m; 920 m; 890 s; 860 w,sh; 845 s; 740 s; 721 m,sh; 683 m; 640 vw; 550 s; 523 w,sh; 450 vw cm^{-1}
Mass spectra: (E.I.) 206 (M^+), 160 ($C_6H_4CNSSN^+$),.128 ($NCC_6H_4CN^+$), 101 ($C_6H_4CN^+$), 78 ($C_6H_4^+$), 50 (?)
(C.I.): 279, 224, 206, 185, 146, 135, 78, 61,.52
Chemical analysis: Found (%) C 40.30 H 1.74 N 17.25
Required (%) C 39.75 H 1.67 N 17.39

Preparation of *para*-[NCC_6H_4CNSSN][AsF_6]

Orange *para*-[NCC_6H_4CNSSN][Cl] (2.42 g, 10.0 mmol) and white $AgAsF_6$ (3.00 g, 10.2 mmol) were placed in the rear leg of a 'dog' containing a magnetic follower. Sufficient SO_2 was condensed into the leg to dissolve both reagents, the solution being a red-brown colour. After sirring (18 h, room temperature) the reaction vessel contained a yellow solution (*para*-[NCC_6H_4CNSSN][AsF_6]) standing over a white solid (AgCl). The yellow solution was removed by filtration and evaporated to dryness *in vacuo*, giving a yellow solid. This crude solid was purified by extraction in SO_2 (c. 10 ml) in a sealed soxhlet extractor for 2 days. The pure product was then dried *in vacuo*.

Appearance: Yellow Solid
Yield: 2.99 g, 9.28 mmol, 93.1 %
IR (Nujol mull, KBr plates): 2200 m; 1308 w; 1158 vw,b; 1026 m; 985 w,b; 769 vw,sh; 718 vw,b; 703 m,sh; 590 w; 551 m; 502 vw; 486 vw; 467 w; 390 s cm^{-1}
Mass spectra: (E.I.) 128 ($NCC_6H_4CN^+$), 101 ($C_6H_4CN^+$), 75 ($C_6H_4^+$), 50 (?)
Chemical Analysis: Found (%) C 24.76 H 1.11 N 11.05
Required (%) C 24.31 H 1.02 N 10.64

Preparation of *para*-$[NSNSCC_6H_4CNSSN][AsF_6]_2$

Yellow *para*-$[NCC_6H_4CNSSN][AsF_6]$ (2.00 g, 5.06 mmol) and beige $[SNS][AsF_6]$ (1.36 g, 5.09 mmol) were placed, together with a magnetic follower, in the rear leg of a 'dog'. Sufficient SO_2 was condensed into the leg to dissolve both reagents, giving a red-brown solution. Stirring commenced and lasted for 60 hours (the reaction appeared to proceed slowly) at room temperature. After this time the solvent was removed and it was found that a bright yellow had been formed. The crude product was washed with back-condensed SO_2 until the washings became colourless, then dried *in vacuo*.

Appearance: Bright yellow solid
Yield: 2.942 g, 3.00 mmol, 59.2 %
IR (Nujol mull, KBr plates): 1515 m; 1401 s; 1302 w; 1167 m; 1020w; 990 m; 925 m; 917 w,sh; 853 m; 847 w; 837 vw; 800 w; 749 vw; 705 vs,b; 612 m,sh; 635 w; 590 vw; 576 vw; 561 w; 442 w; 398 vs cm^{-1}
Mass spectra: (E.I.) 128 ($NCC_6H_4CN^+$), 113 ($C_6H_4CN_2^+$), 101 ($C_6H_4CN^+$), 92 ($C_6H_4N^+$), 78 ($C_6H_4^+$), 64 (S_2^+), 46 (SN^+)
(C.I.): 224, 211, 185, 167, 146, 78, 46
Chemical Analysis: Found (%) C 14.65 H 0.64 N 8.46
Required (%) C 14.51 H 0.61 N 8.46

Preparation of *para*-$[NSNSCC_6H_4CNSSN]^{+\cdot}[AsF_6]^-$

Bright yellow *para*-$[SNSNCC_6H_4CNSSN][AsF_6]_2$ (140 mg, 0.211 mmol) and black *para*-$[SNSNCC_6H_4CNSSN]^{\cdot\cdot}$ (60 mg, 0.213 mmol) were placed in the rear leg of a 'dog' containing a magnetic follower.

Sufficient SO_2 was condensed into the leg to dissolve the reactants, giving a red-brown solution. The reaction was stirred (18 h, room temperature), and a brown solid slowly formed. This crude solid was washed three times with back-condensed SO_2, before being dried *in vacuo*.

Appearance: Brown solid
Yield: 72 mg, 0.077 mmol, 36.3 %
IR (Nujol mull, KBr plates): 1675 m,b; 1603 w; 1510 w; 1423 m; 1400 s; 1303 w,b; 1232 w; 1210 w; 1165 w; 1146 vw; 1128 vw; 1116 vw; 1092 vw; 1015 w; 988 m; 925 vw,sh; 916 w; 903 m; 888 vw; 846 s; 835 m; 826 m; 800 s; 778 vw; 700 vs,b; 642 m; 623 vw; 588 w; 510 m; 441 m; 398 vs; 330 vw,b cm^{-1}
Mass spectra: (E.I.) 128 ($NCC_6H_4CN^+$), 110 (S_3N^+), 93 ($S_2N_2^+$), 84 ($C_2N_2S^+$), 64 (S_2^+)
(C.I.): 156, 77, 65, 60
Chemical Analysis: Found (%) C 21.00 H 1.18 N 10.27
Required (%) C 20.30 H 0.85 N 11.84

References

1. A.J. Banister, I. Lavender, J.M. Rawson and R.J. Whitehead, *J. Chem. Soc., Dalton Commun.*, **1992**, 1449.

2. A.J. Banister, I. Lavender, J.M. Rawson, W. Clegg, B.K. Tanner and R.J. Whitehead, *J. Chem. Soc., Dalton Trans.*, **1993**, 1421.

3. I. Lavender, Personal communication.

Appendix II: [PhN=S=N=S-NPh][AsF_6] as an initiator for the cationic ring-opening polymerisation of tetrahydrofuran

Results

In an attempt to grow single crystals of [PhN=S=N=S-NPh][AsF_6], a powder sample (63 mg, 0.14 mmol.) was placed, along with a magnetic follower, in a 250 ml round bottomed flask, and dry thf (20 ml) was syringed onto the sample against a dry nitrogen counterflow, yielding a very deep green solution. Stirring was then initiated and within 10 minutes the solution was observed to have gelled into a dark green, gelatinous solid; polymerisation of the thf had occurred. This gelatinous solid was then dried *in vacuo* and washed with CH_2Cl_2 (2 x 20 ml) leaving a faintly coloured, rubbery solid, **a**.

A ^{13}C nmr study of **a** showed resonances attributable to monomeric thf (18.5 ppm and 58.5 ppm) and resonances attributable to poly-thf (26.6 ppm and 70.7 ppm), see figure **8.1.1.**. These chemical shifts are in good agreement with the literature values[1]. Molecular weight determinations were carried out on a sample of **a** by G. Forrest of the IRC of Polymer Science and Technology at the University of Durham. These determinations showed the polymer was of high molecular weight and low polydispersity, indicating that only a small amount of branching occurs in the growing polymer chains.

M_n: 221210 g mol^{-1}, M_w: 390219 g mol^{-1}, M_w/M_n (polydipersity): 1.764

^{13}C nmr ($CDCl_3$): 18.5 ppm, 26.6 ppm, 58.5 ppm, 70.7 ppm.

Discussion

The results obtained from this reaction are similar to those previously obtained by Dr Anthony Luke studying the polymerisations of thf by [$[Ph(CNSNS^+)_n]^{n+}[AsF_6^-]_n$] (n = 1,2,3)[2]. These polymerisations take place via a cationic ring-opening polymerisation (C.R.O.P.) mechanism[2], and it seems reasonable to assume that polymerisation of thf by [PhN=S=N=S-NPh][AsF_6] takes place by the same route. The projected mechanism is illustrated in scheme **8.1.1.**. Oxonium ions of the type shown in sheme **8.1.1.** are known to be the active species in thf polymerisations[3-7].

Scheme 8.1.1. The projected mechanism for the [PhN=S=N=S-NPh][AsF_6] initiated C.R.O.P. of thf.

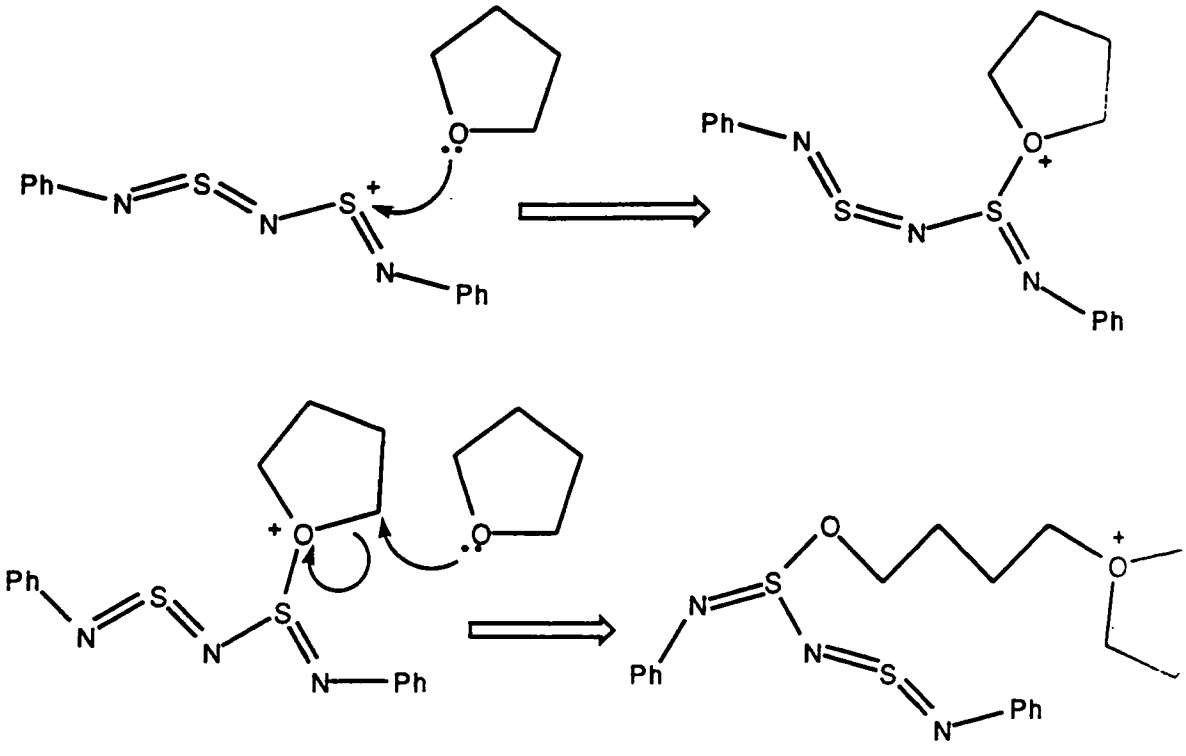

Whilst it seems likely that many dithiadiazolium-related cations may initiate C.R.O.P. of thf, polymerisation of monomers other than thf by these species has not, to the author's knowledge, been investigated.

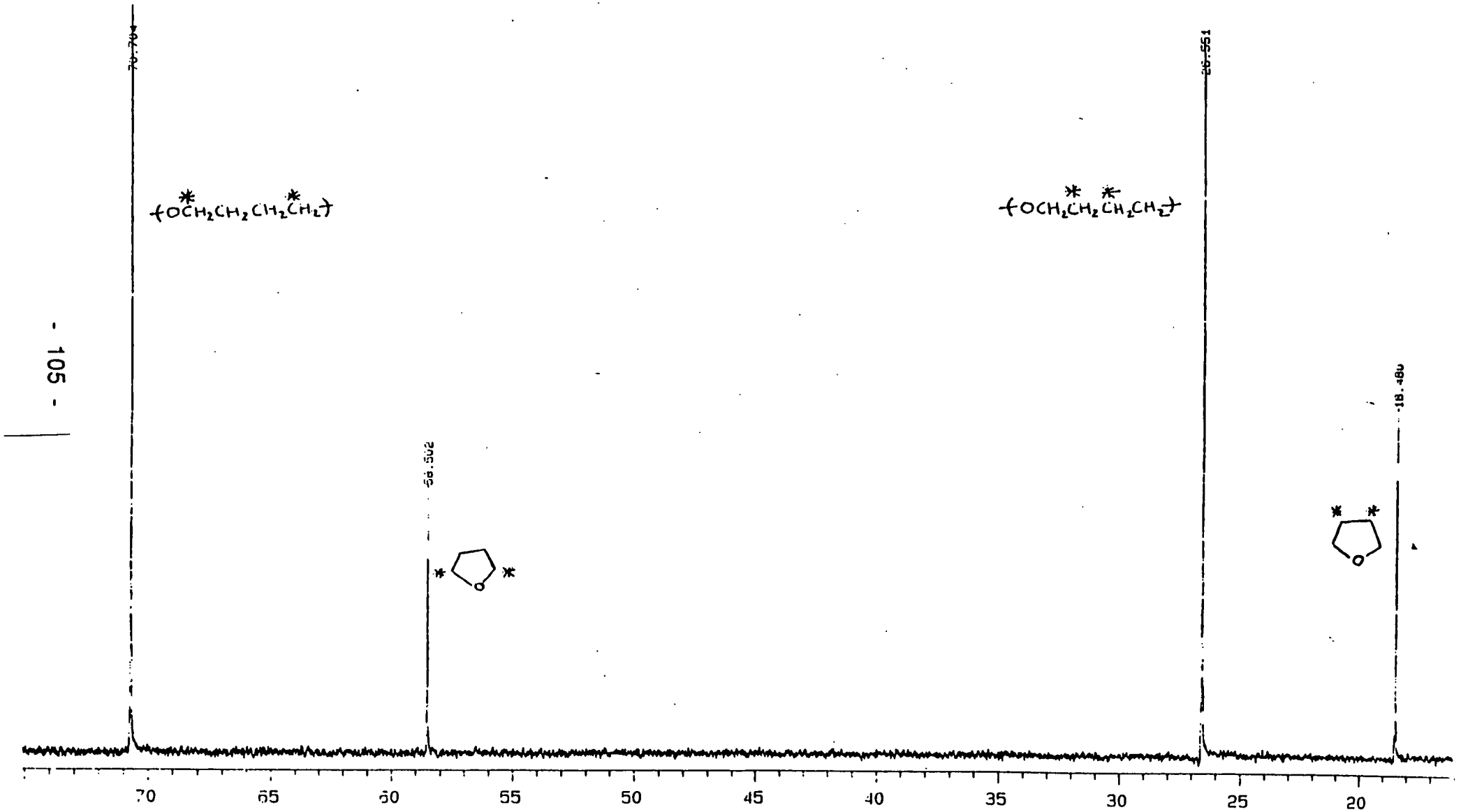
70.704
58.502
26.551
18.480
70
65
60
55
50
45
40
35
30
25
20

References

1. G. Prukmayr and T.K. Wu, in *^{13}C NMR in Polymer Science*, W.M. Pasika (Ed.), ACS symposium series, vol. 103, American Chemical Section, Washington DC, 1979, p.237.

2. A.J. Banister and A.W. Luke, *J. Polym. Sci. A*, **30**, 2653.

3. P.H. Plesch, *The Chemistry of Cationic Polymerisation*, Pergamon, New York, 1963.

4. M.P. Dreyfuss and P. Dreyfuss, *J. Polym. Sci. A-1*, **4**, 2179 (1966).

5. C.C. Price and R.J. Spector, *J. Am. Chem. Soc.*, **88**, 4171 (1966).

6. B.A. Rosenberg and Y.B. Lyndrig, *Polym. Sci. USSR*, **6**, 2253 (1964).

7. S. Penczek and K. Matyjaszewski, *J. Polym. Sci., Polym. Symp.*, **56**, 225 (1976)

Appendix III: COLLOQUIA, LECTURES AND SEMINARS FROM INVITED SPEAKERS

(October 1992 - November 1993)

October 15	Dr M. Glazer (Oxford University) & Dr S. Tarling (Birbeck College, London) The chemist's role as an expert witness in patent litigation
October 20	Dr H.E. Bryndza (Du Pont central research) Synthesis, reactions and thermochemistry of metal (alkyl) cyanide complexes and their impact on olefin hydrocyanation catalysis
October 22 *	Prof. A. Davies (University College, London) *The Ingold-Albert lecture* : The behaviour of hydrogen as a pseudometal
October 28 *	Dr J.K. Cockcroft (Durham University) Recent developments in powder diffraction
October 29 *	Dr J. Emsley (Imperial College, London) The shocking history of phosphorus
November 4 *	Dr T.P. Kee (Leeds University) Synthesis and Coordination chemistry of silylated phosphites
November 5	Dr C.J. Ludman (Durham University) Explosions - a demonstration lecture
November 11	Prof. D. Robins (Glasgow University) Pyrrolizidine alkaloids: biological activity, biosynthesis and benefits
November 12 *	Prof. M.R. Truter (University College, London) Luck and logic in host - guest chemistry

November 18	Dr R. Nix (Queen Mary College, London) Characterisation of heterogeneous catalysis
November 25	Prof. Y. Vallee (Caen University) Reactive thiocarbonyl compounds
November 25 *	Prof. L.D. Quin (Massachusetts University, Amherst) Fragmentation of phosphorous heterocycles as a route to phosphoryl species with uncommon bonding
November 26	Dr D. Humber (Glaxo, Greenford) AIDS - the development of a novel series of inhibitors of HIV
December 2	Prof. A.F. Hegarty (University College, Dublin) Highly reactive enols stabilised by steric protection
December 2	Dr R.A. Aitken (St. Andrews University) The versatile cycloadition chemistry of $Bu_3P.CS_2$
December 3 *	Prof. P. Edwards (Birmingham University) *The SCI lecture* : What is metal?
December 9	Dr A.N. Burgess (ICI, Runcorn) The structure of perfluorinated ionomer membranes
January 20 *	Dr D.C. Clary (Cambridge University) Energy flow in chemical reactions
January 21	Prof. L. Hall (Cambridge University) NMR - window to the human body
January 27	Dr W. Kerr (Strathclyde University) Development of the Pauson-Khand annulation reaction: organocobalt mediated synthesis of natural and unnatural products
January 28 *	Prof. J. Mann (Reading University) Murder, magic and medicine

February 3	Prof. S.M. Roberts (Exeter University) Enzymes in organic synthesis
February 10	Dr D. Gilles (Surrey University) NMR and molecular motion in solution
February 11 *	Prof. S. Knox (Bristol University) *The Tilden lecture* : organic chemistry at polynuclear metal centres
February 17	Dr R.W. Kemmitt (Leicester University) Oxatrimethylenemethane metal complexes
February 18	Dr I. Fraser (ICI, Wilton) Reactive processing of composite materials
February 22	Prof. D.M. Grant (Utah University) Single crystals, molecular structure and chemical shift anisotropy
February 24	Prof. C.J.M. Stirling (Sheffield University) Chemistry on the flat-reactivity of ordered systems
March 10 *	Dr P.K. Baker (University College of North Wales, Bangor) Chemistry of highly versatile 7-coordinate complexes
March 11	Dr R.A.Y. Jones (University of East Anglia) The chemistry of wine making
March 17	Dr R.J.K. Taylor (University of East Anglia) Adventures in natural product synthesis
March 24	Prof. I.O. Sutherland (Liverpool University) Chromogenic reagents for cations
May 13 *	Prof. J.A. Pople (Carnegie-Mellon University, Pittsburgh) *The Boys-Rahman lecture* : Applications of molecular orbital theory

May 21 *	Prof. L. Weber (Bielefeld University) Metallo-phosphaalkenes as synthons in organometallic chemistry
June 1	Prof. J.P. Konopelski (California University, Santa Cruz) Synthetic adventures with enantiomerically pure acetals
June 2	Prof. F. Ciardelli (Pisa University) Chiral discrimination in the stereospecific polymerisation of alpha-olefins
June 7	Prof. R.S. Stein (Massachusetts University, Amherst) Scattering studies of crystalline and liquid crystalline polymers
June 16	Prof. A.K. Covington (Newcastle University) Use of ion-selective electrodes as detectors in ion chromatography
June 17	Prof. O.F. Nielsen (H.C. Ørsted Institute, Kobenhavn University) Low frequency IR and Raman studies of hydrogen bonded liquids
September 13	Prof. A.D. Schlüter (Freie University, Berlin) Synthesis and characterisation of molecular rods and ribbons
September 13	Dr K.J. Wynne (Naval Research Office, Washington D.C.) Polymer surface dsign for minimal adhesion
September 14	Prof. J.M. DeSimone (University of North Carolina, Chapel Hill) Homogeneous and heterogeneous polymerizations in enviromentally responsible carbon dioxide
September 28	Prof. H. Ila (North Eastern Hill University, India) Synthetic strategies for cyclopentanoids via oxoketene dithioacetals

October 4 *	Prof. F.J. Feher (University of California at Irvine) Bridging the gap betwen surfaces and solutions with sessilquioxanes
October 14 *	Dr P. Hubberstey (Nottingham University) Alkali metals: alchemist's nightmare, biochemist's puzzle and technologist's dream
October 20	Dr P. Quayle (Manchester University) Aspects of aqueous ROMP chemistry
October 21	Dr B. Caddy (Strathclyde University) Forensic scientists: do we mean what we say?
October 23 *	Prof. R. Adams (South Carolina University) The chemistry of metal carbonyl cluster complexes containing platinum and iron, ruthenium or osmium and the development of a cluster based alkyne hydrogenation catalyst
October 27	Dr R.A.L. Jones (Cavendish laboratory, Oxford) Perambulating polymers
October 28 *	Dr L. Phillips (Shell Research Ltd., Sittingbourne) Molecular design: a multidisciplinary approach

* indicates lecture attended by the author.

Table 9.1.1. Anisotropic displacement parameters ($Å^2 \times 10^3$) for 1

The anisotropic displacement factor exponent takes the form:
$-2\pi^2(h^2a^{*2}U_{11} + \ldots + 2hka^*b^*U_{12})$.

	U(11)	U(22)	U(33)	U(23)	U(13)	U(12)
Br(1)	52(2)	73(3)	28(2)	8(2)	4(2)	-3(2)
C(1)	48(18)	34(17)	14(14)	-13(13)	-3(12)	-6(15)
C(2)	54(20)	30(17)	8(14)	3(12)	5(13)	5(16)
C(3)	18(15)	51(21)	33(17)	8(16)	-4(13)	-8(15)
C(4)	68(27)	67(28)	51(25)	-1(21)	10(20)	4(23)
C(5)	41(20)	37(20)	46(20)	-17(17)	-18(16)	20(16)
C(6)	43(20)	55(23)	32(18)	-7(17)	-1(15)	-2(18)
C(7)	62(22)	34(19)	29(18)	-12(15)	3(16)	12(17)
S(1)	43(5)	48(5)	31(4)	7(4)	-8(4)	-5(4)
S(2)	33(4)	35(5)	37(4)	-3(4)	4(3)	2(4)
N(1)	35(14)	39(17)	29(14)	-2(12)	-9(11)	12(13)
N(2)	37(15)	38(17)	60(18)	6(14)	2(14)	-6(13)
Br(2)	43(2)	82(3)	35(2)	-4(2)	11(2)	3(2)
C(8)	38(18)	27(18)	31(17)	-4(14)	4(14)	0(15)
C(9)	19(15)	42(20)	29(17)	-10(15)	-9(12)	-7(14)
C(10)	28(17)	83(28)	19(16)	-7(17)	-16(13)	9(18)
C(11)	66(27)	72(29)	33(19)	12(19)	-20(19)	-17(22)
C(12)	33(19)	85(30)	32(20)	12(20)	-16(16)	11(19)
C(13)	42(23)	51(25)	98(35)	-21(23)	-19(21)	38(19)
C(14)	26(16)	40(19)	30(17)	-7(15)	-3(13)	12(15)
S(3)	41(4)	35(5)	25(4)	1(4)	0(3)	1(4)
S(4)	31(4)	40(5)	31(4)	-9(4)	-7(3)	1(4)
N(3)	67(18)	4(12)	26(13)	-3(10)	-6(12)	-3(12)
N(4)	52(16)	15(13)	20(12)	-2(10)	0(11)	0(12)
As(1)	39(2)	31(2)	29(2)	-1.8(14)	4.0(14)	-3(2)
F(1)	100(22)	83(20)	65(17)	-29(15)	-54(15)	15(17)
F(2)	56(15)	35(14)	138(26)	-16(15)	36(16)	-23(12)
F(3)	167(31)	49(16)	50(16)	4(13)	49(18)	-20(18)
F(4)	63(18)	86(23)	218(43)	-99(27)	28(22)	-5(17)
F(5)	104(21)	53(16)	54(15)	15(12)	-9(14)	18(15)
F(6)	102(22)	49(15)	89(19)	-20(15)	-47(16)	4(15)
As(2)	31(2)	24(2)	26(2)	-0.8(14)	-1.5(12)	0.9(14)
F(7)	65(13)	34(11)	49(12)	-3(9)	14(10)	3(10)
F(8)	63(13)	30(11)	48(11)	-10(9)	-7(9)	4(9)
F(9)	33(9)	33(10)	40(10)	-7(8)	-4(8)	-9(8)
F(10)	59(12)	39(11)	68(13)	12(10)	29(11)	10(10)
F(11)	60(12)	29(10)	58(12)	-18(9)	-10(10)	-2(9)
F(12)	41(11)	29(10)	68(13)	9(9)	-10(9)	24(9)

Table 9.1.2. Hydrogen atom coordinates (x 10^4) and isotropic displacement parameters ($Å^2$ x 10^3) for 1

	x	y	z	U
H(3)	-1917(21)	284(42)	3091(12)	51
H(4)	-3395(32)	399(53)	2448(15)	93
H(5)	-3126(25)	1778(40)	1634(14)	63
H(6)	-1468(26)	2259(45)	1323(13)	65
H(10)	1779(24)	2340(48)	-1555(12)	66
H(11)	192(30)	3039(51)	-1993(14)	86
H(12)	-1260(26)	3316(50)	-1499(14)	76
H(13)	-1164(29)	3139(47)	-606(19)	97

Table 9.1.3. Anisotropic displacement parameters ($Å^2 \times 10^3$) for 2

The anisotropic displacement factor exponent takes the form: $-2\pi^2(h^2a^{*2}U_{11} + \ldots + 2hka^*b^*U_{12})$.

	U(11)	U(22)	U(33)	U(23)	U(13)	U(12)
As(1)	30.3(4)	21.5(4)	24.1(4)	-1.1(3)	13.9(3)	-0.7(3)
F(1)	38(2)	36(3)	39(2)	-4(2)	9(2)	5(2)
F(2)	65(3)	30(3)	30(2)	-5(2)	29(2)	-5(2)
F(3)	48(3)	31(3)	48(3)	-5(2)	31(2)	-10(2)
F(4)	63(3)	34(3)	37(2)	-6(2)	33(2)	-4(2)
F(5)	43(2)	30(2)	40(2)	1(2)	23(2)	-7(2)
F(6)	38(2)	29(3)	51(3)	5(2)	9(2)	3(2)
As(2)	36.3(4)	29.0(5)	33.3(4)	-1.1(4)	10.2(4)	-2.8(4)
F(7)	211(11)	37(4)	203(11)	9(5)	185(10)	-8(5)
F(8)	38(4)	51(5)	219(12)	-1(6)	3(5)	22(4)
F(9)	118(7)	34(4)	61(4)	-18(3)	-23(4)	8(4)
F(10)	201(9)	50(5)	93(6)	17(4)	112(6)	9(5)
F(11)	43(4)	43(4)	104(6)	9(4)	5(4)	0(3)
F(12)	120(6)	36(4)	54(4)	-23(3)	39(4)	-28(4)
As(3)	38.3(4)	26.6(4)	29.6(4)	-0.2(3)	12.7(3)	-1.7(4)
F(13)	37(3)	66(4)	121(6)	26(4)	30(4)	-4(3)
F(14)	162(8)	42(4)	128(7)	11(4)	112(6)	36(4)
F(15)	71(4)	61(4)	98(5)	14(4)	37(4)	-24(3)
F(16)	118(5)	33(3)	59(4)	0(3)	60(4)	12(3)
F(17)	68(4)	64(4)	31(3)	4(3)	15(3)	-6(3)
F(18)	106(6)	66(4)	40(3)	22(3)	-4(3)	12(4)
As(4)	36.3(4)	23.8(4)	24.9(4)	0.0(3)	14.7(3)	-0.9(3)
F(19)	47(3)	46(3)	54(3)	11(2)	32(2)	17(2)
F(20)	70(3)	61(4)	37(3)	-2(2)	4(2)	-29(3)
F(21)	82(3)	34(3)	56(3)	8(2)	43(3)	22(3)
F(22)	42(3)	36(3)	49(3)	-9(2)	10(2)	-9(2)
F(23)	77(3)	34(3)	38(2)	8(2)	40(2)	3(2)
F(24)	72(3)	41(3)	31(2)	10(2)	29(2)	4(2)
Cl(1)	36.1(11)	68(2)	34.6(11)	-1.6(10)	6.1(9)	-3.6(11)
S(1)	36.1(10)	31.1(11)	38.9(11)	-5.9(9)	24.3(9)	-7.9(9)
S(2)	42.8(11)	29.4(11)	24.6(9)	1.2(8)	16.1(8)	-1.3(9)
N(1)	31(3)	19(3)	29(3)	-5(3)	14(3)	-5(3)
N(2)	48(4)	29(4)	39(4)	-6(3)	32(3)	-4(3)
C(1)	35(4)	17(4)	25(4)	0(3)	15(3)	0(3)
C(2)	35(4)	18(4)	32(4)	-3(3)	18(3)	-2(3)
C(3)	37(4)	39(5)	27(4)	1(3)	14(4)	-1(4)
C(4)	32(4)	69(7)	57(6)	3(5)	22(4)	-14(4)
C(5)	48(5)	65(7)	57(6)	10(5)	36(5)	-7(5)
C(6)	57(6)	48(6)	40(5)	3(4)	31(4)	-9(4)
C(7)	36(4)	38(5)	30(4)	1(4)	17(4)	3(4)
Cl(2)	60.1(14)	88(2)	32.3(11)	-14.9(12)	13.4(10)	-24.9(14)
S(3)	38.8(11)	33.9(12)	37.0(11)	-1.0(9)	18.2(9)	-3.8(9)
S(4)	59.1(13)	38.3(12)	30.6(10)	-2.3(9)	25.4(10)	-1.1(10)
N(3)	60(4)	28(4)	47(4)	0(3)	35(4)	-5(3)
N(4)	37(3)	36(4)	24(3)	-2(3)	12(3)	-3(3)
C(8)	45(4)	22(4)	26(4)	1(3)	18(4)	0(3)
C(9)	43(4)	23(4)	29(4)	3(3)	18(3)	0(3)
C(10)	64(5)	30(5)	26(4)	0(3)	21(4)	2(4)
C(11)	76(7)	42(5)	37(5)	1(4)	32(5)	6(5)
C(12)	86(7)	44(6)	48(5)	15(4)	49(5)	15(5)
C(13)	55(5)	60(6)	57(6)	25(5)	36(5)	10(5)

C(14)	47(5)	28(5)	37(4)	3(4)	21(4)	-5(4)
Cl(3)	46.8(12)	74(2)	26.5(10)	-2.8(10)	7.0(9)	-12.2(11)
S(5)	31.2(10)	38.3(12)	34.4(10)	0.8(9)	14.5(8)	0.1(9)
S(6)	48.1(12)	36.2(12)	29.1(10)	-0.9(9)	22.5(9)	1.4(10)
N(5)	58(4)	28(4)	50(4)	5(3)	38(4)	3(3)
N(6)	36(3)	29(4)	29(3)	-3(3)	16(3)	2(3)
C(15)	33(4)	25(4)	28(4)	5(3)	12(3)	1(3)
C(16)	36(4)	26(4)	24(4)	3(3)	15(3)	3(3)
C(17)	43(4)	39(5)	24(4)	7(3)	15(4)	1(4)
C(18)	63(6)	49(6)	30(4)	0(4)	24(4)	4(5)
C(19)	78(7)	36(5)	45(5)	11(4)	48(5)	21(5)
C(20)	45(5)	54(6)	47(5)	17(4)	33(4)	15(4)
C(21)	40(5)	46(5)	30(4)	1(4)	16(4)	6(4)
Cl(4)	32.4(12)	188(4)	45.5(14)	-17(2)	6.7(11)	6(2)
S(7)	35.1(10)	34.6(12)	25.2(9)	-1.4(8)	14.2(8)	2.2(9)
S(8)	31.9(10)	47.7(13)	36.5(11)	8.8(10)	19.3(9)	7.3(9)
N(7)	44(4)	34(4)	40(4)	5(3)	27(3)	5(3)
N(8)	27(3)	27(4)	30(3)	2(3)	16(3)	0(3)
C(22)	36(4)	18(4)	27(4)	-1(3)	13(3)	3(3)
C(23)	33(4)	33(5)	43(5)	1(4)	21(4)	3(4)
C(24)	34(5)	102(9)	43(5)	-1(5)	15(4)	17(5)
C(25)	39(6)	199(16)	74(8)	-1(9)	32(6)	29(8)
C(26)	71(8)	139(12)	88(8)	-4(8)	58(7)	23(8)
C(27)	70(7)	76(8)	59(6)	-6(5)	47(6)	5(6)
C(28)	52(5)	28(5)	43(5)	-5(4)	30(4)	4(4)

.1.4. Hydrogen atom coordinates (x 10^4) and isotropic displacement
eters ($Å^2$ x 10^3) for 2

	x	y	z	U
H(4)	5333(3)	2905(12)	4536(4)	78
H(5)	4951(4)	3148(12)	3589(4)	78
H(6)	3977(4)	2609(11)	3045(3)	67
H(7)	3382(3)	1781(10)	3443(3)	50
H(11)	6427(4)	-6740(11)	1324(3)	74
H(12)	7403(4)	-6208(11)	1664(4)	79
H(13)	7922(4)	-5120(12)	2539(4)	79
H(14)	7462(3)	-4709(9)	3101(3)	54
H(18)	8615(4)	-2552(11)	8688(3)	69
H(19)	7635(4)	-2959(10)	8385(3)	68
H(20)	7055(4)	-3898(11)	7493(3)	66
H(21)	7476(3)	-4364(10)	6897(3)	58
H(25)	4686(4)	-2080(20)	396(5)	152
H(26)	5025(5)	-1537(18)	1332(5)	136
H(27)	6014(4)	-1581(13)	1915(4)	93
H(28)	6661(4)	-2235(9)	1561(3)	56

ortho-[BrC_6H_4CNSNS][AsF_6]
ortho-[ClC6H4CNSNS][AsF_6]

isolated by filtration and washed with ethanol (5 x 10 ml) to remove impurities before being dried *in vacuo*.

Appearance: White solid
Yield: 5.82 g, 17.3 mmol, 58.5 %
IR (Nujol mull, KBr plates): 2299 vw,b; 1731 w; 1709 vw; 1643 vw; 1589 s; 1337 vw; 1309 vw; 1292 w; 1271 vw; 1204 w; 1153 m,b; 1079 w; 1027 m; 993 vw; 972 w; 888 vw; 782 vw,sh; 743 vs; 722 vs; 680 s; 664 vw,sh; 636 m; 616 w; 606 m; 508 m; 492 m; 453 m; 418 vw,sh cm^{-1}
DSC: Melting point at 145.8 +/- 2 ^{0}C (cf. literature[9] value; 149 °C)

5.3.2. The preparation of $[Ph_2N\text{-}S\text{-}N{=}S\text{-}NPh_2][AsF_6]$

Beige [SNS][AsF_6] (107 mg, 0.401 mmol) and white $Ph_2N\text{-}NPh_2$ (145 mg, 0.432 mmol) were placed in the rear leg of a 'dog', together with a magnetic follower. Sufficient SO_2 was then condensed into the leg to dissolve the reagents, forming a red-brown solution. After stirring (24 h, room temperature) the solution was observed to have turned green. The solvent was removed, and the crude product was washed with hexane (3 x 10 ml) to remove unreacted $Ph_2N\text{-}NPh_2$ and impurities. This was followed by drying of the product *in vacuo*.

Appearance: Dark green solid
Yield: 213 mg, 0.353 mmol, 88.1 %
IR (Nujol mull, KBr plates): 1565 s; 1150 s,b; 1080 w; 999 vw; 816 m; 746 m,sh; 721 s,sh; 696 vs,b; 671 w,sh; 506 m; 398 vs cm^{-1}
Mass spectrum (E.I.): 199 (Ph_2NS^+), 169 (Ph_2N^+), 77 (Ph^+), 51 (SF^+).
(C.I.): 200, 170.
Chemical Analysis: Found (%) C 33.08 H 2.54 N 8.99
Required (%) C 32.74 H 2.29 N 9.55

5.3.3. The preparation of $[Ph_2P\text{-}S\text{-}N{=}S\text{-}PPh_2][AsF_6]$

Beige [SNS][AsF_6] (254 mg, 0.951 mmol) and white $Ph_2P\text{-}PPh_2$ (403 mg, 1.09 mmol) were placed, along with a magnetic follower, in the rear leg of 'dog'. Sufficient SO_2 was condensed into the leg to

dissolve the reagents, giving a red-brown solution. After stirring (24 h, room temperature) the solution was observed to have become slightly lighter in colour. Removal of the solvent was followed by extraction of the crude product in pentane (15 ml) for 3 days to remove unreacted Ph_2P-PPh_2 and impurities. The product was then dried *in vacuo*.

Appearance: Golden yellow solid
Yield: 578 mg, 0.838 mmol, 89.9 %
IR (Nujol mull,KBr plates): 2356 m; 1732 w; 1642 vw; 1587 m; 1568 m; 1305 w; 1132 m; 1027 w,sh; 998 w; 962 s,b; 848 vw,sh; 722 vs; 701 vs,b; 669 vw,sh; 614 vw,sh; 544 s; 500 s; 418 vw,sh; 398 vs cm^{-1}
Mass spectra:(E.I.): 199 (Ph_2PN^+); 193 ($PhS_2NF_2^+$); 147 ($PhSF_2^+$); 123 ($PhNS^+$); 74 (P_2N^+); 62 (P_2^+)
(C.I.): 419, 220
NMR: ^{31}P (161.903 MHz; CD_3CN solvent) δ = 43.62 ppm (doublet; $^1J_{PP}$ = 1012.2 Hz), δ = 34.07 ppm (doublet; $^1J_{PP}$ = 902.8 Hz), δ = 32.24 ppm (singlet; impurity)
Chemical Analysis: Found (%) C 43.94 H 3.17 N 2.09
Required (%) C 44.52 H 3.12 N 2.16

5..4. The preparation of [^{t}Bu-O-S=N-S-O-^{t}Bu][AsF_6]

Beige [SNS][AsF_6] (261 mg, 0.978 mmol) was placed in a 250 ml three-necked, round bottomed flask, together with a magnetic follower. Hexane (30 ml) was then syringed into the flask against a dry nitrogen counterflow, and a reflux condenser was fitted to the apparatus. A pressure-equilibrating dropping funnel containing colourless t-butyl peroxide (0.4 ml, excess) dissolved in hexane (20 ml) was also attached to the flask. The flask was then placed in an ice bath and after stirring was commenced, the t-butyl peroxide solution was added dropwise to the flask. Reaction proceeded slowly, producing a dull orange solid, and was complete after 24 hours, having warmed to room temperature. The hexane was then removed by cannulation and the crude solid was washed with hexane (3 x 20 ml) to ensure removal of all the unreacted peroxide. The product was further purified by recrystallisation from anhydrous diethyl ether (40 ml) and dried *in vacuo*, giving a peach-coloured product.

Appearance: Peach-coloured solid
Yield:
Mass spectrum (C.I.): 173 ($^tBuNS^tBu^+$); 156 ($^tBuS_2O^+$); 139 ($^tBuSNO^+$); 122 ($^tBuS_2^+$); 107 ($^tBuSF^+$); 96 ($S_2O_2^+$); 67 (SOF_2^+); 57 ($^tBu^+$)
(E.I.): 185, 154, 123, 109, 92, 62
Chemical Analysis: Found (%) C 23.67 H 4.22 N 4.00
Required (%) C 23.25 H 4.40 N 3.39

5.3.5. The preparation of [4,5-cyclohexo-1,3,2-dithiazol-1-oxo-2-ylium][AsF_6]

Beige [SNS][AsF_6] (255 mg, 0.955 mmol) was placed, along with a magnetic follower, in the rear leg of a 'dog'. Colourless cyclohexene oxide (vacuum distilled, 0.3 ml, excess) was syringed into the front leg against a dry nitrogen counterflow. Sufficient SO_2 was condensed into each leg to dissolve the reagents, the [SNS][AsF_6] solution being red-brown. The cyclohexene oxide was then transferred to the rear leg, and stirring (18 h, room temperature) was commenced. Immediately upon addition of the cyclohexene oxide to the [SNS][AsF_6] solution, a bright yellow precipitate was formed which slowly redissolved to give a deep red-brown solution. Removal of the solvent was followed by extraction of the crude solid in hexane (10 ml) in a sealed soxhlet extractor for 2 days. The product was then dried *in vacuo*.

Appearance: Light brown solid
Yield: 293 mg, 0.802 mmol, 84.0%
IR (Nujol mull,KBr plates): 2360 w; 1731 w; 1641 vw; 1567 s; 1303 m; 1155 w; 1098 m; 973 m; 847 vw; 778 w; 720 vs; 700 vs,b; 676 vw,sh; 398 vs cm^{-1}
Chemical Analysis: Found (%) C 20.14 H 2.73 N 3.55
Required (%) C 19.73 H 2.77 N 3.84

5.4 References

1. W.V.F. Brooks, G.K. MacLean, J. Passmore, P.S. White and C.M. Wong, *J. Chem. Soc., Dalton Trans.*, **1983**, 1961.

2. J.E. Huheey, E.A. Keiter and R.L. Keiter, *Inorganic Chemistry: Principles of Structure and Reactivity.*, 4th edn., Harper Collins, New York, 1993.

3. H. Wieland and S. Gambarjan, *Chem. Ber.*, 1906, 1499.

4. M.J. Schriver, PhD Thesis, University of New Brunswick, 1988.

5. I.B. Gorrell, PhD Thesis, University of Durham, 1989.

6. W.A. Patterson, *Anal. Chem.*, **26**, 823, 1954.

7. *The Aldrich Library of Infrared Spectra*, 3rd edn., ed. C.J. Pouchert, Aldrich Chemical Company Inc., Milwaukee, WI, 1981.

8. A.J. Banister, J.A. Durrant, I.B. Gorrell and R.S. Roberts, *J. Chem. Soc., Faraday Trans. 2*, 1985, **81**, 1771.

9. *Handbook of Chemistry and Physics*, 70th edn., ed. R.C. Weast, CRC Press, Boca Raton, FL, 1989.

Chapter 6. The plasma oxidation/reduction of silver

6.1. Introduction

6.1.1. General uses of plasma techniques

Over the past 25 years research into plasma techniques has concentrated on, amongst other things, the areas outlined below[1,2]:

(i) SURFACE DEPOSITION OF FILMS

Much lower temperatures (c. 100 °C) are required for plasma chemical vapour deposition than for thermal chemical vapour deposition, and plasma techniques produce cleaner products.

(ii) POLYMER SYNTHESIS

Supported or unsupported substrates can be used. Plasma induced polymer syntheses occur by mechanisms different from those in the solution state, hence many different products may be formed.

(iii) POLYMER MODIFICATION

Modifications may be obtained by cross-linking, adhesive bonding or by surface grafting to create reactive sites.

(iv) NUCLEAR FUSION RESEARCH

The chief difficulties in this field are in attaining the required temperatures, and keeping the hot plasmas in contact for sufficient time for fusion to occur.

(v) NOVEL SYNTHESES

The plasma synthesis of C_{60} has led to a considerable number of fullerenes being prepared via plasma routes. The chemistry of these compounds has excited much recent interest.

(vi) SURFACE MODIFICATION

The work described in this chapter falls under this broad heading.

6.1.2. Silver morphology alteration via plasma oxidation/reduction cycles

A.J. Banister and Z.V. Hauptman at Durham University have examined the use of a two stage plasma oxidation/reduction cycle to increase the surface area and alter the morphology of silver and silver alloys[3]. The four main conclusions of this work are set out below.

(i) Thermal decomposition vapours of several S/N/Cl compounds passed over a silver(I) selenide catalyst converted 50 μm thick silver wires into porous hollow tubes at 180 °C. The walls of these tubes were composed of a mixture of silver(I) sulphide and silver(I) chloride. Reduction of the tubes in a hydrogen plasma (c. 150 °C) produced porous silver tubes.

(ii) Reaction of S_4N_4 vapour with silver/copper alloy wire (*c.* 200 °C) produced a mixed silver/copper sulphide, and caused a tripling of the wire diameter. Reduction with plasma hydrogen gave an alloy of finely divided silver strands and largely unaltered copper.

(iii) Cycling between sulphochlorination of silver and hydrogen plasma reduction gave highly porous silver.

(iv) Cycling between oxygen plasma oxidation and hydrogen plasma reduction also gave highly porous silver[4].

The work described in this chapter was a partial continuation of section (iv), above, with a view to studying the morphologies of silver samples that have undergone several plasma oxidation/reduction cycles.

6.2. Results and discussions

6.2.1. A brief overview of the apparatus

All plasma experiments were carrried out using the same apparatus, illustrated in a simplified schematic form in figure **6.2.1.**, and the plasma disharge equipment used was of the A.C. glow, capacitance-coupled type. The key points of operation of the plasma apparatus are summarised below.

(i) Samples were be entered into the plasma chamber either in quartz boats or on a ceramic tray.

(ii) The displacement of the samples from the anode in the plasma chamber could be measured (+/- 0.5 mm) using a metal rule.

(iii) The entire apparatus was evacuated (c. 1 x 10^{-2} Torr) before plasma discharge was begun.

(iv) The oxygen was drawn from a BOC white spot cylinder and used without further purification. The hydrogen was also drawn from a BOC cylinder and purified by passage through a Pd/Ag hydrogen diffuser at 300 °C.

(v) Heating of the samples was provided solely by the plasma discharge (ie. no external heating source was employed).

(vi) In each cycle of each sample the duration of plasma discharge was three hours.

Samples were studied by electron microscopy, using a Cambridge Stereoscan 600 scanning electron microscope at the Applied Physics section of the School of Engineering and Applied Science at Durham University. This electron microscope is the source of all the photographs in this chapter.

Figure 6.2.1. Simplified schematic of the plasma apparatus

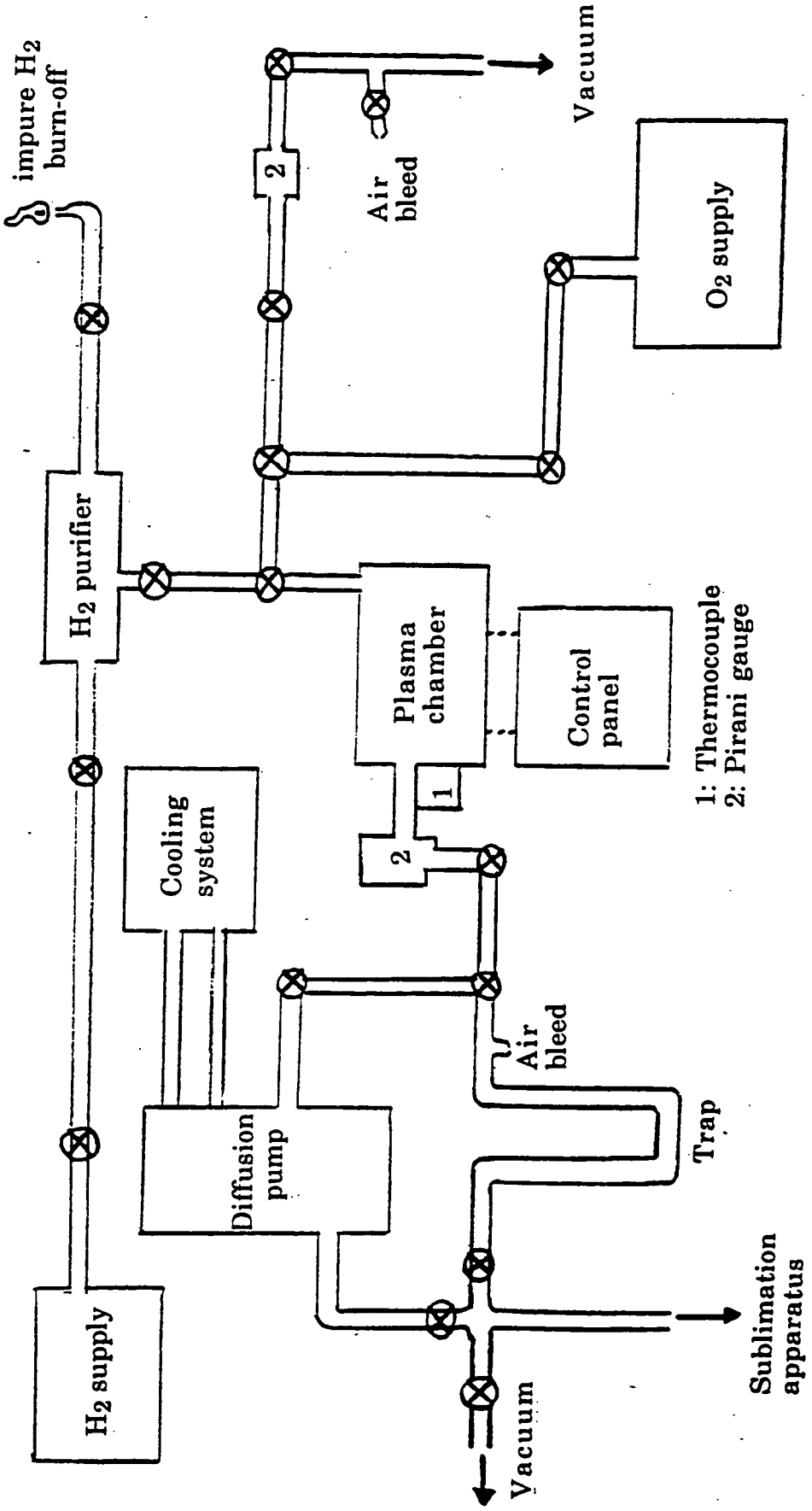

6.2.2. Plasma oxidation/reduction of 50 μm thick silver wire

Pure silver 50 μm thick wire was cut into three approximately 0.2 gram samples, which were shaped into rough spheres. The samples were degreased with a small amount of acetone and left to dry, prior to being placed in the discharge chamber of the plasma apparatus. The spheres were weighed accurately and their displacements from the anode in the plasma chamber were recorded.

Sphere **A**: initial mass = 0.19601 g; 13 mm from anode
Sphere **B**: initial mass = 0.19940 g; 66 mm from anode
Sphere **C**: initial mass = 0.19622 g; 145 mm from anode

The conditions of this experiment, in terms of temperature and pressure inside the plasma chamber, and the dial reading of the gas inlet valve (arbitary units), are given in table **6.2.1.**. After five complete oxidation/reduction cycles the spheres were removed from the plasma chamber and reweighed.

Sphere **A**: final mass = 0.19385 g (0.00216 g less than initial mass)
Sphere **B**: final mass = 0.19722 g (0.00218 g less than initial mass)
Sphere **C**: final mass = 0.19383 g (0.00239 g less than initial mass)

The mass lost by the spheres is assumed to be lost in the form of silver hydrides[4].

Table 6.2.1. Plasma oxidation/reduction of 50μm thick silver wire

Plasma	Pressure/Torr	Temp/°C	Inlet Dial
1st O_2	0.411	92	0.435
1st H_2	0.410	82	0.453
2nd O_2	0.385	92	0.436
2nd H_2	0.502	79	0.475
3rd O_2	0.485	91	0.438
3rd H_2	0.479	80	0.453
4th O_2	0.490	92	0.431
4th H_2	0.488	77	0.452
5th O_2	0.468	91	0.430
5th H_2	0.476	81	0.450

Figure 6.2.2. Treated 50 μm silver wire (50 times magnification).

Figure 6.2.3. Treated 50 μm silver wire (100 times magnification)

Figure 6.2.4. Treated 50 μm silver wire (200 times magnification).

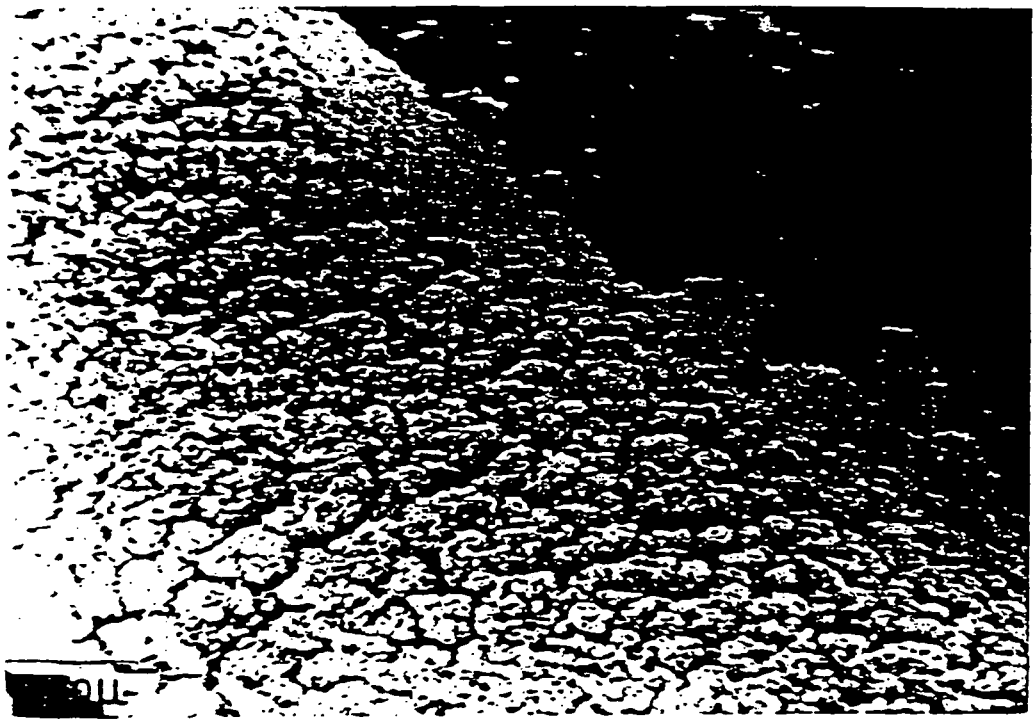

Figure 6.2.5. Treated 50 μm silver wire (500 times magnification)

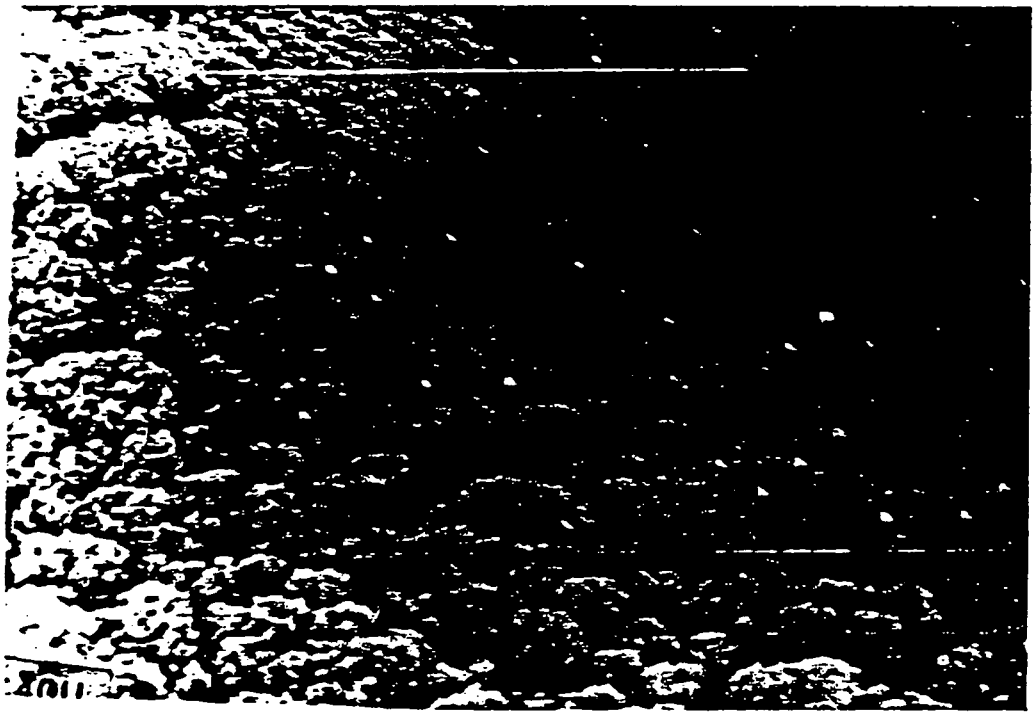

The spheres were then studied by scanning electron microscopy. Figure **6.2.2.** shows the treated wire at 50 times magnification, clearly illustrating the porous expansion of the silver and an area where mounting of the sample has caused removal of the porous fraction. Figure **6.2.3.** shows a similar section of wire at 100 times magnification. Figures **6.2.4.** and **6.2.5.** again show treated wire (at 200 and 500 times magnification respectively), with the highly irregular surface of the silver clearly visible. With these, as with all subsequent plasma experiments, the samples closest to the anode were the most thoroughly treated.

6.2.3. Plasma oxidation/reduction of silver ballotini

Samples of silver ballotini (tiny glass spheres coated with silver) were placed in quartz boats and underwent four complete oxidation/reduction cycles, as shown in table **6.2.2.**. A scanning electron microscope photograph of the ballotini before treatment (figure **6.2.6.**, 5000 times magnification) shows the smooth surfaces of the spheres, whereas after treatment (figure **6.2.7.**, 5000 times magnification) the surfaces of the spheres can be seen to be distinctly irregular. It can also be seen from figure **6.2.7.** that after treatment the ballotini remain as individual spheres, rather than being fused into much larger aggregations.

Table 6.2.2. Plasma oxidation/reduction of silver ballotini

Plasma	Pressure/Torr	Temp/°C	Inlet Dial
1st O_2	0.355	82	0.431
1st H_2	0.439	79	0.420
2nd O_2	0.371	76	0.433
2nd H_2	0.423	65	0.432
3rd O_2	0.436	79	0.434
3rd H_2	0.374	66	0.440
4th O_2	0.408	74	0.425
4th H_2	0.412	70	0.431

6.2.4. Plasma oxidation/reduction of 5 μm thick silver wire

Pure silver 5 μm thick wire was cut into three approximately 0.1 gram samples, which were shaped into rough spheres. The samples were degreased with a little acetone and left to dry, prior to being placed in the discharge chamber of the plasma apparatus. The samples underwent four complete oxidation/reduction cycles as shown in table **6.2.3.**.

Table 6.2.3. Plasma oxidation/reduction of 5μm thick silver wire

Plasma	Pressure/Torr	Temp/°C	Inlet Dial
1st O_2	0.410	86	0.415
1st H_2	0.411	76	0.439
2nd O_2	0.411	86	0.442
2nd H_2	0.438	77	0.463
3rd O_2	0.442	89	0.460
3rd H_2	0.459	80	0.427
4th O_2	0.420	85	0.437
4th H_2	0.437	78	0.435

6.2.5. Plasma oxidation/reduction of silver powder

Samples of silver powder (average particle size of roughly 5 μm diameter) were placed in quartz boats and underwent four complete plasma oxidation/reduction cycles, as shown in table **6.2.4.**.

The treated samples were then viewed using a scanning electron microscope. Figure **6.2.8.** shows a sample of the wire (200 times magnification) before treatment, illustrating the generally smooth surface of the wire. Figure **6.2.9.**, on the other hand, shows a sample of the wire (1000 times magnification) after treatment, with the expansion of surface area clearly visible.

Figure 6.2.6. Untreated silver ballotini (5000 times magnification).

Figure 6.2.7. Treated silver ballotini (5000 times magnification)

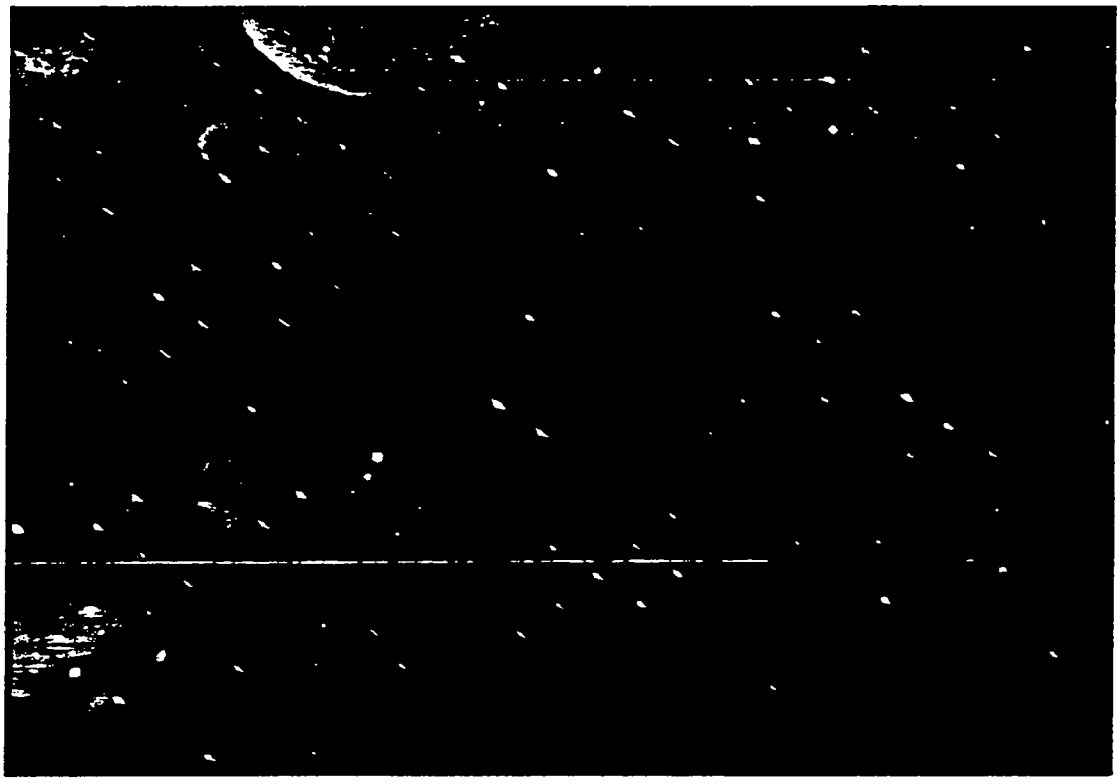

Figure 6.2.8. Untreated 5 μm silver wire (200 times magnification).

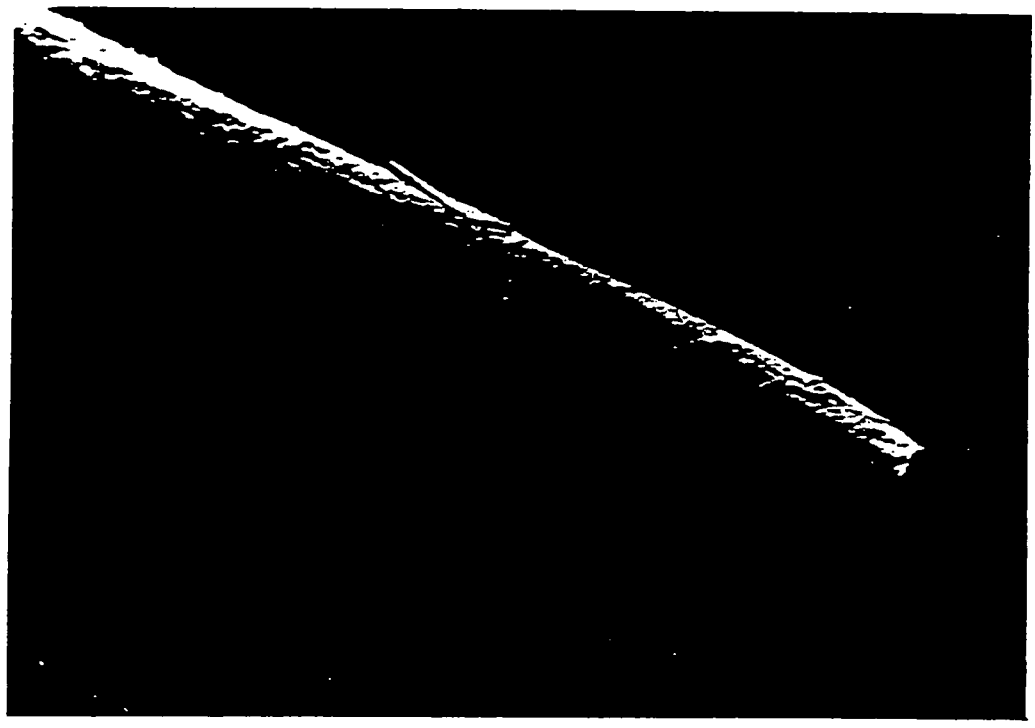

Figure 6.2.9. Treated 5 μm silver wire (1000 times magnification)

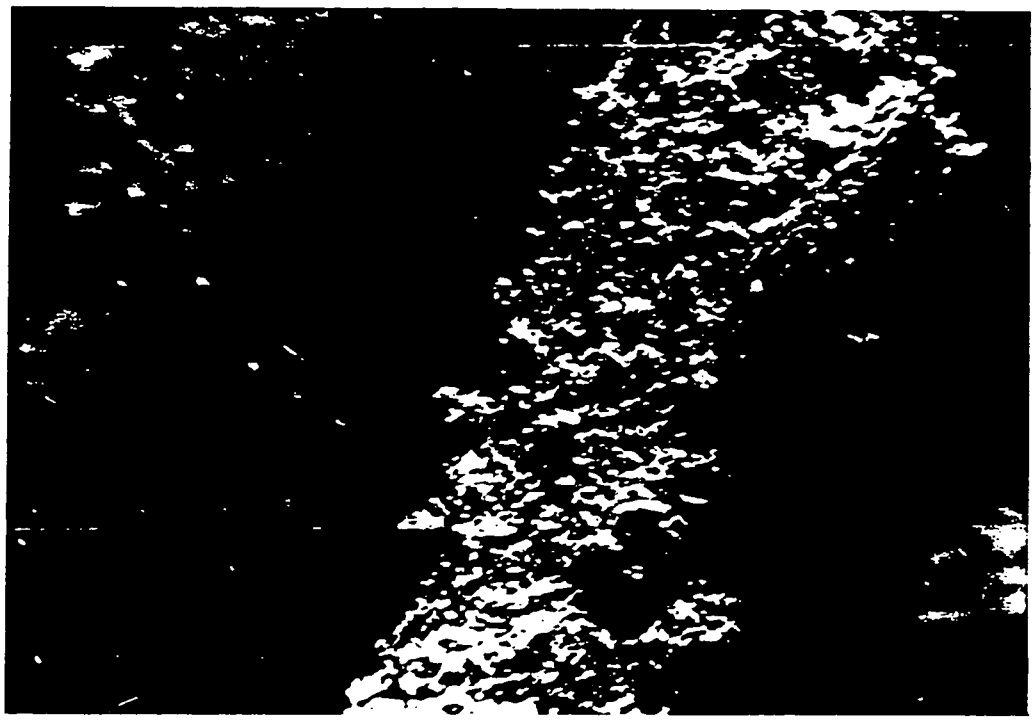

Figure 6.2.10. Untreated silver powder (1000 times magnification).

Figure 6.2.11. Treated silver powder (2000 times magnification)

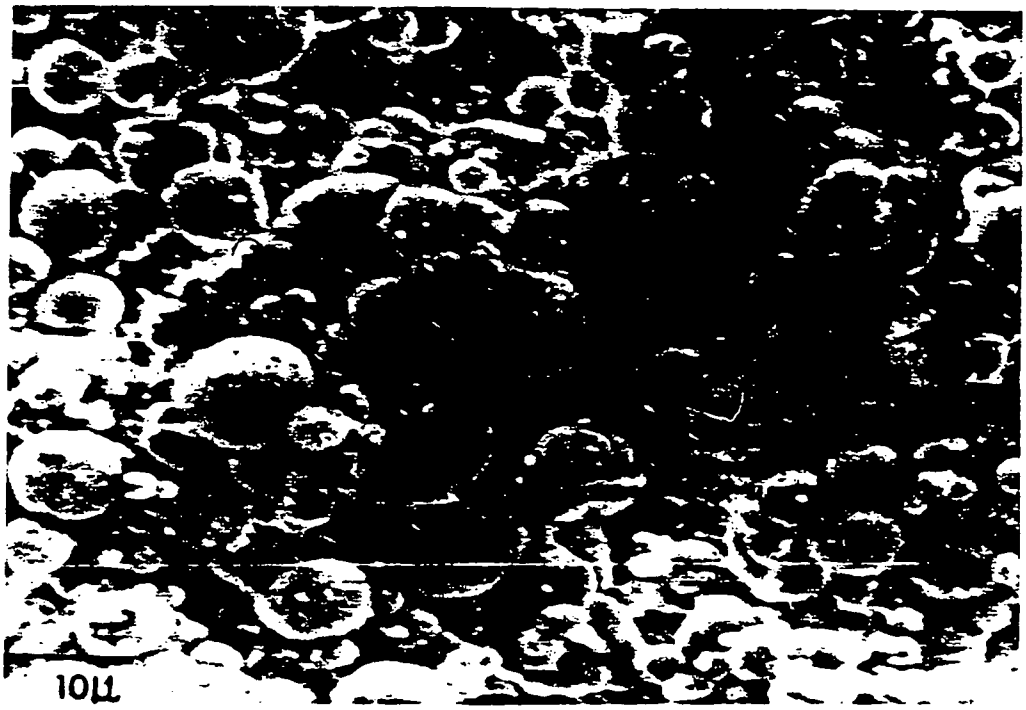

Table 6.2.4. Plasma oxidation/reduction of silver powder

Plasma	Pressure/Torr	Temp/°C	Inlet Dial
1st O_2	0.423	86	0.416
1st H_2	0.426	82	0.474
2nd O_2	0.402	92	0.469
2nd H_2	0.427	81	0.451
3rd O_2	0.442	84	0.405
3rd H_2	0.391	69	0.405
4th O_2	0.418	86	0.416
4th H_2	0.399	70	0.430

Unfortunately, the scanning electron microscope photographs of the samples are somewhat indistinct. Figure **6.2.10.** shows the silver powder (1000 times magnification) before treatment, posessing smooth surfaces. Figure **6.2.11.** shows the powder (2000 times magnification) after treatment, with irregular surfaces visible on some of the central flakes of powder.

6.3. References

1. H.F. Winters, *Top. Curr. Chem.*, **94**, 1980, 69.

2. M. Wittmer, *J. Vac. Technol. A*, Vol. 2, **2**, 1984, 273.

3. A.J. Banister and Z.V. Hauptman, SERC grant final report No. GR/G16519, February 1993.

4. Z.V. Hauptman, personal communication.

Appendix I. Synthesis of *para*-$[NSSNCC_6H_4CNSNS]^{+\cdot}$ $[AsF_6]^-$

Introduction

Bis-dithiadiazolyl compounds are, like dithiadiazolyl dimers, essentially diamagnetic[1], but the radical cation (*para*-$[SNSNCC_6H_4CNSSN]^{+\cdot}$) is paramagnetic (S = 1/2)[2]. The radical cation chloride has been synthesised by Dr I. Lavender (as has its selenium analogue[3]) and the Weiss constant for this compound, θ = -7 K, indicates antiferromagnetic ordering of the radical centres. This result can be explained by the fact that the solid state packing in *para*-$[SNSNCC_6H_4CNSSN][Cl]$ is determined by the coulombic interactions of the ions, thus preventing the radical centres from aligning in 'spin pairs'.

The unusual magnetic behaviour arising from this property prompted further research. As the properties of the radical cation are highly dependant on the solid state packing, changing the anion may have important consequences for its magnetic behaviour. It was for this reason that the preparation of *para*-$[SNSNCC_6H_4CNSSN][AsF_6]$ was attempted.

Results and discussions

Synthesis of the starting materials

The starting materials for the preparation of the target radical cation (see figure **7.1.1.**) are *para*-$[SNSNCC_6H_4CNSSN]^{2+}[AsF_6^-]_2$ and *para*-$[SNSNCC_6H_4CNSSN]^{\cdot\cdot}$. The *para*-dication was prepared by the author by standard literature routes[2] (mentioned in the experimental section of this appendix). The *para*-diradical was prepared[1] by Dr I. Lavender from a sample of the *para*-dication.

Figure 7.1.1. The radical cation *para*-$[SNSCC_6H_4CNSSN][AsF_6]$

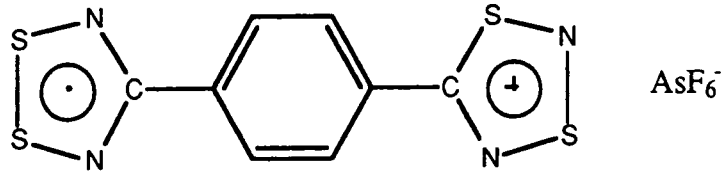

The reaction of *para*-$[SNSCC_6H_4CNSSN]^{2+}[AsF_6^-]_2$ and *para*-$[SNSNCC_6H_4CNSSN]$-

The reaction of *para*-$[SNSCC_6H_4CNSSN]^{2+}[AsF6^-]_2$ and *para*-$[SNSNCC_6H_4CNSSN]$.. in liquid SO_2 over 18 hours gave para-$[SNSNCC_6H_4CNSSN]^{+\cdot}$ $[AsF_6]^-$, **a**, in 36.3 % yield. The product, a brown solid, was sparingly soluble in SO_2. An I.R. spectrum of **a** was run and compared with spectra of the starting materials, showing that **a** was <u>not</u> a mixture of the *para*-dication and *para*-diradical. The spectrum of **a** shows peaks that are present in the spectra of both the *para*-dication and *para*-diradical, but also other peaks (at 1423, 1092, 988 and 846 cm^{-1}) not present in the spectra of either the dication or diradical.

The mass spectrum of **a** showed a reasonably clear breakdown pattern, considering that AsF_6^- salts are notoriously involatile. Despite numerous attempts, fairly poor chemical analysis figures (C,H,N) were obtained for **a** .Differential scanning calorimetry measurements gave a melting point for **a** of 310 °C +/- 2 °C, compared with 253 °C +/- 2 °C for the diradical and > 330 °C for the dication. An esr study of **a** by Dr L.H. Sutcliffe of the Department of Chemistry, University of Sussex, showed a 1:1:1 triplet, typical of a dithiadiazolyl mono-radical. A cyclic voltammagram of **a** was also run (by Miss C.M. Aherne) as shown in figure **7.1.2.**, below.

Figure 7.1.2. Cyclic voltammagram of *para*-$[SNSNCC_6H_4CNSSN][AsF_6]$

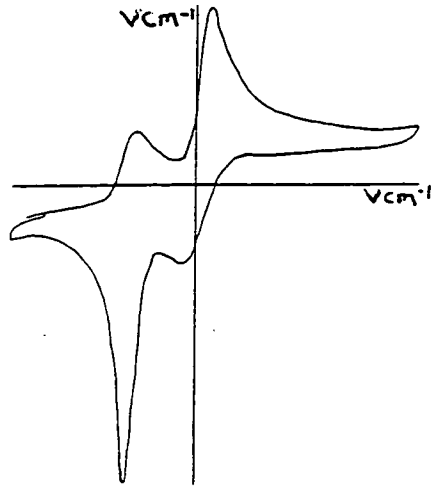

Experimental

Preparation of *para*-[NCC_6H_4CNSSN][Cl]

White $LiN(SiMe_3)_2$ (6.52g, 39 mmol) and white *para*-dicyanobenzene (5.00 g, 39 mmol) were placed, along with a magnetic follower, in a two-necked 250 ml round bottomed flask. Diethyl ether (30 ml) was added and the mixture was left to stir for 18 hours, at room temperature. An off-white precipitate ($[Li][NCC_6H_4C(NSiMe_3)_2]$) was observed to have formed, which was dried *in vacuo*. Yellow SCl_2 (6 ml, excess) was dissolved in CH_2Cl_2 (35 ml) and then added by cannulation to the $[Li][NCC_6H_4C(NSiMe_3)_2]$. An orange solid was formed, *para*-[NCC_6H_4CNSSN][Cl], which was purified by extraction with CH_2Cl_2 (10 ml) in a sealed soxhlet extractor for 2 days. The pure product was dried *in vacuo*.

Appearance: Bright orange solid
Yield: 8.05 g, 33.3 mmol, 85.4 %
IR (Nujol mull): 2100 s,b; 1285 vw,b; 1145 m; 1012 m; 920 m; 890 s; 860 w,sh; 845 s; 740 s; 721 m,sh; 683 m; 640 vw; 550 s; 523 w,sh; 450 vw cm^{-1}
Mass spectra: (E.I.) 206 (M^+), 160 ($C_6H_4CNSSN^+$),.128 ($NCC_6H_4CN^+$), 101 ($C_6H_4CN^+$), 78 ($C_6H_4^+$), 50 (?)
(C.I.): 279, 224, 206, 185, 146, 135, 78, 61,.52
Chemical analysis: Found (%) C 40.30 H 1.74 N 17.25
Required (%) C 39.75 H 1.67 N 17.39

Preparation of *para*-[NCC_6H_4CNSSN][AsF_6]

Orange *para*-[NCC_6H_4CNSSN][Cl] (2.42 g, 10.0 mmol) and white $AgAsF_6$ (3.00 g, 10.2 mmol) were placed in the rear leg of a 'dog' containing a magnetic follower. Sufficient SO_2 was condensed into the leg to dissolve both reagents, the solution being a red-brown colour. After sirring (18 h, room temperature) the reaction vessel contained a yellow solution (*para*-[NCC_6H_4CNSSN][AsF_6]) standing over a white solid (AgCl). The yellow solution was removed by filtration and evaporated to dryness *in vacuo*, giving a yellow solid. This crude solid was purified by extraction in SO_2 (c. 10 ml) in a sealed soxhlet extractor for 2 days. The pure product was then dried *in vacuo*.

Appearance: Yellow Solid
Yield: 2.99 g, 9.28 mmol, 93.1 %
IR (Nujol mull, KBr plates): 2200 m; 1308 w; 1158 vw,b; 1026 m; 985 w,b; 769 vw,sh; 718 vw,b; 703 m,sh; 590 w; 551 m; 502 vw; 486 vw; 467 w; 390 s cm^{-1}
Mass spectra: (E.I.) 128 ($NCC_6H_4CN^+$), 101 ($C_6H_4CN^+$), 75 ($C_6H_4^+$), 50 (?)
Chemical Analysis: Found (%) C 24.76 H 1.11 N 11.05
Required (%) C 24.31 H 1.02 N 10.64

Preparation of *para*-$[NSNSCC_6H_4CNSSN][AsF_6]_2$

Yellow *para*-$[NCC_6H_4CNSSN][AsF_6]$ (2.00 g, 5.06 mmol) and beige $[SNS][AsF_6]$ (1.36 g, 5.09 mmol) were placed, together with a magnetic follower, in the rear leg of a 'dog'. Sufficient SO_2 was condensed into the leg to dissolve both reagents, giving a red-brown solution. Stirring commenced and lasted for 60 hours (the reaction appeared to proceed slowly) at room temperature. After this time the solvent was removed and it was found that a bright yellow had been formed. The crude product was washed with back-condensed SO_2 until the washings became colourless, then dried *in vacuo*.

Appearance: Bright yellow solid
Yield: 2.942 g, 3.00 mmol, 59.2 %
IR (Nujol mull, KBr plates): 1515 m; 1401 s; 1302 w; 1167 m; 1020w; 990 m; 925 m; 917 w,sh; 853 m; 847 w; 837 vw; 800 w; 749 vw; 705 vs,b; 612 m,sh; 635 w; 590 vw; 576 vw; 561 w; 442 w; 398 vs cm^{-1}
Mass spectra: (E.I.) 128 ($NCC_6H_4CN^+$), 113 ($C_6H_4CN_2^+$), 101 ($C_6H_4CN^+$), 92 ($C_6H_4N^+$), 78 ($C_6H_4^+$), 64 (S_2^+), 46 (SN^+) (C.I.): 224, 211, 185, 167, 146, 78, 46
Chemical Analysis: Found (%) C 14.65 H 0.64 N 8.46
Required (%) C 14.51 H 0.61 N 8.46

Preparation of *para*-$[NSNSCC_6H_4CNSSN]^{+\cdot}[AsF_6]^-$

Bright yellow *para*-$[SNSNCC_6H_4CNSSN][AsF_6]_2$ (140 mg, 0.211 mmol) and black *para*-$[SNSNCC_6H_4CNSSN]^{\cdot\cdot}$ (60 mg, 0.213 mmol) were placed in the rear leg of a 'dog' containing a magnetic follower.

Sufficient SO_2 was condensed into the leg to dissolve the reactants, giving a red-brown solution. The reaction was stirred (18 h, room temperature), and a brown solid slowly formed. This crude solid was washed three times with back-condensed SO_2, before being dried *in vacuo*.

Appearance: Brown solid
Yield: 72 mg, 0.077 mmol, 36.3 %
IR (Nujol mull, KBr plates): 1675 m,b; 1603 w; 1510 w; 1423 m; 1400 s; 1303 w,b; 1232 w; 1210 w; 1165 w; 1146 vw; 1128 vw; 1116 vw; 1092 vw; 1015 w; 988 m; 925 vw,sh; 916 w; 903 m; 888 vw; 846 s; 835 m; 826 m; 800 s; 778 vw; 700 vs,b; 642 m; 623 vw; 588 w; 510 m; 441 m; 398 vs; 330 vw,b cm^{-1}
Mass spectra: (E.I.) 128 ($NCC_6H_4CN^+$), 110 (S_3N^+), 93 ($S_2N_2^+$), 84 ($C_2N_2S^+$), 64 (S_2^+)
(C.I.): 156, 77, 65, 60
Chemical Analysis: Found (%) C 21.00 H 1.18 N 10.27
Required (%) C 20.30 H 0.85 N 11.84

References

1. A.J. Banister, I. Lavender, J.M. Rawson and R.J. Whitehead, *J. Chem. Soc., Dalton Commun.*, **1992**, 1449.

2. A.J. Banister, I. Lavender, J.M. Rawson, W. Clegg, B.K. Tanner and R.J. Whitehead, *J. Chem. Soc., Dalton Trans.*, **1993**, 1421.

3. I. Lavender, Personal communication.

Appendix II: [PhN=S=N=S-NPh][AsF_6] as an initiator for the cationic ring-opening polymerisation of tetrahydrofuran

Results

In an attempt to grow single crystals of [PhN=S=N=S-NPh][AsF_6], a powder sample (63 mg, 0.14 mmol.) was placed, along with a magnetic follower, in a 250 ml round bottomed flask, and dry thf (20 ml) was syringed onto the sample against a dry nitrogen counterflow, yielding a very deep green solution. Stirring was then initiated and within 10 minutes the solution was observed to have gelled into a dark green, gelatinous solid; polymerisation of the thf had occurred. This gelatinous solid was then dried *in vacuo* and washed with CH_2Cl_2 (2 x 20 ml) leaving a faintly coloured, rubbery solid, **a**.

A ^{13}C nmr study of **a** showed resonances attributable to monomeric thf (18.5 ppm and 58.5 ppm) and resonances attributable to poly-thf (26.6 ppm and 70.7 ppm), see figure **8.1.1.**. These chemical shifts are in good agreement with the literature values[1]. Molecular weight determinations were carried out on a sample of **a** by G. Forrest of the IRC of Polymer Science and Technology at the University of Durham. These determinations showed the polymer was of high molecular weight and low polydispersity, indicating that only a small amount of branching occurs in the growing polymer chains.

M_n: 221210 g mol^{-1}, M_w: 390219 g mol^{-1}, M_w/M_n (polydipersity): 1.764

^{13}C nmr ($CDCl_3$): 18.5 ppm, 26.6 ppm, 58.5 ppm, 70.7 ppm.

Discussion

The results obtained from this reaction are similar to those previously obtained by Dr Anthony Luke studying the polymerisations of thf by [$[Ph(CNSNS^+)_n]^{n+}[AsF_6^-]_n$] (n = 1,2,3)[2]. These polymerisations take place via a cationic ring-opening polymerisation (C.R.O.P.) mechanism[2], and it seems reasonable to assume that polymerisation of thf by [PhN=S=N=S-NPh][AsF_6] takes place by the same route. The projected mechanism is illustrated in scheme **8.1.1.**. Oxonium ions of the type shown in sheme **8.1.1.** are known to be the active species in thf polymerisations[3-7].

Scheme 8.1.1. The projected mechanism for the [PhN=S=N=S-NPh][AsF_6] initiated C.R.O.P. of thf.

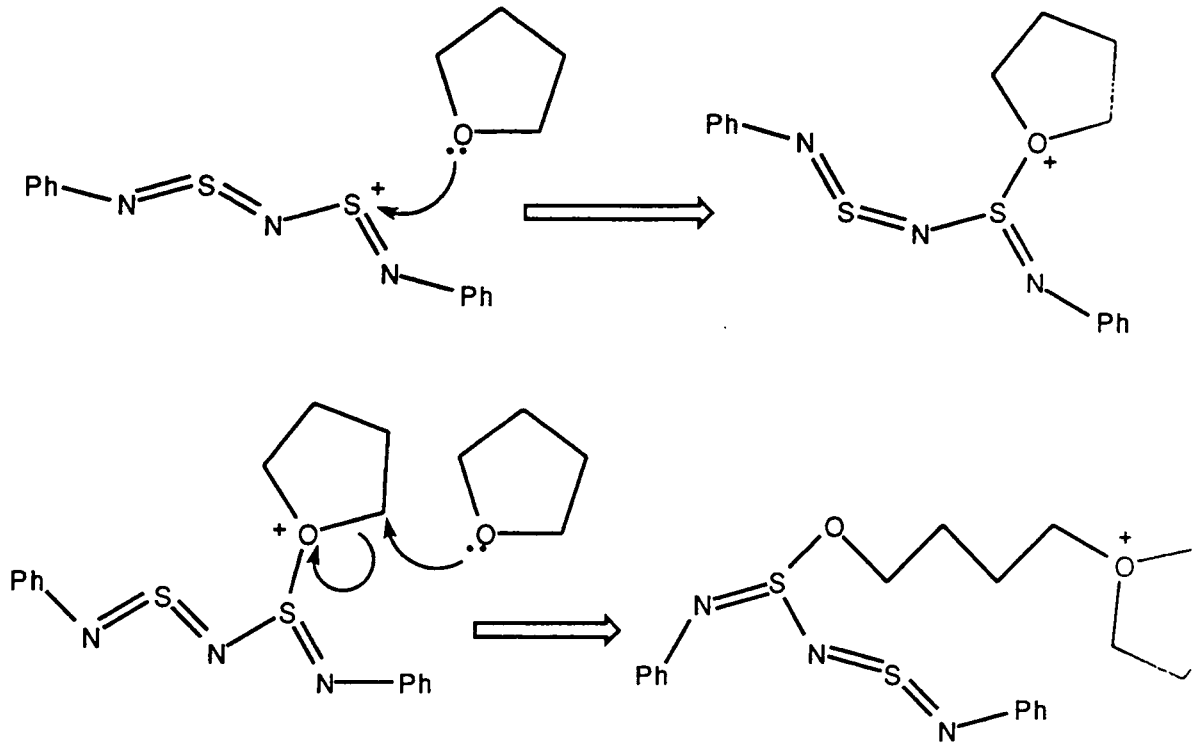

Whilst it seems likely that many dithiadiazolium-related cations may initiate C.R.O.P. of thf, polymerisation of monomers other than thf by these species has not, to the author's knowledge, been investigated.

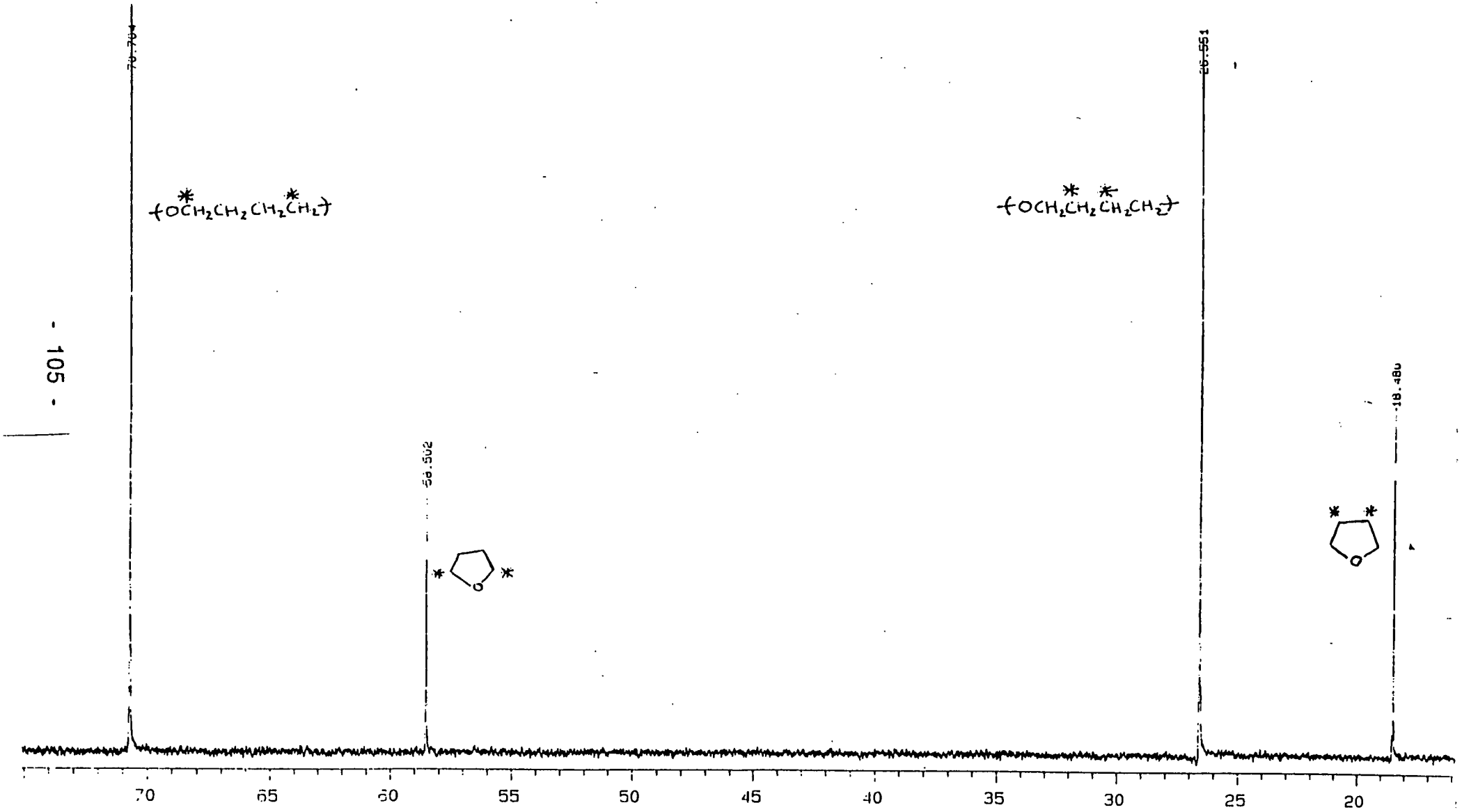
70.764
56.502
26.551
18.480
70
65
60
55
50
45
40
35
30
25
20

References

1. G. Prukmayr and T.K. Wu, in *^{13}C NMR in Polymer Science*, W.M. Pasika (Ed.), ACS symposium series, vol. 103, American Chemical Section, Washington DC, 1979, p.237.

2. A.J. Banister and A.W. Luke, *J. Polym. Sci. A*, **30**, 2653.

3. P.H. Plesch, *The Chemistry of Cationic Polymerisation*, Pergamon, New York, 1963.

4. M.P. Dreyfuss and P. Dreyfuss, *J. Polym. Sci. A-1*, **4**, 2179 (1966).

5. C.C. Price and R.J. Spector, *J. Am. Chem. Soc.*, **88**, 4171 (1966).

6. B.A. Rosenberg and Y.B. Lyndrig, *Polym. Sci. USSR*, **6**, 2253 (1964).

7. S. Penczek and K. Matyjaszewski, *J. Polym. Sci., Polym. Symp.*, **56**, 225 (1976)

Appendix III: COLLOQUIA, LECTURES AND SEMINARS FROM INVITED SPEAKERS

(October 1992 - November 1993)

October 15	Dr M. Glazer (Oxford University) & Dr S. Tarling (Birbeck College, London) The chemist's role as an expert witness in patent litigation
October 20	Dr H.E. Bryndza (Du Pont central research) Synthesis, reactions and thermochemistry of metal (alkyl) cyanide complexes and their impact on olefin hydrocyanation catalysis
October 22 *	Prof. A. Davies (University College, London) *The Ingold-Albert lecture* : The behaviour of hydrogen as a pseudometal
October 28 *	Dr J.K. Cockcroft (Durham University) Recent developments in powder diffraction
October 29 *	Dr J. Emsley (Imperial College, London) The shocking history of phosphorus
November 4 *	Dr T.P. Kee (Leeds University) Synthesis and Coordination chemistry of silylated phosphites
November 5	Dr C.J. Ludman (Durham University) Explosions - a demonstration lecture
November 11	Prof. D. Robins (Glasgow University) Pyrrolizidine alkaloids: biological activity, biosynthesis and benefits
November 12 *	Prof. M.R. Truter (University College, London) Luck and logic in host - guest chemistry

November 18	Dr R. Nix (Queen Mary College, London) Characterisation of heterogeneous catalysis
November 25	Prof. Y. Vallee (Caen University) Reactive thiocarbonyl compounds
November 25 *	Prof. L.D. Quin (Massachusetts University, Amherst) Fragmentation of phosphorous heterocycles as a route to phosphoryl species with uncommon bonding
November 26	Dr D. Humber (Glaxo, Greenford) AIDS - the development of a novel series of inhibitors of HIV
December 2	Prof. A.F. Hegarty (University College, Dublin) Highly reactive enols stabilised by steric protection
December 2	Dr R.A. Aitken (St. Andrews University) The versatile cycloadition chemistry of $Bu_3P.CS_2$
December 3 *	Prof. P. Edwards (Birmingham University) *The SCI lecture* : What is metal?
December 9	Dr A.N. Burgess (ICI, Runcorn) The structure of perfluorinated ionomer membranes
January 20 *	Dr D.C. Clary (Cambridge University) Energy flow in chemical reactions
January 21	Prof. L. Hall (Cambridge University) NMR - window to the human body
January 27	Dr W. Kerr (Strathclyde University) Development of the Pauson-Khand annulation reaction: organocobalt mediated synthesis of natural and unnatural products
January 28 *	Prof. J. Mann (Reading University) Murder, magic and medicine

February 3	Prof. S.M. Roberts (Exeter University) Enzymes in organic synthesis
February 10	Dr D. Gilles (Surrey University) NMR and molecular motion in solution
February 11 *	Prof. S. Knox (Bristol University) *The Tilden lecture* : organic chemistry at polynuclear metal centres
February 17	Dr R.W. Kemmitt (Leicester University) Oxatrimethylenemethane metal complexes
February 18	Dr I. Fraser (ICI, Wilton) Reactive processing of composite materials
February 22	Prof. D.M. Grant (Utah University) Single crystals, molecular structure and chemical shift anisotropy
February 24	Prof. C.J.M. Stirling (Sheffield University) Chemistry on the flat-reactivity of ordered systems
March 10 *	Dr P.K. Baker (University College of North Wales, Bangor) Chemistry of highly versatile 7-coordinate complexes
March 11	Dr R.A.Y. Jones (University of East Anglia) The chemistry of wine making
March 17	Dr R.J.K. Taylor (University of East Anglia) Adventures in natural product synthesis
March 24	Prof. I.O. Sutherland (Liverpool University) Chromogenic reagents for cations
May 13 *	Prof. J.A. Pople (Carnegie-Mellon University, Pittsburgh) *The Boys-Rahman lecture* : Applications of molecular orbital theory

May 21 *	Prof. L. Weber (Bielefeld University) Metallo-phosphaalkenes as synthons in organometallic chemistry
June 1	Prof. J.P. Konopelski (California University, Santa Cruz) Synthetic adventures with enantiomerically pure acetals
June 2	Prof. F. Ciardelli (Pisa University) Chiral discrimination in the stereospecific polymerisation of alpha-olefins
June 7	Prof. R.S. Stein (Massachusetts University, Amherst) Scattering studies of crystalline and liquid crystalline polymers
June 16	Prof. A.K. Covington (Newcastle University) Use of ion-selective electrodes as detectors in ion chromatography
June 17	Prof. O.F. Nielsen (H.C. Ørsted Institute, Kobenhavn University) Low frequency IR and Raman studies of hydrogen bonded liquids
September 13	Prof. A.D. Schlüter (Freie University, Berlin) Synthesis and characterisation of molecular rods and ribbons
September 13	Dr K.J. Wynne (Naval Research Office, Washington D.C.) Polymer surface dsign for minimal adhesion
September 14	Prof. J.M. DeSimone (University of North Carolina, Chapel Hill) Homogeneous and heterogeneous polymerizations in enviromentally responsible carbon dioxide
September 28	Prof. H. Ila (North Eastern Hill University, India) Synthetic strategies for cyclopentanoids via oxoketene dithioacetals

October 4 *	Prof. F.J. Feher (University of California at Irvine) Bridging the gap betwen surfaces and solutions with sessilquioxanes
October 14 *	Dr P. Hubberstey (Nottingham University) Alkali metals: alchemist's nightmare, biochemist's puzzle and technologist's dream
October 20	Dr P. Quayle (Manchester University) Aspects of aqueous ROMP chemistry
October 21	Dr B. Caddy (Strathclyde University) Forensic scientists: do we mean what we say?
October 23 *	Prof. R. Adams (South Carolina University) The chemistry of metal carbonyl cluster complexes containing platinum and iron, ruthenium or osmium and the development of a cluster based alkyne hydrogenation catalyst
October 27	Dr R.A.L. Jones (Cavendish laboratory, Oxford) Perambulating polymers
October 28 *	Dr L. Phillips (Shell Research Ltd., Sittingbourne) Molecular design: a multidisciplinary approach

* indicates lecture attended by the author.

Table 9.1.1. Anisotropic displacement parameters ($Å^2 \times 10^3$) for 1

The anisotropic displacement factor exponent takes the form:
$-2\pi^2(h^2a^{*2}U_{11} + \ldots + 2hka^*b^*U_{12})$.

	U(11)	U(22)	U(33)	U(23)	U(13)	U(12)
Br(1)	52(2)	73(3)	28(2)	8(2)	4(2)	-3(2)
C(1)	48(18)	34(17)	14(14)	-13(13)	-3(12)	-6(15)
C(2)	54(20)	30(17)	8(14)	3(12)	5(13)	5(16)
C(3)	18(15)	51(21)	33(17)	8(16)	-4(13)	-8(15)
C(4)	68(27)	67(28)	51(25)	-1(21)	10(20)	4(23)
C(5)	41(20)	37(20)	46(20)	-17(17)	-18(16)	20(16)
C(6)	43(20)	55(23)	32(18)	-7(17)	-1(15)	-2(18)
C(7)	62(22)	34(19)	29(18)	-12(15)	3(16)	12(17)
S(1)	43(5)	48(5)	31(4)	7(4)	-8(4)	-5(4)
S(2)	33(4)	35(5)	37(4)	-3(4)	4(3)	2(4)
N(1)	35(14)	39(17)	29(14)	-2(12)	-9(11)	12(13)
N(2)	37(15)	38(17)	60(18)	6(14)	2(14)	-6(13)
Br(2)	43(2)	82(3)	35(2)	-4(2)	11(2)	3(2)
C(8)	38(18)	27(18)	31(17)	-4(14)	4(14)	0(15)
C(9)	19(15)	42(20)	29(17)	-10(15)	-9(12)	-7(14)
C(10)	28(17)	83(28)	19(16)	-7(17)	-16(13)	9(18)
C(11)	66(27)	72(29)	33(19)	12(19)	-20(19)	-17(22)
C(12)	33(19)	85(30)	32(20)	12(20)	-16(16)	11(19)
C(13)	42(23)	51(25)	98(35)	-21(23)	-19(21)	38(19)
C(14)	26(16)	40(19)	30(17)	-7(15)	-3(13)	12(15)
S(3)	41(4)	35(5)	25(4)	1(4)	0(3)	1(4)
S(4)	31(4)	40(5)	31(4)	-9(4)	-7(3)	1(4)
N(3)	67(18)	4(12)	26(13)	-3(10)	-6(12)	-3(12)
N(4)	52(16)	15(13)	20(12)	-2(10)	0(11)	0(12)
As(1)	39(2)	31(2)	29(2)	-1.8(14)	4.0(14)	-3(2)
F(1)	100(22)	83(20)	65(17)	-29(15)	-54(15)	15(17)
F(2)	56(15)	35(14)	138(26)	-16(15)	36(16)	-23(12)
F(3)	167(31)	49(16)	50(16)	4(13)	49(18)	-20(18)
F(4)	63(18)	86(23)	218(43)	-99(27)	28(22)	-5(17)
F(5)	104(21)	53(16)	54(15)	15(12)	-9(14)	18(15)
F(6)	102(22)	49(15)	89(19)	-20(15)	-47(16)	4(15)
As(2)	31(2)	24(2)	26(2)	-0.8(14)	-1.5(12)	0.9(14)
F(7)	65(13)	34(11)	49(12)	-3(9)	14(10)	3(10)
F(8)	63(13)	30(11)	48(11)	-10(9)	-7(9)	4(9)
F(9)	33(9)	33(10)	40(10)	-7(8)	-4(8)	-9(8)
F(10)	59(12)	39(11)	68(13)	12(10)	29(11)	10(10)
F(11)	60(12)	29(10)	58(12)	-18(9)	-10(10)	-2(9)
F(12)	41(11)	29(10)	68(13)	9(9)	-10(9)	24(9)

Table 9.1.2. Hydrogen atom coordinates (x 10^4) and isotropic displacement parameters ($Å^2$ x 10^3) for **1**

	x	y	z	U
H(3)	-1917(21)	284(42)	3091(12)	51
H(4)	-3395(32)	399(53)	2448(15)	93
H(5)	-3126(25)	1778(40)	1634(14)	63
H(6)	-1468(26)	2259(45)	1323(13)	65
H(10)	1779(24)	2340(48)	-1555(12)	66
H(11)	192(30)	3039(51)	-1993(14)	86
H(12)	-1260(26)	3316(50)	-1499(14)	76
H(13)	-1164(29)	3139(47)	-606(19)	97

Table 9.1.3. Anisotropic displacement parameters ($Å^2 \times 10^3$) for **2**

The anisotropic displacement factor exponent takes the form: $-2\pi^2(h^2a^{*2}U_{11} + \ldots + 2hka^*b^*U_{12})$.

	U(11)	U(22)	U(33)	U(23)	U(13)	U(12)
As(1)	30.3(4)	21.5(4)	24.1(4)	-1.1(3)	13.9(3)	-0.7(3)
F(1)	38(2)	36(3)	39(2)	-4(2)	9(2)	5(2)
F(2)	65(3)	30(3)	30(2)	-5(2)	29(2)	-5(2)
F(3)	48(3)	31(3)	48(3)	-5(2)	31(2)	-10(2)
F(4)	63(3)	34(3)	37(2)	-6(2)	33(2)	-4(2)
F(5)	43(2)	30(2)	40(2)	1(2)	23(2)	-7(2)
F(6)	38(2)	29(3)	51(3)	5(2)	9(2)	3(2)
As(2)	36.3(4)	29.0(5)	33.3(4)	-1.1(4)	10.2(4)	-2.8(4)
F(7)	211(11)	37(4)	203(11)	9(5)	185(10)	-8(5)
F(8)	38(4)	51(5)	219(12)	-1(6)	3(5)	22(4)
F(9)	118(7)	34(4)	61(4)	-18(3)	-23(4)	8(4)
F(10)	201(9)	50(5)	93(6)	17(4)	112(6)	9(5)
F(11)	43(4)	43(4)	104(6)	9(4)	5(4)	0(3)
F(12)	120(6)	36(4)	54(4)	-23(3)	39(4)	-28(4)
As(3)	38.3(4)	26.6(4)	29.6(4)	-0.2(3)	12.7(3)	-1.7(4)
F(13)	37(3)	66(4)	121(6)	26(4)	30(4)	-4(3)
F(14)	162(8)	42(4)	128(7)	11(4)	112(6)	36(4)
F(15)	71(4)	61(4)	98(5)	14(4)	37(4)	-24(3)
F(16)	118(5)	33(3)	59(4)	0(3)	60(4)	12(3)
F(17)	68(4)	64(4)	31(3)	4(3)	15(3)	-6(3)
F(18)	106(6)	66(4)	40(3)	22(3)	-4(3)	12(4)
As(4)	36.3(4)	23.8(4)	24.9(4)	0.0(3)	14.7(3)	-0.9(3)
F(19)	47(3)	46(3)	54(3)	11(2)	32(2)	17(2)
F(20)	70(3)	61(4)	37(3)	-2(2)	4(2)	-29(3)
F(21)	82(3)	34(3)	56(3)	8(2)	43(3)	22(3)
F(22)	42(3)	36(3)	49(3)	-9(2)	10(2)	-9(2)
F(23)	77(3)	34(3)	38(2)	8(2)	40(2)	3(2)
F(24)	72(3)	41(3)	31(2)	10(2)	29(2)	4(2)
Cl(1)	36.1(11)	68(2)	34.6(11)	-1.6(10)	6.1(9)	-3.6(11)
S(1)	36.1(10)	31.1(11)	38.9(11)	-5.9(9)	24.3(9)	-7.9(9)
S(2)	42.8(11)	29.4(11)	24.6(9)	1.2(8)	16.1(8)	-1.3(9)
N(1)	31(3)	19(3)	29(3)	-5(3)	14(3)	-5(3)
N(2)	48(4)	29(4)	39(4)	-6(3)	32(3)	-4(3)
C(1)	35(4)	17(4)	25(4)	0(3)	15(3)	0(3)
C(2)	35(4)	18(4)	32(4)	-3(3)	18(3)	-2(3)
C(3)	37(4)	39(5)	27(4)	1(3)	14(4)	-1(4)
C(4)	32(4)	69(7)	57(6)	3(5)	22(4)	-14(4)
C(5)	48(5)	65(7)	57(6)	10(5)	36(5)	-7(5)
C(6)	57(6)	48(6)	40(5)	3(4)	31(4)	-9(4)
C(7)	36(4)	38(5)	30(4)	1(4)	17(4)	3(4)
Cl(2)	60.1(14)	88(2)	32.3(11)	-14.9(12)	13.4(10)	-24.9(14)
S(3)	38.8(11)	33.9(12)	37.0(11)	-1.0(9)	18.2(9)	-3.8(9)
S(4)	59.1(13)	38.3(12)	30.6(10)	-2.3(9)	25.4(10)	-1.1(10)
N(3)	60(4)	28(4)	47(4)	0(3)	35(4)	-5(3)
N(4)	37(3)	36(4)	24(3)	-2(3)	12(3)	-3(3)
C(8)	45(4)	22(4)	26(4)	1(3)	18(4)	0(3)
C(9)	43(4)	23(4)	29(4)	3(3)	18(3)	0(3)
C(10)	64(5)	30(5)	26(4)	0(3)	21(4)	2(4)
C(11)	76(7)	42(5)	37(5)	1(4)	32(5)	6(5)
C(12)	86(7)	44(6)	48(5)	15(4)	49(5)	15(5)
C(13)	55(5)	60(6)	57(6)	25(5)	36(5)	10(5)

C(14)	47(5)	28(5)	37(4)	3(4)	21(4)	-5(4)
Cl(3)	46.8(12)	74(2)	26.5(10)	-2.8(10)	7.0(9)	-12.2(11)
S(5)	31.2(10)	38.3(12)	34.4(10)	0.8(9)	14.5(8)	0.1(9)
S(6)	48.1(12)	36.2(12)	29.1(10)	-0.9(9)	22.5(9)	1.4(10)
N(5)	58(4)	28(4)	50(4)	5(3)	38(4)	3(3)
N(6)	36(3)	29(4)	29(3)	-3(3)	16(3)	2(3)
C(15)	33(4)	25(4)	28(4)	5(3)	12(3)	1(3)
C(16)	36(4)	26(4)	24(4)	3(3)	15(3)	3(3)
C(17)	43(4)	39(5)	24(4)	7(3)	15(4)	1(4)
C(18)	63(6)	49(6)	30(4)	0(4)	24(4)	4(5)
C(19)	78(7)	36(5)	45(5)	11(4)	48(5)	21(5)
C(20)	45(5)	54(6)	47(5)	17(4)	33(4)	15(4)
C(21)	40(5)	46(5)	30(4)	1(4)	16(4)	6(4)
Cl(4)	32.4(12)	188(4)	45.5(14)	-17(2)	6.7(11)	6(2)
S(7)	35.1(10)	34.6(12)	25.2(9)	-1.4(8)	14.2(8)	2.2(9)
S(8)	31.9(10)	47.7(13)	36.5(11)	8.8(10)	19.3(9)	7.3(9)
N(7)	44(4)	34(4)	40(4)	5(3)	27(3)	5(3)
N(8)	27(3)	27(4)	30(3)	2(3)	16(3)	0(3)
C(22)	36(4)	18(4)	27(4)	-1(3)	13(3)	3(3)
C(23)	33(4)	33(5)	43(5)	1(4)	21(4)	3(4)
C(24)	34(5)	102(9)	43(5)	-1(5)	15(4)	17(5)
C(25)	39(6)	199(16)	74(8)	-1(9)	32(6)	29(8)
C(26)	71(8)	139(12)	88(8)	-4(8)	58(7)	23(8)
C(27)	70(7)	76(8)	59(6)	-6(5)	47(6)	5(6)
C(28)	52(5)	28(5)	43(5)	-5(4)	30(4)	4(4)

Table 9.1.4. Hydrogen atom coordinates (x 10^4) and isotropic displacement parameters ($Å^2$ x 10^3) for **2**

	x	y	z	U
H(4)	5333(3)	2905(12)	4536(4)	78
H(5)	4951(4)	3148(12)	3589(4)	78
H(6)	3977(4)	2609(11)	3045(3)	67
H(7)	3382(3)	1781(10)	3443(3)	50
H(11)	6427(4)	-6740(11)	1324(3)	74
H(12)	7403(4)	-6208(11)	1664(4)	79
H(13)	7922(4)	-5120(12)	2539(4)	79
H(14)	7462(3)	-4709(9)	3101(3)	54
H(18)	8615(4)	-2552(11)	8688(3)	69
H(19)	7635(4)	-2959(10)	8385(3)	68
H(20)	7055(4)	-3898(11)	7493(3)	66
H(21)	7476(3)	-4364(10)	6897(3)	58
H(25)	4686(4)	-2080(20)	396(5)	152
H(26)	5025(5)	-1537(18)	1332(5)	136
H(27)	6014(4)	-1581(13)	1915(4)	93
H(28)	6661(4)	-2235(9)	1561(3)	56

1 = *ortho*-[BrC_6H_4CNSNS][AsF_6]

2 = *ortho*-[$ClC_6H4CNSNS$][AsF_6]

" Tom.....what makes Teflon waterproof ? "
" Go to sleep "